

In the Name of God

# Journal of Information Systems & Telecommunication

Vol. 14, Special Issue, Winter 2026

Research Institute for Information and Communication Technology  
Iranian Association of Information and Communication Technology  
Affiliated to: Academic Center for Education, Culture and Research (ACECR)

**Manager-in-Charge:** Dr. Ali Mokhtarani, ACECR, Iran

**Editor-in-Chief:** Dr. Masoud Shafiee, Amir Kabir University of Technology, Iran

## Editorial Board

Dr. Abdolali Abdipour, Professor, Amirkabir University of Technology, Iran  
Dr. Ali Akbar Jalali, Professor, Iran University of Science and Technology, Iran  
Dr. Alireza Montazemi, Professor, McMaster University, Canada  
Dr. Ali Mohammad-Djafari, Associate Professor, Le Centre National de la Recherche Scientifique (CNRS), France  
Dr. Hamid Reza Sadegh Mohammadi, Associate Professor, ACECR, Iran  
Dr. Mahmoud Moghavvemi, Professor, University of Malaya (UM), Malaysia  
Dr. Mehrnosh Shamsfard, Associate Professor, Shahid Beheshti University, Iran  
Dr. Omid Mahdi Ebadati, Associate Professor, Kharazmi University, Iran  
Dr. Rahim Saeidi, Assistant Professor, Aalto University, Finland  
Dr. Ramezan Ali Sadeghzadeh, Professor, Khajeh Nasireddin Toosi University of Technology, Iran  
Dr. Sha'ban Elahi, Professor, Vali-e-asr University of Rafsanjan, Iran  
Dr. Shohreh Kasaei, Professor, Sharif University of Technology, Iran  
Dr. Habibollah Asghari, Associate Professor, ACECR, Iran  
Dr. Zabih Ghasemlooy, Professor, Northumbria University, UK  
Dr. Saeed Ghazi Maghrebi, Associate Professor, ACECR, Iran

**Executive Editor:** Dr. Fatemeh Kheirkhah

**Executive Manager:** Mahdokht Ghahari

**Print ISSN:** 2322-1437

**Online ISSN:** 2345-2773

**Publication License:** 91/13216

**Editorial Office Address:** No.5, Saeedi Alley, Kalej Intersection., Enghelab Ave., Tehran, Iran,  
P.O.Box: 13145-799 Tel: (+9821) 88930150 Fax: (+9821) 88930157

E-mail: info@jst.ir, infojst@gmail.com

URL: jst.acecr.org

## Indexed by:

- |   |                  |
|---|------------------|
| - SCOPUS  | www.Scopus.com   |
| - Islamic World Science Citation Center (ISC)                     | www.isc.gov.ir   |
| - Directory of open Access Journals (DOAJ)                        | www.Doaj.org     |
| - Scientific Information Database (SID)                           | www.sid.ir       |
| - Regional Information Center for Science and Technology (RICEST) | www.ricest.ac.ir |
| - Magiran   | www.magiran.com  |

## Publisher:

Iranian Academic Center for Education, Culture and Research (ACECR)

This Journal is published under scientific support of  
Advanced Information Systems (AIS) Research Group and  
Telecommunication Research Group, ICTRC

## **Acknowledgement**

JIST Editorial-Board would like to gratefully appreciate the following distinguished referees for spending their valuable time and expertise in reviewing the manuscripts and their constructive suggestions, which had a great impact on the enhancement of this issue of the JIST Journal.

### **(A-Z)**

- Afsharirad, Majid, Kharazmi University, Tehran, Iran
- Agahi, Hamed, Islamic Azad University, Shiraz, Iran
- Azarkasb, Seyed Omid, K.N. Toosi University of Technology, Tehran, Iran
- Ebadati, Omid Mahdi, Kharazmi University, Tehran, Iran
- Kheirkhah, Fatemeh, ACECR, Tehran, Iran
- Nasersharif, Babak, K. N. Toosi University of Technology, Tehran, Iran
- Tanhaei, Mohammad, Ilam University, Ilam , Iran
- Taghipour, Mohammad, ACECR, Tehran, Iran
- Yaghoobi, Kaebeh, Ale Taha Institute of Higher Education, Tehran, Iran

## Table of Contents

- **Gated Fusion Transformer for English-Hindi Multimodal Translation..... 1**  
Priyanka Suram and Pramoda Patro
- **Transforming Public Healthcare Supply Chains: A Framework to Measure Efficiency of Heterogeneous Public Healthcare Supply Chains across Nation for Improving Drug Availability .....9**  
Abhishek Verma , Dr. Rekha Agarwal and Jitendra Singh
- **Maize Leaf Disease Detection using Deep Learning Models and a DenXNet Ensemble Model..25**  
Meghna Gupta, Sarika Jain and Manoj Kumar
- **Detecting Synchronized Hate Speech in Online Social Networks Via Social Synchrony and Ant Colony Optimization ..... 39**  
Shabana Nargis Rasool , Sarika Jain and Ajay Vikram Singh
- **Optimized Gradient Boosting for Financial Forecasting : A Data Driven Approach to Gold Stock Prediction ..... 50**  
Shreya Garag, Jossy George, Akhil M Nair, Bosco Paul Alapatt and Riya Baby
- **Enhancing Industrial Intraction Practices Through AI Based Parameter Modeling ..... 59**  
Ashwini Kumar, Rekha Agrawal and Archana Singh

# Gated Fusion Transformer for English-Hindi Multimodal Translation

Priyanka Suram<sup>1\*</sup> Pramoda Patro<sup>2</sup>

<sup>1</sup>.School of Computer Science and Artificial Intelligence, SR University, Warangal Telangana-506371, India

Received: 26 Jul 2025/ Revised: 04 Oct 2025/ Accepted: 02 Nov 2025

## Abstract

Machine translation is fundamental in closing the gap between different languages, especially in the areas of concern and expertise such as agriculture. With the increase of digital tool usages in the agricultural practice, such an accurate and context-sensitive translation is increasingly significant. Proper delivery of agricultural information, including farm methods, weather advisories, and crop suggestions is essential among farmers, farm laborers, policymakers and researchers. Nevertheless, typical text-based translation frameworks tend to be less than optimal because of uncertainty and a restricted knowledge of context. To address these shortcomings, the proposed study refers to Multimodal Machine Translation (MMT) to incorporate textual and visual information to enhance accuracy. Gated Fusion Transformer (GFT) model has been customized to the agricultural field so that the problem of ambiguity in contexts and inconsistencies in translation can be eliminated. Training and evaluation were done using the multilingual benchmark dataset known as FLORES-200. Two commonly employed measures of performance were used, i.e. BLEU and METEOR. The system under proposal produced a BLEU of 58.2; METEOR score of 0.71, a high level and contextually relevant translation indicator. Besides benchmarking the GFT model in agricultural terms, this work adds value to the research community by offering a basis on which future development of multimodal translation systems in low-resource settings with domain-specific applications may be done.

**Keywords:** Machine Translation; Domain Specific Translation; Multimodal Machine Translation; Multi Modal Fusion Mechanisms; Gated Fusion Transformer; Agricultural Translation.

## 1- Introduction

Machine Translation (MT) plays a critical role in cross-lingual communication, especially in specialized fields, such as agriculture, where integrating textual and visual data can significantly enhance meaning. Conventional text-based translation models frequently encounter semantic inconsistencies because of a lack of contextual depth. MMT aims to overcome these challenges by integrating multiple modalities, including images, structured data, and linguistic contexts, to improve translation accuracy.

Several studies have sought to enhance the MT performance through multimodal integration. However, existing approaches, such as mBART [1], M2M-100 [2], and T5 [3], primarily rely on pre-trained multilingual text models and fail to effectively utilize visual information for context enhancement. Previous research has explored multimodal fusion, but often lacks efficient fusion mechanisms to balance information from different modalities. Additionally, most research has focused on general-purpose

MT, neglecting the specialized requirements of domain-specific translation such as agriculture, which demands models adapted to unique terminology and contextual meanings. Although some studies have experimented with multimodal integration in medical and technical translations, there is a scarcity of research on agriculture-specific multimodal MT. Another major challenge is the absence of dedicated fusion mechanisms that can optimally integrate multimodal data without introducing redundancies. Current methods also fall short in quantifying the impact of different fusion techniques on translation quality, leaving a gap in the understanding of how multimodal interactions influence accuracy.

In this paper, a Gated Fusion Transformer (GFT) is introduced, which is a novel multimodal architecture specifically designed for domain-specific MT in agriculture. The key innovation of the GFT is its gated fusion mechanism, which effectively balances textual and visual features and addresses the limitations of existing models. The methodology includes detailed explanations of the GFT

model architecture, data pre-processing using the FLORES-200 dataset, and evaluation metrics, such as BLEU and METEOR.

The research analyzes Multimodal Machine Translation (MMT) performance within specific applications by translating English texts to Hindi for agricultural purposes. Text-only translation models face limitations in modern translation because they cannot utilize the rich contextual information provided by combined text and visual data. The research presents the Gated Fusion Transformer model (GFT) along with evaluating its translation capabilities against dominant models in the field. This work makes several notable contributions: (1) we introduce a Gated Fusion Transformer that adjusts the flow of text and image information with gating, (2) we suggest new fusion methods targeted at translating terms related to agriculture, (3) we show that our method has better results than current language translation models and (4) we are the first to comprehensively study multimodal machine translation in the agricultural domain. Comparison of GFT performance with five leading MT models: mBART, M2M-100, T5, GPT-4 [4], and Seq2Seq [5]. Proof from the study indicates that combining multiple linguistic modes enhances the quality of translated content related to agriculture.

This discussion assesses the effectiveness of various fusion processes and suggests areas for further improvement. It explores how multimodal fusion affects translation accuracy across domains and compares domain-specific multimodal models to general-purpose multilingual MT models. Furthermore, this study investigated the contributions of several fusion mechanisms to translation quality and optimal configuration.

In this we proposed a Gated Fusion Transformer (GFT) as an innovative solution to the problems encountered by classic text-based translation models in domain-specific applications. This paper emphasizes the important findings, contributions, and implications for future multimodal translation research, addressing a critical research need in English-to-Hindi MMT for agriculture.

Machine translation (MT) is critical for improving cross-linguistic communication. It has a big impact in specific domains such as agriculture. In these domains, textual, visual, and structured data all contribute to meaning. Traditional text-only trans-

lation models often fail to capture the contextual depth required in specialized domains, leading to semantic inconsistencies [6]. Recent advancements in Multimodal Neural Machine Translation (MMT) have addressed these limitations by integrating multiple modalities such as images, structured data, and linguistic context, thereby enhancing translation accuracy [7]. In this study, a Gated Fusion Transformer (GFT), a multimodal transformer-based architecture, was designed to efficiently integrate textual and visual information. The performance of the GFT

was compared against five leading MT models in the context of English-to-Hindi translation for the agriculture domain. This study addressed the following research questions:

1. How does multimodal integration enhance domain-specific translations?
2. Does the GFT model outperform the traditional and pretrained multilingual models?
3. What is the impact of the fusion mechanisms on translation quality?

The remaining of this paper is organized as follows. Section 2 literature review analyzes prior studies on MMT, fusion mechanisms, and domain-specific MT, identifying their limitations. Next the section 3 is methodology explains the GFT model architecture, data preprocessing (FLORES-200 dataset), and evaluation metrics (BLEU and METEOR). After that the section 4 is experiments and results presents a comparative performance analysis of GFT against mBART, M2M-100, T5, GPT-4, and Seq2Seq with Attention. In Section 5 (Discussion), the impact of the fusion mechanisms is evaluated and directions for future improvements are proposed. Section 6 (Conclusion) summarizes the key findings, contributions, and implications for future research on multimodal translations.

## 2- Related Work

Recent developments in machine translation and multimodal learning have led to the emergence of several state-of-the-art architectures, each employing unique strategies to improve translation quality. This section reviews key advances in neural machine translation (NMT) and multimodal MT.

According to the author [8][58] English to Hindi translation using multimodal concepts and monolingual data to improve the translation quality, the models are considered as multimodal neural machine translation, the dataset is Hindi Visual Genome 3, and the evaluation metrics are BLEU Score, Ribes Score, and AMFM Score. The authors [9] and [10] stated that gated fusion transformers have been explicitly utilized in multimodal machine translation (MMT) for English-Hindi tasks to improve translation quality by integrating textual and visual features, with clear experimental success reported in low-resource settings. However, no study has focused directly on the agricultural domain.

The features of the image were extracted using pre-trained visual encoders or advanced techniques such as latent diffusion models for the enhancement of synthetic data [11], [12]. These enhanced translations resolve ambiguities in low-resource settings such as English-Hindi. The advancement of neural machine translation (mBART) [13] is a multilingual auto-encoder-based translation model that leverages denoising pre-training for sequence-to-sequence

taks. M2M-100 [14] is a fully multilingual transformer model designed for more than 100 languages, eliminating dependency on English-centric translation pipelines. T5 [15] is a text-to-text transformer model that is trained for multiple NLP tasks, for machine translation utilizing transfer learning across language pairs.

Multimodal MT incorporates visual cues alongside text, leading to more accurate translation. Recent efforts in image-assisted translation, such as ViLBERT, CLIP, and Vision Transformers, have influenced the design of MMT architectures, including GFT [16]. Gated fusion mechanisms have been introduced to effectively balance textual and visual contributions [17]. [18], presents a bidirectional Recurrent Neural Network (RNN) encoder combined with a doubly attentive transformer decoder for multimodal translation. The model was fine-tuned on the Hindi Visual Genome dataset, which comprises 28,929 parallel English-Hindi sentences. The primary research gap addressed in this study is the scarcity of resources for Hindi translation and the need for improved multimodal feature integration. The proposed approach significantly advances state-of-the-art methodologies, achieving an impressive BLEU score of 42.47 on the evaluation set.

The review process joyful multiple metrics, incorporating BLEU, RIBES, and AMFM, to guarantee a comprehensive performance assessment. The creation of the Hindi Visual Genome dataset specifically for Hybrid-modal machine translation applications is a remarkable addition to Hybrid-modal translation search. With the use of this dataset, English parts can be self-operating translated into Hindi while taking related images into account and advancing contextual awareness. A challenge test set of 1,400 sections was included in the dataset, offering a reliable standard by which to assess Hybrid-modal translation models. This study highlights how significant it is to grow Hybrid-modal attribute incorporation to increase translation accuracy. The efficacy of this dataset for multimodal translation tasks was validated by trials that showed a BLEU score of 37.50 on the challenge test set. Recent developments underlined the need of combining textual and visual modalities for machine interpretation. Improved contextual alignment between textual and visual data has been shown by refined models on the Visual Genome dataset, improving rendering accuracy. BLEU ratings, which offer a normalize indicator of conversion quality, were a major component of the evaluation calculate employed in these examinations. To enhance the robustness of the model in practical appeal and optimize the fusion mechanisms, more examinations is necessary.

### 3- Experimental Setup

#### 3-1- Dataset Selection

Agriculture-related English-Hindi conversion were release from the FLORES-200 dataset [19], which offers high-quality parallel conversions for 200 languages. To ensure relevance for agricultural appeal, the dataset consists of domain-specific terms (such as crop diseases, irrigation techniques, and agricultural implements).

#### 3-2- Preprocessing

Several Technique were working to prepare the data for the model during preprocessing. Initially, the mBART tokenizer was used to computing the series, which helped to efficiently encode them. By doing this, the textual data was support to be roughly formatted for the model input. Apart from text processing, the image data was subjected to particular accommodation in order to conform to the model's specifications. To guarantee consistency across all samples, the photos were scaled to match the expect input measurements. Additionally, the image data was normalized to preserve uniformity and enhance the model's performance. Techniques for data amplification are applied to increase the dataset's stability. One such method is synonym replacement, which adds difference to the text by replacing specific words with their synonyms. Back-translation, which creates a difference of phrase patterns by translating a text into another language and then back again, was another enlargement skill used.

### 4- Methodology

A Gated Fusion Transformer (GFT) expands the classic transformer architecture by including a gated fusion module. This module adaptively weights text and image embeddings before sending them to the encoder, leading in improved domain-specific knowledge preservation. For Hybrid-modal machine translation, gated fusion transformers give a number of advantages, particularly for agricultural content. By merging textual and visual data, the translation process was Upgraded, becoming more Precise and contextually relevant. The Gated Fusion Transformer uses that both text and images contribute effectively. A feedforward network (FFN) operates as part of the representation refinement process.

$$\text{FFN} = \text{ReLU}((W_{\text{ffn}} * \text{Attention}) + b_{\text{ffn}}) \quad (6)$$

The learnable weight and bias term consists of  $W_{\text{ffn}}$  and  $b_{\text{ffn}}$ . a gate fusion technique to combine generated visual information with upgraded text data, which refines the Linguistic accuracy of translations [20]. This model grabs the connection between visuals and text, Consequent in a

more advanced understanding of agricultural phraseology and concepts, which are tough in this sector. In agricultural uses, the model has exhibited good accuracy and rates of up to 0.95, 0.92, and 0.94 in disease detection tasks. Enhanced BLEU scores in comparative studies demonstrate that the integration of multimodal data greatly improves translation performance [20]. Better object detection and classification results are achieved by the Gated Fusion Transformer's efficient handling of complex agricultural data, including fine-grained picture features and detailed textual descriptions [21]. Accurate translation of agricultural content, which frequently includes complex and varied information, requires robustness. On the other hand, although the Gated Fusion Transformer is highly effective in Hybrid-modal settings, there are still problems with securing the cable layer of the visual data that is created and the necessity for large training datasets, which may limit its use in settings with restricted resources [20]. The Gated Fusion Transformer (GFT) approach for Hybrid-modal machine translation merges textual and visual input to rise translation precision. The method starts with a visual encoder, which extracts image features using an attention mechanism to create a visual output while also grasping tough contextual information. Textual data is also encoded positionally, ensuring that the model honors word order. The Gated Fusion Module merges both textual and visual characteristics, and the fusion process is directed by the equation:

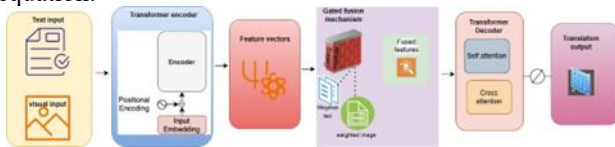


Fig. 1. Gated Fusion Transformer

The Gated Fusion Transformer (GFT) figure 1 stands as an advanced architectural design which enhances translation quality through the fusion of visual information into text-based machine translation systems. The model requires two main inputs which are the text and image data. The language input receives embedding processing after tokenization and image processing involves the application of visual feature extractors through pre-trained CNN or ViT before feature extraction. The features are jointly aligned with text features to achieve dimensional compatibility between elements.

During Transformer Encoder in figure 1, text embeddings receive positional encodings for maintaining word order details. Self-attention together with feed-forward layers operate on the inputs in an encoder to generate contextual feature vectors. The core innovation of GFT model involves the Gated Fusion Mechanism because it receives text and visual features together. A gating function based on sigmoid activation governs the amount of visual information that

will contribute to the process. A dynamic gating function within the system determines how  $X$  is transformed into query  $Q$ , Key  $K$ , and Value  $V$  representation is mechanism aims to improve translation outcomes while avoiding noise contamination.

#### 4-1- Detailed Architecture Components

##### Visual Feature Extractor

Input : Image  $I \in \mathbb{R}^{(H \times W \times 3)}$  Process :

- ResNet - 50 / ViT feature extraction
- Global Average Pooling

Output : Visual features  $V \in \mathbb{R}^{d_v}$

##### 1. Text Encoder

Input : Source text tokens  $S = \{s_1, s_2, \dots, s_n\}$  Process :

- Embedding layer :  $E_s = \text{Embed}(S)$
- 
- Positional encoding :  $P_s = \text{PosEnc}(E_s)$
- Multi-head self-attention layers

Output : Text features  $T \in \mathbb{R}^{(n \times d_t)}$

##### Gated Fusion Mechanism (Proposed Innovation)

Algorithm 1: Gated Fusion Process

Text features  $T$ , Visual features  $V$  Fused features  $F$  Concatenate features:  $C \leftarrow [T; V_{\text{expanded}}]$  Compute gate weights:

$$G_t = \sigma(W_{gt} \cdot C + b_{gt})$$

$$G_v = \sigma(W_{gv} \cdot C + b_{gv})$$

Apply gating:

$$F_t = G_t \odot T$$

$$F_v = G_v \odot V_{\text{expanded}}$$

Combine:  $F = F_t + F_v$  Layer

normalization:  $\text{LayerNorm}(F)$

2. Transformer Decoder

- Masked self-attention
- Cross-attention with fused features
- Feed-forward networks
- Residual connections
- 
-

## 4-2- Training Algorithm

Algorithm 2: GFT Training process

Dataset  $D = \{(S_i, I_i, T_i)\}$  Parameters:  $\theta = W_{enc}, W_{dec}, W_{gate}, W_{ffn}$  Initialize parameters  $\theta$  randomly each epoch each batch  $B$  in  $D$  Extract visual features:

$V \leftarrow \text{VisualEncoder}(I)$

Encode text:

$H_s \leftarrow \text{TextEncoder}(S)$  Apply gated fusion:

$F \leftarrow \text{GatedFusion}(H_s, V)$

## 4-3- Innovation Highlights

### Novel Contributions

1. Adaptive Gating Strategy: Dynamic weight assignment based on contextual relevance
2. Domain-Specific Fusion: Agricultural terminology-aware integration
3. Multi-Scale Visual Processing: Hierarchical feature extraction
4. Cross-Modal Attention: Bidirectional information flow

## 4-4- Architectural Novelty

- Learnable gate parameters for modality weighting
- Context-aware fusion avoiding information redundancy
- Agricultural domain vocabulary enhancement
- Robust handling of low-resource language pairs

## 5- Results and Comparative Analysis

This part provides performance comparisons between the Gated Fusion Transformer (GFT) model and existing top machine translation models currently available. Evaluation relied on BLEU and METEOR scores to calculate translation accuracy through measuring the shared content between generated output and reference translations. The evaluation demonstrates how multi-modal fusion powers translation improvement when analyzing the agricultural domain.

The evaluation included well-recognized metrics from machine translation assessment to provide both a thorough and trustworthy assessment of performance. The assessed BLEU score evaluates translation quality through its assessment of the accurate usage of n-grams between generated text and reference materials to detect lexical similarities. The BLEU score is calculated by using below equation.

$$\text{BLEU} = \text{BP} \times \exp \sum_{n=1}^N \frac{1}{n} \log p_n \quad (9)$$

where:

- $\text{BP}(\text{Brevity Penalty}) = \min(1, \exp(1 - r))$

5-1-1.1.  $r$  = reference length

5-1-1.2.  $c$  = candidate length

5-1-1.3.  $p_n$  = modified  $n$ -gram precision

5-1-1.4.  $w_n$  = uniform weights =  $\frac{1}{n}$

Additionally, the Metric for Evaluation of Translation with Explicit Ordering (METEOR) offers a more nuanced assessment by incorporating factors such as synonymy, stemming, and word order, providing a holistic measure of translation accuracy. These metrics collectively facilitated a robust evaluation of the system's effectiveness in producing high-quality translations.

METEOR Score is determined by using below formula

$$\text{METEOR} = \frac{(1 - \beta) \cdot P \cdot R}{\alpha P + (1 - \alpha)R} \quad (10)$$

Where:

- $P(\text{Precision}) = \frac{|\text{matched unigrams}|}{|\text{candidate unigrams}|}$
- $R(\text{Recall}) = \frac{|\text{matched unigrams}|}{|\text{reference unigrams}|}$
- $\alpha, \beta$  = tuning parameters

Table 1: Comparison of Translation Models Based on Bleu Scores

NO	Dataset	Language Pair	Model	BLEU Score
1	wmt 2014	English to French	SMT+iterative backtranslation [22]	26.22
2	wmt 2016	English to French	Delight [23]	40.5
3	wmt 2014 wmt2016	German to English English to German	SMT+iterative backtranslation [22]	17.43 23.05
4	wmt 2016	German to English	Attentional encoder decoder+ BPE [24]	38.6
5	wmt 2016	German to English	Linguistic Input features [25]	28.7
6	wmt 2016	German to English	Exploiting Mono at Scale [26]	47.5
7	wmt 2014	French to English	SMT+iterative backtranslation [22]	17.43
8	wmt 2016	English to Czech	Attentional encoder decoder+ BPE [24]	25.8
9	wmt 2016	Czech to english	Attentional encoder decoder+ BPE [24]	25.8

The various translation models and different language pairs by using WMT-2014 and WMT-2016 dataset the performance of BLEU Score is describing in Table I. For the English to French Language pair, the SMT+iterative back translation model, the BLEU Score is 26.22 on the WMT dataset, and the model Delight BLEU Score is 40.5 on dataset WMT-2016 exhibited a significant enhancement in the quality of translation. For the German-to- English language pair, the SMT+iterative back translation model BLEU Score is 17.43 on the WMT 2014 dataset and on the

WMT- 2016 dataset, showing notable enhancements in the quality of translation. The Attentional encoder decoder+BPE model performs well for German-to-English translation with a BLEU Score of 38.6 on the WMT 2016 dataset. The Linguistic input features model BLEU Score is 28.7 and Exploiting Mono at Scale model achieves the highest BLEU Score of 47.5 indicating excellent translation quality of the language pair German to English. The SMT+iterative back translation model also scores 17.43 for the french to English language pair on the WMT 2014 dataset. The Attentional encoder decoder+BPE model achieves a BLEU Score of 25.8 for English to Czech and Czech to English translation with the WMT-2016 dataset, reflecting the performance. The performance of translation models with different Languagepairs and datasets showed significant improvements in certain models and language pairs. Translation quality was evaluated using the BLEU and METEOR scores. The results are summarized below.

Table 2: comparison of models with accuracy

Model	BLEU Score	METEOR Score
GFT	58.2	0.71
mBART	54.6	0.68
M2M-100	52.3	0.65
T5	50.7	0.63
GPT-4	48.9	0.60
Seq2Seq	45.2	0.58

The experimental results in Table II reveal several key insights regarding the performance of different models in English-to- Hindi multimodal machine translation for the agricultural do- main. The Gated Fusion Transformer (GFT) model consistently outperformed the other evaluated models and achieved the highest BLEU and METEOR scores. This superior performance underscores the effectiveness of its gated fusion mechanism in integrating multimodal contexts, thereby enhancing context retention and producing more precise and semantically relevant translations. By dynamically balancing textual and visual in- formation, the GFT model mitigates ambiguities and ensures accurate translation of domain-specific terminology.

In contrast, mBART and M2M-100 demonstrated competitive performance, largely because of their extensive multilingual pre- training. However, their lack of explicit multimodal fusion capa- bilities limits their ability to effectively translate domain-specific terminology, particularly in cases where textual context alone is insufficient. Similarly, general-purpose models, such as T5 and GPT-4, exhibit suboptimal results in domain-specific translation despite their state-of-the-art performance in broader natural language processing (NLP) tasks. The absence of mechanisms to incorporate visual context leads

to reduced contextual accuracy, particularly for specialized agricultural terms. Furthermore, the traditional Seq2Seq model, which relies solely on textual input, struggles to capture domain-specific nuances, resulting in the lowest performance among the evaluated models.

The impact of multimodal fusion is evident in the superior translation quality achieved by the GFT. The model's ability to seamlessly integrate textual and visual features enables it to resolve textual ambiguities by using complementary visual information. Moreover, it effectively translates domain-specific terms by leveraging both modalities and demonstrates adapt- ability to low-resource settings by utilizing supplementary infor mation from the images. This capability is particularly crucial in specialized domains, where textual data alone may be insufficient for accurate translation.

Despite these advancements, several avenues for future re- search and optimization remain. Expanding the training cor- pus with additional agricultural datasets can further enhance the robustness and generalizability of the model. In addition, refining fusion mechanisms to optimize performance across di- verse domains can strengthen multimodal translation capabilities. Exploring hybrid fusion techniques that combine gated fusion with attention-based enhancements presents another promising direction for improving the translation accuracy and contextual understanding. These refinements have the potential to further advance multimodal machine translation, ensuring more effective and domain-specific translations.

Table 3: score comparison of multimodal machine translation models

Dataset	Model	BLEU
Hindi Visual Genome	ViTA [27]	44.6
Multi30k, flickr	opus-mt-te-base-gnw-gnw [28]	32.2
Multi30k	VAG-NMT [29]	31.6
Multi30k	ERINE-UniX2 [30]	49.3
Multi30k	IKD-MMT [31]	41.28
Multi30k	DCCN [32]	39.7
Multi30k	caglayan [33]	39.4
Multi30k	Gumbel-Attention MMT [34]	39.2
Multi30k	multimodal transformer [35]	38.7
Multi30k	ImagiT [36]	38.4
Multi30k	del+obj [37]	38
Multi30k	VMMTF [38]	37.6
Multi30k	IMGD [39]	37.3
Multi30k	NMTSRC+IMG [40]	37.1
Multi30k	VAG-NMT [29]	31.6
Multi30k	PS-KD [41]	32.3

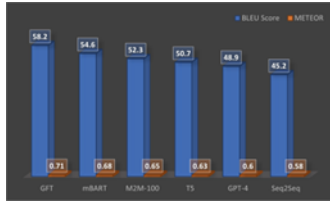


Fig. 2. Results analysis of accuracy on multimodal machine translation

## 6- Conclusion

This study demonstrates the effectiveness of the GFT for English-to-Hindi multimodal translation in the agricultural domain. By leveraging gated fusion mechanisms, the GFT achieves superior BLEU and METEOR scores, underscoring its practical applicability for domain-specific MT tasks. Future research should focus on scaling GFT to larger datasets, fine-tuning additional agricultural data, and extending its application to other multimodal domains.

## References

- [1] Navarro A, Casacuberta F. Exploring multilingual pretrained machine translation models for interactive translation. In Proceedings of Machine Translation Summit XIX, Vol. 2: Users Track 2023 Sep (pp. 132-142).
- [2] Nimma D, Srinivas VS, Gupta SS, Nair H, Devi RL, Bala BK. Comparative Analysis of Deep Learning Models for Multilingual Language Translation. In 2024 8th SLAAI International Conference on Artificial Intelligence (SLAAI-ICAI) 2024 Dec 18 (pp. 1-6). IEEE.
- [3] Zaki MZ. Revolutionising Translation Technology: A Comparative Study of Variant Transformer Models—BERT, GPT and T5. Computer Science and Engineering—An International Journal. 2024;14(3):15-27.
- [4] Raunak V, Sharaf A, Wang Y, Awadallah HH, Menezes A. Leveraging GPT-4 for automatic translation post-editing. arXiv preprint arXiv:2305.14878. 2023 May 24.
- [5] Barrault L, Chung YA, Meglioli MC, Dale D, Dong N, Duquenne PA, Elsahar H, Gong H, Heffernan K, Hoffman J, Klaiher SeamlessM4T: Massively Multilingual Multimodal Machine Translation. arXiv preprint arXiv:2308.11596. 2023 Aug 22.
- [6] Bahdanau D, Cho K, Bengio Y. Neural machine translation by jointly learning to align and translate. arXiv preprint arXiv:1409.0473. 2014 Sep 1.
- [7] Caglayan O, Aransa W, Wang Y, Masana M, Garc'ia-Mart'inez M, Bougares F, Barrault L, Van de Weijer J. Does multimodality help human and machine for translation and image captioning?. arXiv preprint arXiv:1605.09186. 2016 May 30.
- [8] Laskar SR, Khilji AF, Pakray P, Bandyopadhyay S. Multimodal neural machine translation for English to Hindi. In Proceedings of the 7th Workshop on Asian Translation 2020 Dec (pp. 109-113).
- [9] Hatami A, Banerjee S, Arcan M, Chakravarthi B, Buitelaar P, Mccrae J. English-to-low-resource translation: A multimodal approach for hindi, malayalam, bengali, and hausa. In Proceedings of the Ninth Conference on Machine Translation 2024 Nov (pp. 815-822).
- [10] Singh TD, Bonet CE, Bandyopadhyay S, van Genabith J. Proceedings of the First Workshop on Multimodal Machine Translation for Low Resource Languages (MMTLRL 2021). In Proceedings of the First Workshop on Multimodal Machine Translation for Low Resource Languages (MMTLRL 2021) 2021 Sep.
- [11] Dash A, Gupta HR, Sharma Y. Bits-p at wat 2023: Improving indic language multimodal translation by image augmentation using diffusion models. In Proceedings of the 10th Workshop on Asian Translation 2023 Sep (pp. 41-45).
- [12] Laskar SR, Singh RP, Pakray P, Bandyopadhyay S. English to Hindi multi-modal neural machine translation and Hindi image captioning. In Proceedings of the 6th Workshop on Asian Translation 2019 Nov (pp. 62-67).
- [13] Liu Y, Gu J, Goyal N, Li X, Edunov S, Ghazvininejad M, Lewis M, Zettlemoyer L. Multilingual denoising pre-training for neural machine translation. Transactions of the Association for Computational Linguistics. 2020 Nov 1;8:726-42.
- [14] Fan A, Bhosale S, Schwenk H, Ma Z, El-Kishky A, Goyal S, Baines M, Celebi O, Wenzek G, Chaudhary V, Goyal N. Beyond english-centric multilingual machine translation. Journal of Machine Learning Research. 2021;22(107):1-48.
- [15] Raffel C, Shazeer N, Roberts A, Lee K, Narang S, Matena M, Zhou Y, Li W, Liu PJ. Exploring the limits of transfer learning with a unified text-to-text transformer. Journal of machine learning research. 2020;21(140):1-67.
- [16] Su W, Zhu X, Cao Y, Li B, Lu L, Wei F, Dai J. Vi-bert: Pre-training of generic visual-linguistic representations. arXiv preprint arXiv:1908.08530. 2019 Aug 22.
- [17] Tan H, Bansal M. Lxmert: Learning cross-modality encoder representations from transformers. arXiv preprint arXiv:1908.07490. 2019 Aug 20.
- [18] Gain B, Bandyopadhyay D, Ekbal A. IITP at WAT 2021: System description for English-Hindi multimodal translation task. arXiv preprint arXiv:2107.01656. 2021 Jul 4.
- [19] Goyal N, Gao C, Chaudhary V, Chen PJ, Wenzek G, Ju D, Krishnan S, Ranzato MA, Guzman F, Fan A. The flores-101 evaluation benchmark for low-resource and multilingual machine translation. Transactions of the Association for Computational Linguistics. 2022 May 4;10:522-38.
- [20] Yuan J, Shi X, Niu Y, Niu Y, Wang X. Multimodal Machine Translation with Fusion of Generated Visual Information. In International Conference on Computer Engineering and Networks 2023 Nov 3 (pp. 150-156). Singapore: Springer Nature Singapore.
- [21] Lu Y, Lu X, Zheng L, Sun M, Chen S, Chen B, Wang T, Yang J, Lv C. Application of multimodal transformer model in intelligent agricultural disease detection and question-answering systems. Plants. 2024 Mar 28;13(7):972.
- [22] Artetxe M, Labaka G, Agirre E. Unsupervised statistical machine translation. arXiv preprint arXiv:1809.01272. 2018 Sep 4.
- [23] Mehta S, Ghazvininejad M, Iyer S, Zettlemoyer L, Hajishirzi H. Delight: Deep and light-weight transformer. arXiv preprint arXiv:2008.00623. 2020 Aug 3.
- [24] Sennrich R, Haddow B, Birch A. Edinburgh neural machine translation systems for WMT 16. arXiv preprint arXiv:1606.02891. 2016 Jun 9.
- [25] Sennrich R, Haddow B. Linguistic input features improve neural machine translation. arXiv preprint arXiv:1606.02892. 2016 Jun 9.

- [26] Wu L, Wang Y, Xia Y, Qin T, Lai J, Liu TY. Exploiting Aug 24. monolingual data at scale for neural machine translation. In Proceedings of the 2019 Conference on Empirical Methods in Natural Language Processing and the 9th International Joint Conference on Natural Language Processing (EMNLP-IJCNLP) 2019 Nov (pp. 4207-4216).
- [27] Gupta K, Gautam D, Mamidi R. ViTA: Visual-linguistic translation by aligning object tags. arXiv preprint arXiv:2106.00250. 2021 Jun 1.
- [28] Tiedemann J. The tatoeba translation challenge—realistic data sets for low resource and multilingual MT. arXiv preprint arXiv:2010.06354. 2020 Oct 13.
- [29] Zhou M, Cheng R, Lee YJ, Yu Z. A visual attention grounding neural model for multimodal machine translation. arXiv preprint arXiv:1808.08266. 2018
  
- [30] Shan B, Han Y, Yin W, Wang S, Sun Y, Tian H, Wu H, Wang H. Ernie-unix2: A unified cross-lingual cross-modal framework for understanding and generation. arXiv preprint arXiv:2211.04861. 2022 Nov 9.
- [31] Peng R, Zeng Y, Zhao J. Distill the image to nowhere: Inversion knowledge distillation for multimodal machine translation. arXiv preprint arXiv:2210.04468. 2022 Oct 10.
- [32] Lin H, Meng F, Su J, Yin Y, Yang Z, Ge Y, Zhou J, Luo J. Dynamic context-guided capsule network for multimodal machine translation. In Proceedings of the 28th ACM international conference on multimedia 2020 Oct 12 (pp. 1320-1329).
- [33] Sulubacak U, Caglayan O, Gro'nroos SA, Rouhe A, Elliott D, Specia L, Tiedemann J. Multimodal machine translation through visuals and speech. *Machine Translation*. 2020 Sep;34:97-147.
- [34] Liu P, Cao H, Zhao T. Gumbel-attention for multi-modal machine translation. arXiv preprint arXiv:2103.08862. 2021 Mar 16.
- [35] Yao S, Wan X. Multimodal transformer for multimodal machine translation. In Proceedings of the 58th annual meeting of the association for computational linguistics 2020 Jul (pp. 4346-4350).
- [36] Long Q, Wang M, Li L. Generative imagination elevates machine translation. arXiv preprint arXiv:2009.09654. 2020 Sep 21.
- [37] Ive J, Madhyastha P, Specia L. Distilling translations with visual awareness. arXiv preprint arXiv:1906.07701. 2019 Jun 18.
- [38] Calixto I, Rios M, Aziz W. Latent variable model for multi-modal translation. arXiv preprint arXiv:1811.00357. 2018 Nov 1.
- [39] Calixto I, Liu Q, Campbell N. Incorporating global visual features into attention-based neural machine translation. arXiv preprint arXiv:1701.06521. 2017 Jan 23.
- [40] Calixto I, Liu Q, Campbell N. Doubly-attentive decoder for multi-modal neural machine translation. arXiv preprint arXiv:1702.01287. 2017 Feb 4.
- [41] Kim K, Ji B, Yoon D, Hwang S. Self-knowledge distillation with progressive refinement of targets. In Proceedings of the IEEE/CVF international conference on computer vision 2021 (pp. 6567-6576).



# Transforming Public Healthcare Supply Chains: A Framework to Measure Efficiency of Heterogeneous Public Healthcare Supply Chains across Nation for Improving Drug Availability

Abhishek Verma<sup>1\*</sup>, Dr. Rekha Agarwal<sup>1</sup>, Jitendra Singh<sup>2</sup>

<sup>1</sup>.AIIT, Amity University, Noida, Uttar Pradesh

<sup>2</sup>.Centre For development of Advanced Computing, Delhi

Received: 25 Jul 2025/ Revised: 13 Oct 2025/ Accepted: 02 Nov 2025

## Abstract

Health in Indian scenario is a state subject which means that states usually use their independent respective IT systems based on their specific needs and requirements. This brings a big challenge in terms of diversified nomenclatures used in across Indian states and Union Territories (UTs). Centralized data analysis is required by central agencies like Ministry of Health and Family Welfare (MoHFW) and the National Health Systems Resource Centre (NHSRC) for performance monitoring and policy making. This diversified nomenclature poses a significant hindrance in the process. The aggregation, standardization, deduplication, and visualization of data from these heterogeneous sources is both complex and resource intensive. This paper presents solution for the above challenges and propose a comprehensive framework for analyzing data from heterogeneous sources related to supply chain of drugs and vaccines. The framework incorporates fuzzy logic-based algorithms for deduplication of drug and vaccine nomenclature and supports real-time data analysis through the use of Key Performance Indicators (KPIs). It further enables centralized monitoring and decision-making via a built-in visualization layer, accessible to stakeholders at multiple administrative levels. While the framework has been tailored to the Indian public health context, its modular design makes it broadly applicable to other domains requiring integration of diverse data sources for strategic planning and policy implementation. The use of open-source technologies for development of various configurable and integrated layers like ETL, Deduplication, Standardization and Visualization layers encompassing into a single framework ensuring cost effectiveness in delivering the end-to-end solution makes it a novel and impactful for adoption specially in resource constrained environments.

**Keywords:** Public Health Informatics; Indian Health Framework; Deduplication; Digital Health; Drugs and Vaccines Availability; Essential Drugs and Vaccines; Extraction Transformation and loading (ETL); Public Health; Supply Chain; Warehouse.

## 1- Introduction

Health is a state subject in India, with 36 States and Union Territories (UTs) each using independent systems with unique nomenclatures. [1]described India as a "Nation within Nations" due to its vast population. Population of each state is comparable to that of many countries, which

makes the implementation of health initiatives really challenging. Effective health improvement requires studying prevalent health systems, disease burden, and risk mitigation.

The Global Burden of Disease (GBD) study highlighted the need for consistent health systems across states [1]. [2] emphasized the importance of state-level health investments and the federal government's role in encouraging such initiatives and increasing public

---

✉ Corresponding Author  
abhishekverma@cdac.in

healthcare investment. For effective informed decision-making, standardized data is essential for central agencies like National Health Systems Resource Centre (NHSRC) and the Ministry of Health and Family Welfare (MoHFW). They also require effective visualization on standardized data for analysis and further use in the centralized health system.

India's health system is divided into several major programs, with each state having its own IT-enabled systems to address health issues [3]. Reports indicate a high dependence on central agencies for smooth implementation of health services. (Atreya, 2020) noted that deficiencies in technical strength available with states were highlighted during pandemic, emphasising the role of central government in providing expertise, funds, and policy guidance.

This paper proposes a comprehensive framework for central agencies for Extraction, Transformation, and Loading (ETL) of diverse health data from various sources with a aim to make data usable and ready for analysis at central level along with providing visualization for analysis to them for effective decision making.

The objective is to design and develop a framework for handling large health data for drug and vaccine availability in Indian context. The authors propose utilizing open-source technologies to ensure cost effective and scalable solution for ETL, deduplication, standardization, and visualization, facilitating data analysis for central agencies through Key Performance Indicators (KPIs).

This novel framework involves six components for an end-to-end solution, from remote data extraction to visualization, assisting users in making informed decisions. The implementation uses open-source technologies like J2EE, jQuery, and JavaScript to reduce costs. Each component is detailed in the following sections of this paper

## 2- Literature Review

[4] describe ETL systems as "resource-intensive, costly, and highly complex," accounting for approximately 70% of the workload in data warehouse development. They highlight the lack of systematic methodologies and supporting tools to meet ETL quality requirements, noting that most implementations rely heavily on developer experience.

[5] and [6] describe ETL (Extract, Transform, Load) as a fundamental process in data warehousing. Extraction involves gathering data from diverse sources; Transformation includes cleaning and restructuring the data for analysis; and Loading refers to inserting the processed data into the target system such as a database, data mart, data lake, or warehouse.

In the ELT approach, data is loaded into the target system before transformation occurs, allowing transformations to

leverage the processing capabilities of modern data warehouses. Sivabalan et al. (2021) describe ELT as a process of collecting data from APIs or SQL/NoSQL sources, followed by validation, transformation, and storage—all scheduled systematically [7].

[8] states that ECL-TL method reduces coupling between these stages and enhances adaptability for complex transformation scenarios.

[9] cites various challenges of the ETL process like high velocity data, strive for low latency, security etc and discusses various strategies for addressing these challenges [10] , [11] ETL remains critical for integrating and processing data before analysis. Variants such as ELT (Extract, Load, Transform) and ECL-TL (Extract, Clean, Load – Transform, Load) have emerged to address challenges in traditional ETL pipelines –.

In the healthcare context, Dixit et al. (2019) review the supply chain of drugs and vaccines, emphasizing the importance of IT-based systems to improve efficiency and reliability [12]. Atinga et al. (2019) explore supply chain gaps in Ghana, recommending improvements in human resources, technical infrastructure, and IT-based systems to enhance performance [13].

[14] addressed the scenario of the IFA supplementation program under the Anemia Mukht Bharat (AMB) program, wherein they refer to the problems related to the supply chain of drugs and vaccines and calls for the requirement of supply chain review framework for performance monitoring through measurement of defined Key Performance Indicators

A survey of software used across Indian states and Union Territories revealed varying practices for procurement and distribution of pharmaceuticals [15]. The study aimed to identify a solution that meets regional requirements using available software resources.

Popular ETL tools were reviewed for their applicability in healthcare data integration:

**SAS Enterprise Guide (EG) 7.1** is a Windows-based application providing GUI-driven SAS functionality, metadata storage, and automation features. However, it has limitations in consuming web services (SOAP/REST), deduplication, and advanced visualization [16] , [17] , [18]. **Microsoft SSIS** supports integration from XML, flat files, and RDBMS sources. It offers built-in transformations and a graphical design interface but lacks robust dashboard visualization capabilities [19].

**Informatica PowerCenter** is noted for its robust ETL features, automated testing, and support for zero-downtime operations, though it comes with premium licensing and optional add-ons [20].

**Pentaho Data Integration (PDI)**, formerly Kettle, is Java-based and supports reporting and OLAP through additional subprojects. Enterprise editions are available [21] , (<https://en.wikipedia.org/>, 2019).

**IBM DataStage** is recognized as a leading data integration tool enabling the development and execution of data movement and transformation jobs [23].

**Adeptia** focuses on reducing integration complexity, offering real-time data access and user-defined transformations for business productivity (Adipati, 2022a, 2022b).

**Talend** provides ETL solutions for integration, quality control, and big data, with products like Talend Open Studio offering an open-source environment for pipeline management [26] [27].

**CloverETL** supports automation, scheduling, and integration through a J2EE-compatible platform with SOAP/HTTP APIs for control [28].

**Hevo Data** emphasizes ease of use, automation, and pricing based on usage. It facilitates integration from various sources into warehouses for analytics readiness (Hevo-Features, 2021).

**Oracle Data Integrator** is positioned as a comprehensive integration solution that integrates seamlessly with Oracle's enterprise suite [30].

(Khan & Hoque, 2015;2017), [32] and [33] underscore the relevance of ETL tools in healthcare systems –, [10], [34], [35], [36] shares insight about the large resources that are consumed during the ETL processes. Comparative analysis of seven tools across 33 different criteria are provided by (Biplob et al., 2018).

### Summary and Research Gap

The literature reveals a consensus on the complexity and centrality of ETL processes in data warehousing, particularly in healthcare applications. Existing tools vary in functionality, integration capabilities, cost, and user experience. Despite the availability of numerous ETL solutions, there is a lack of customizable, open-source platforms tailored for Indian healthcare supply chain management needs.

### Proposed Framework

Based on the literature review, this study proposes an open-source, configurable framework designed for aggregating data from all Indian states and Union Territories. The framework supports data cleaning, standardization, centralized storage, and a visualization layer for decision-makers. It aims to bridge the gap between available ETL solutions and the specific needs of regional health departments.

## 3- Proposed Solution and Methodology

The following components are envisaged by the proposed framework:

**Component 1** represents the remote repositories of data where IT-based systems are in place, these can be understood as the respective Indian states and union territories that have their IT-based systems for the supply chain of drugs and vaccines. These states and UTs have their respective rulesets and nomenclature as well that are being used in their respective systems. The respective systems work well to satisfy the needs of respective states / UTs.

**Component 2** represents the ETL Layer. It is proposed to be configurable as ETL or ELT or ETLT as per the requirements of the KPIs under consideration.

**Component 3** represents the Standardization Layer. This needs to be adaptive to handle the needs of all Indian states and UTs. It can be understood as the mapping process to ensure common nomenclature for drugs/vaccines/health facilities/suppliers etc.

**Component 4** represents the Deduplication Layer. The authors propose the ruleset specific to the drugs and vaccine's nomenclature and corresponding weights. Multiple levels of fuzzy logic functions are included in it for predicting the duplicity chances and then presenting the probability of 2 entities being duplicates or not. The final Decision for the removal of such entities is left to the central users, as of now. However automatic removal can also be configured in this framework.

**Component 5** represents the Visualization Layer. Support for multiple and configurable options for visualization using libraries from Google Charts, Bootstrap, Hi-charts, etc. is proposed for this component.

**Component 6** represents the final users for whom the system will generate the visualizations based on the required Key Performance Indicators (KPIs). This can be understood as the States / Union Territories / Central Agencies like NHSRC, CHI, MoHFW, etc.

The following figure presents the components of the proposed framework.

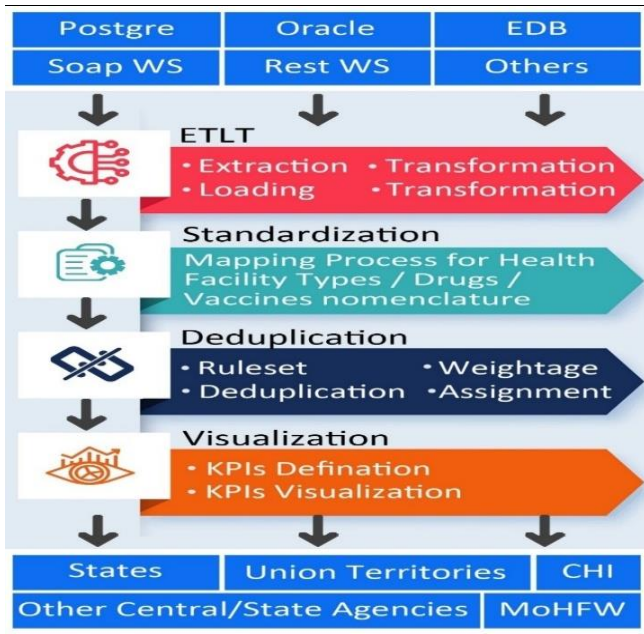


Figure 1: Components of the Proposed Framework.

[37] in his work mentions that data errors increase once the integration of data across the system is sought due to heterogeneity in the data, He outlines the value of clean and quality data and stresses the role of technology in providing quality data. In the health systems, data formats, and nomenclatures vary significantly between states and union territories. The states / UTs have their IT-based solutions for Health Systems for the distribution of drugs and vaccines. A detailed study of such systems used in India was carried out by the authors. The systems have their own databases which store the data of specific states / UTs [15]. Although the systems were similar the data across the systems is heterogeneous both in terms of structure and nomenclature. The problem of heterogeneity of the data is resolved by the pre and post-processing components and the standardization component of the proposed framework. The various components of the proposed framework are described in the following sections.

**3.1 ETLT Component:**

The authors adopted a configurable approach wherein the ETL can be configured as ETL ELT or ETLT depending on a case-to-case basis. The proposed 5 Layered Approach as follows:

**Layer 1:** Remote Layer – represents remote data repositories like Postgres, EDB, Oracle, SQL Server, MySQL, etc.

**Layer 2:** Extraction Layer – represents the extraction part. The extraction can be through REST-based Web Service

APIs, SOAP-based Web Service APIs, direct DB connection, Stub-based DB connection, etc.

**Layer 3:** Transformation Layer –This layer represents pre-processing requirements. This can be an optional layer that is used for pre-processing for cleaning of main repository/table, versioning, DSS creation, or for implementation of misc. logic which may be required to be performed before loading.

**Layer 4:** Loading Layer – represents loading activity. The loading can be simple loading in which data is simply pushed into the repository as it is fetched.

**Layer 5:** Transformation Layer – This layer represents post-processing requirements that may include data standardizations, partitioned tables, multi-table inserts, and implementation of misc. logic which may be required to be performed after loading.

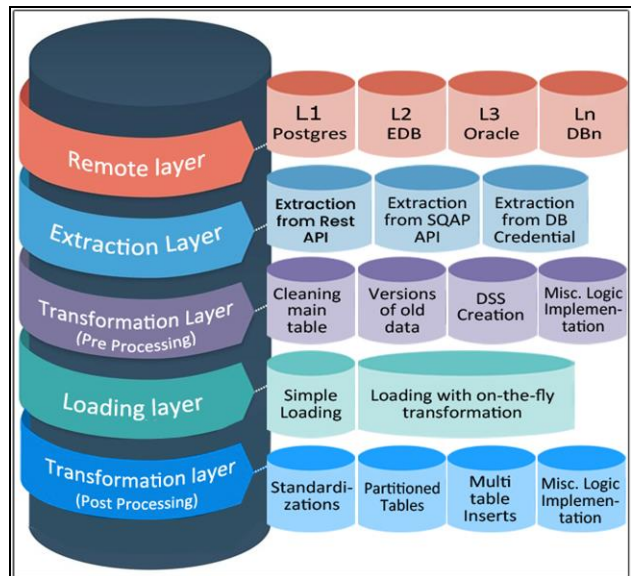


Figure 2: Proposed Architecture for ETL Component.

The Authors designed a utility system based on the designed framework which consists of screens for configuration of remote locations, configuration of jobs on those locations, and provision of one-time, manual, or scheduled execution of created jobs. The Proposed ETL Solution consists of the following steps.

Step 1: Configuration for connection and extraction (State / UT Configuration)

- i. When the Destination DB details can be provided to the utility
- ii. When the Destination DB details cannot be provided to the utility, Through Web Services (APIs)

The normal flow is presented in the following figure:

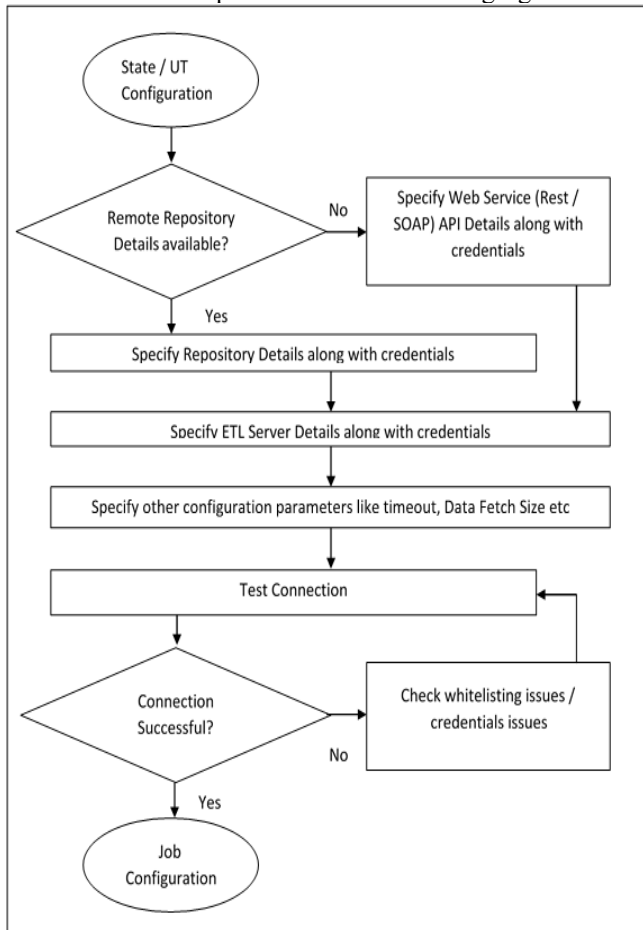


Figure 3: Configuration for connection and extraction (State / UT Configuration)

Step 2: Creation of Jobs for states for the ETL Process which includes.

- i. Select Fetch Query [Extraction]
- ii. Preprocessing Activity [Transformation] [Optional Transformation BEFORE Loading. It can be used for the creation of history tables / DSS tables or the creation of versions of past data and cleaning of the main table.]
- iii. Insert into the Central Warehouse [Loading]
- iv. Post Processing Activity [Transformation] [Optional Transformation AFTER Loading. It can be used for standardization via updating of codes from the mapping tables of the centralized Repository. It can also be used for creating partitioned tables or different tables based on some Key parameters like location etc.]

The normal flow is presented through the following figure:

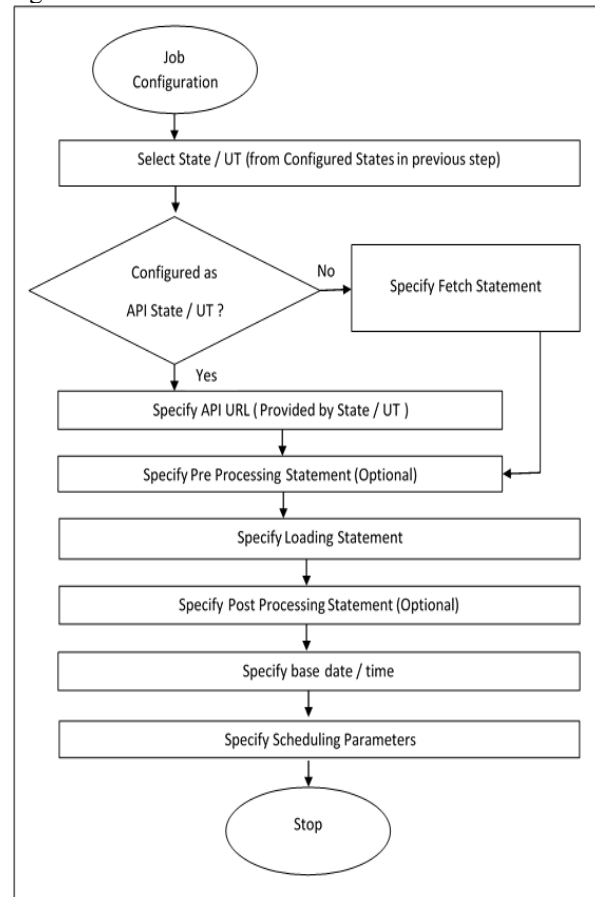


Figure 4: Configuration for ETL Jobs.

The authors found the Extraction Transformation Load Transformation (ETLT) approach most useful.

### 3.2 Standardization Component:

Different states / UTs have implemented different systems as per their respective needs. There are different masters available for the same object. For instance, the nomenclature for Drugs is different for every state / UT e.g. Paracetamol 500 mg tablet is present with different codes/IDs and different names at respective states. So, the need was to standardize such objects. For standardization, the Authors decided to create a master set at a central location with unique instances of objects from every state. Secondly, a mapping process was envisaged to enable states / UTs to map their drug with the drug created in the central master. The following figure illustrates this concept in greater detail:

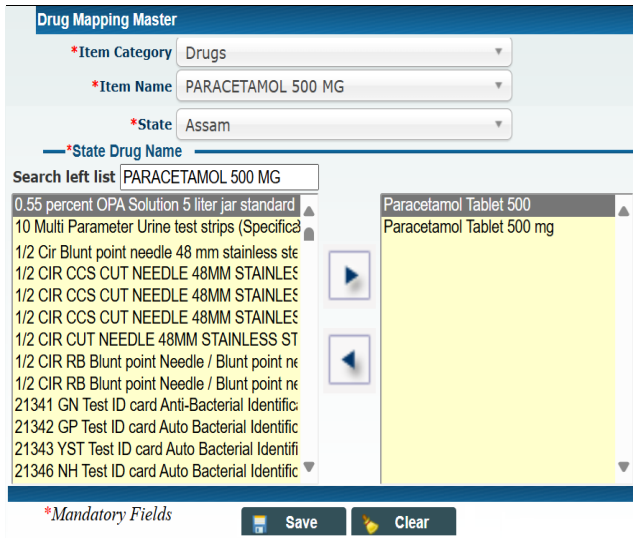


Figure 5: Standardization component.

So here a screen is divided into three parts (Top Pane, Left Pane, and Right Pane). The top Pane represents the drugs from Central Master, Left pane shows the unmapped drugs of the selected state. Now when any state wants to map its drug with a central drug, it selects the drug in the Left pane and moves it to the Right Pane. This way drug nomenclature is standardized for all states / UTs. Similarly, provision for standardization of Health Facilities and Suppliers, etc. is conceptualized in our framework.

### 3.3 Deduplication Component:

Authors faced the challenge of the absence of exact salt information in the data repositories of state / UTs, authors devised an algorithm for finding duplicate records via probabilities. The following steps are proposed:

- 3.3.1 Decide upon the parameters for determining the probability of duplicity.
- 3.3.2 Decide upon the initial weights for parameters.
- 3.3.3 Storage of two compared data.
- 3.3.4 Execution of the algorithm to calculate the probable percentage that any 2 drugs are probably duplicated by 'x' percent. It includes implementations of Fuzzy Logic for string comparison.

This calls for gathering the drug data and assigning weights to related parameters which will eventually help in deduplication.

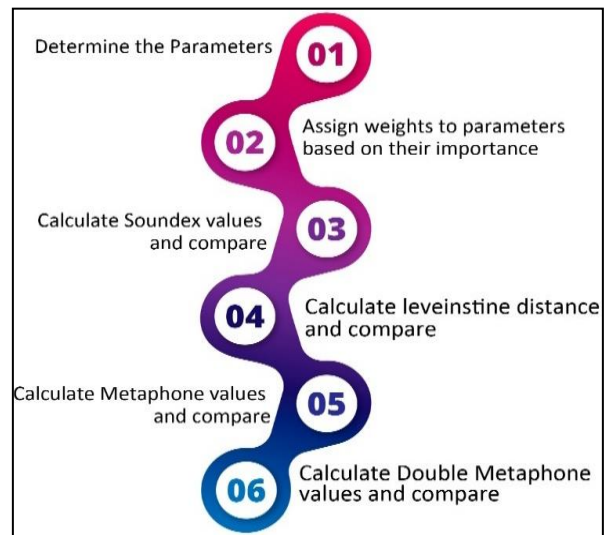


Figure 6: Steps followed for deduplication of drugs.

For finding duplicate drugs, weights need to be given to the various parameters based on our experience (initially) like:

- a. Parameter - Drug Name – Initial Weight - .75  
Drug nomenclature is the systematic naming of drugs, mainly pharmaceutical drugs. The name given by the producing company or based on the active ingredient a drug produces of the brand name drug [38], [39], [40], [41], [42].
- b. Parameter - Strength – Initial Weight - .05  
Strength is the amount of drug in a given dosage form, for example, 500 mg/tablet [12].
- c. Parameter - Group – Initial Weight – .02  
Each drug is classified by its presence of active substances which are divided into different like Anaesthetic agents, Adrenocortical steroids, Analgesics Antipyretics Nonsteroidal Anti-inflammatory Medicines & Anti-Rheumatic Drugs, Anti-Depressants, Immunological, Psychotropic Drugs, etc.
- d. Parameter - Subgroup – Initial Weight - .01  
Each drug is classified by its presence of active substances and divided into groups based on certain pharmacological properties [13].
- e. Parameter - Drug\_Type – Initial Weight - .02  
Based on different types of packaging and the way it can be consumed. For example, injections, inhalators, oral drugs, vials, etc.
- f. Parameter - Drug\_VED– Initial Weight - 0  
Classification of any drug belonging to the Vital, Essential, or Desirable category. Vital drugs are those which are expected to be present in all types of health facilities, they can be termed as “Life-Saving Drugs”. Essential are those that are relatively less important as

Lifesaving but are required to be present for treatment of common illnesses, The Desirable category is for those drugs that are not required to always be in stock, they can be understood as “Good to Have” drugs.

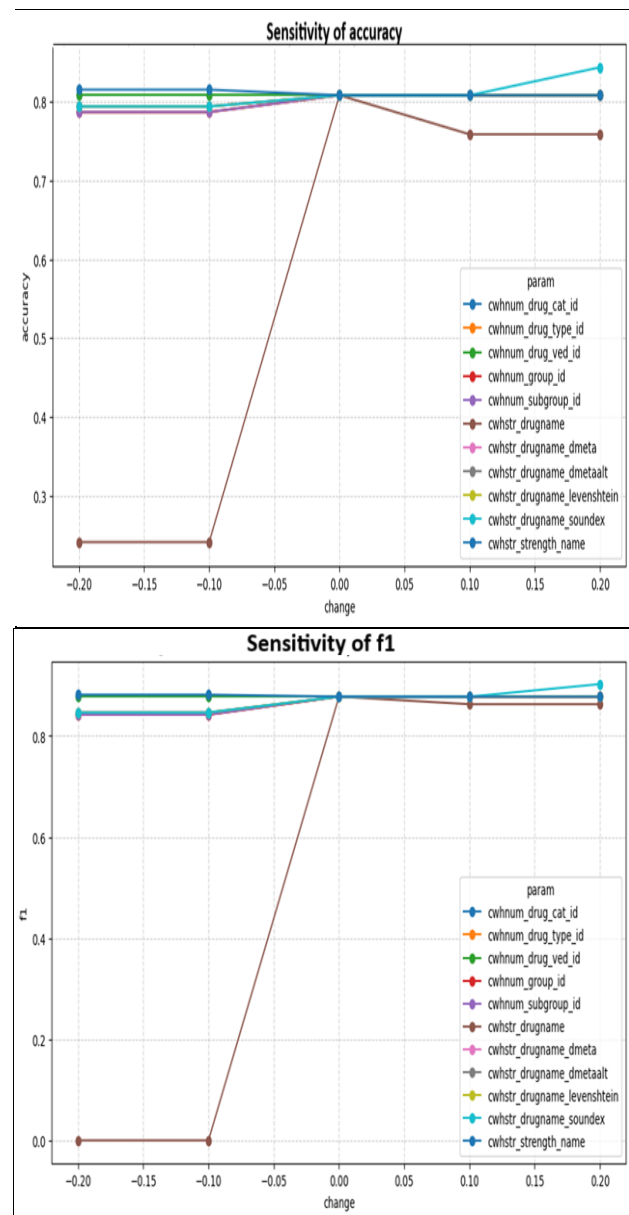
- g. Parameter - Drug\_CAT – Initial Weight – 0  
The Public Health System in India is categorized into three levels.  
Primary level (sub-centers and Primary Health Centres (PHCs)),  
Secondary level (Community Health Centres (CHCs) and smaller Sub-District hospitals) and  
Tertiary level (Medical Colleges and District/General Hospitals).  
Classification of any drug belonging to Primary, Secondary, or Tertiary category. Accordingly.
- h. Parameter - Drug\_Soundex – Initial Weight – .08  
Soundex is a phonetic algorithm that helps in indexing names by sound the way they are pronounced in English. This algorithm aims to match homophones despite minor differences in spelling. Also, it encodes consonants and vowels will not be encoded till it is the first letter [43]. The Soundex function is used in this framework to find the matches between two drug names and to address the issue of spelling mistakes. Limitations of Soundex include sensitivity to spelling variations, dependence on the initial letter, noise intolerance (mistyping, extra consonants, swapped consonants), and differing transcription systems. Other potential errors can be the use of initials, particles in names, perceptual differences, and silent consonants.
- i. Parameter - Drug\_Double\_Metaphone – Initial Weight – .02  
Metaphone is an improved version of the Soundex algorithm as it uses information about variations and inconsistencies in pronunciation of English spellings to produce a more accurate encoding [44]. The Double Metaphone provides an improved algorithm over the original Metaphone algorithm. [45]. Rudrappa, Agarkhed, and Vaidya (2019) while describing the implementation of Double Metaphone mentions it as a second-generation algorithm, which contains fundamental design improvements [42]. To handle ambiguous cases as well as multiple variants of surnames with common ancestry, it returns two codes for a string i.e. a primary and a secondary code and hence the name double is attached to the algorithm. [46]
- j. Parameter - Drug\_Double\_Metaphone\_Alt – Initial Weight – .02  
This is the secondary code for a string in double metaphone.
- k. Parameter - Drug\_Levenshtein – Initial Weight - .03  
The Levenshtein distance is a string metric that measures the difference between two sequences to convert one into

the other by the minimum number of single-character edits (insertions, deletions, or substitutions) [47].

The total weights need to be 1 for ease of comparison of results.

### Sensitivity Analysis

Sensitivity Analysis of the Initial Weights is as follows:



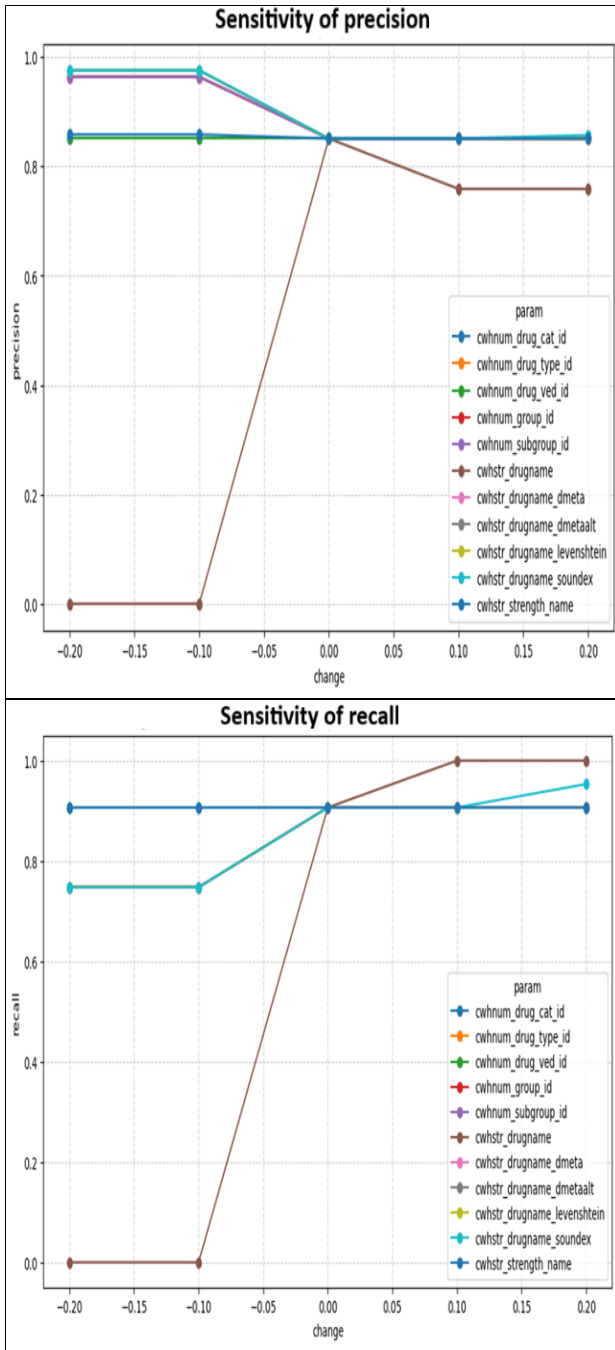


Figure 7: Sensitivity Analysis with original weights.

**Summary:**

1. Drug name exact match (cwhstr\_drugname) dominates.  
 Too low = model breaks.  
 Too high = recall increases, precision decreases.  
 Current baseline looks balanced.

2. Phonetic + Levenshtein features are valuable.  
 Increasing their weight slightly improves recall and F1.  
 Recommend boosting these to catch spelling variations / typos.
3. group-level features (group\_id, subgroup\_id, drug\_type\_id, etc.) are less sensitive.  
 They stabilize the model but don't strongly shift performance.  
 Safe to keep their weights moderate.

**Weights Optimization:**

Although the weights provided accurate results, models were tested with multiple values of weights and minor optimizations were done in the weights  
 After various rounds, optimized weights are as follows:

```
param_weights_optimized =
{
  "cwhnum_group_id": .02,
  "cwhnum_subgroup_id": .01,
  "cwhnum_drug_type_id": .02,
  "cwhnum_drug_cat_id": 0,
  "cwhnum_drug_ved_id": 0,
  "cwhstr_strength_name": .04,
  "cwhstr_drugname": .72, # keep dominant but slightly reduced
  "cwhstr_drugname_soundex": .10, # boosted
  "cwhstr_drugname_dmeta": .03, # boosted
  "cwhstr_drugname_dmetaalt": .03, # boosted
  "cwhstr_drugname_levenshtein": .05 # boosted
}
```

Sensitivity analysis shows that although the weights which were chosen initially based on purely experience basis were sufficient, still they have minor scope of improvements wherein minor boosting is recommended in parameters related to fuzzy matching of the stings like Soundex, Metaphone and Levenshtein while the weights for the drug name can be slightly reduced to have better performance of the model.

Sensitivity Analysis shows following improvements:

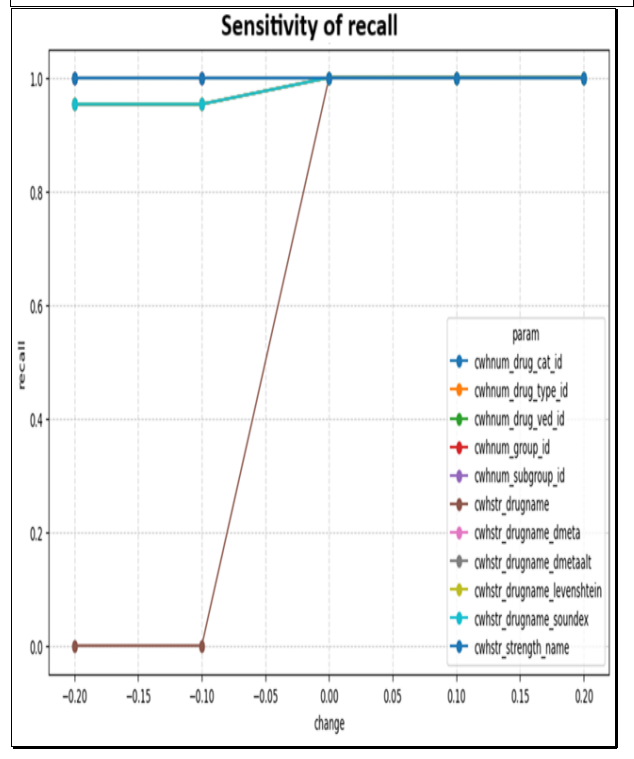
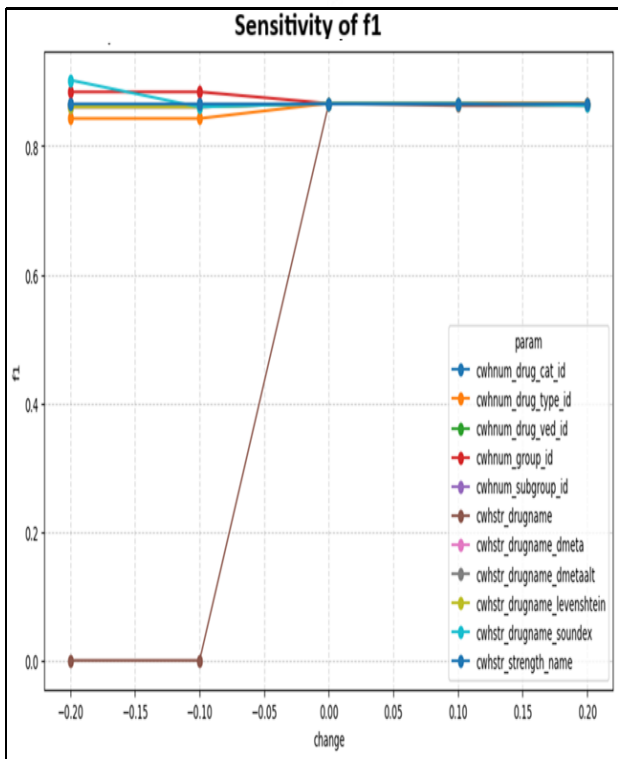
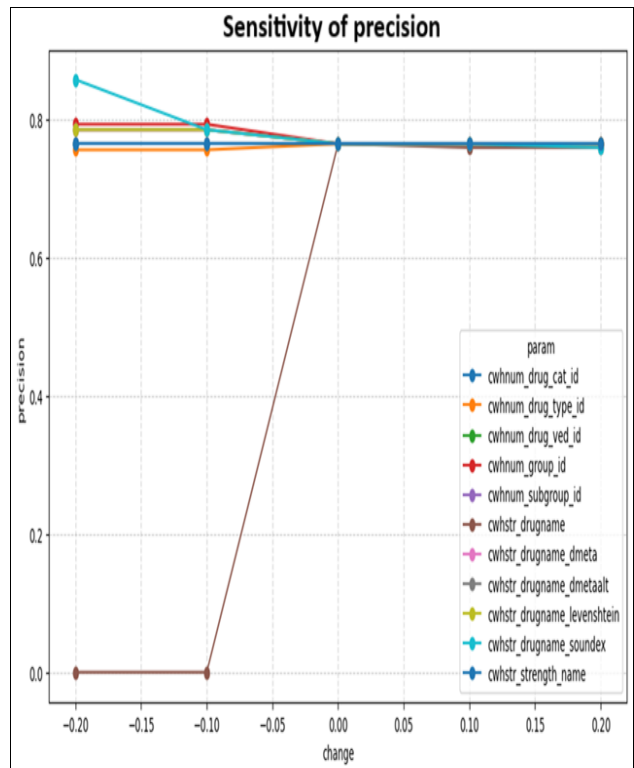
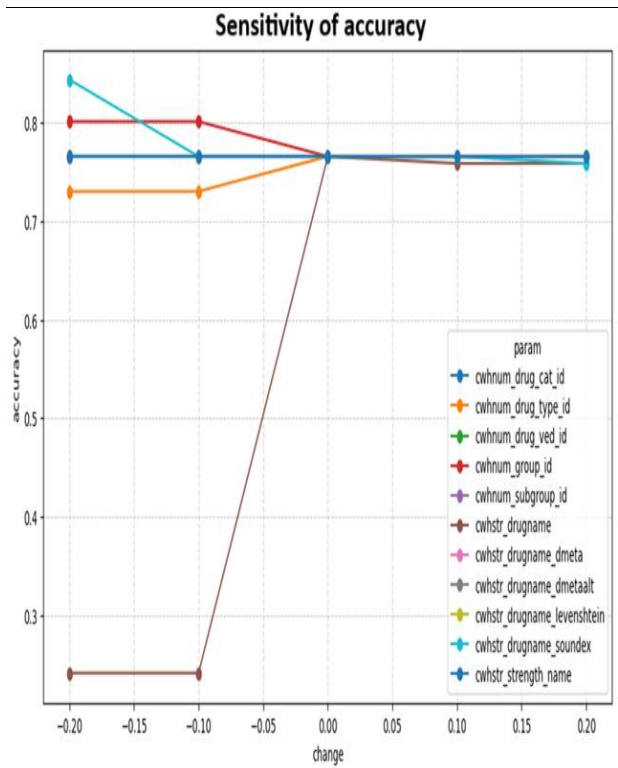


Figure 8: Sensitivity Analysis with optimized weights.

**Results of Weights Optimization:**

Overall F1 range: ~0.84 → 0.90 (pretty stable, good performance).

Accuracy: ~0.73 → 0.84.

Recall: Mostly 1.0 (catching all true matches), except some cases where it drops to 0.95.

Precision: Varies 0.75 - 0.97 depending on the parameter - main driver of changes in accuracy/F1.

So the model is recall-heavy (it rarely misses matches).

Algorithm: The designed algorithm below briefs out the fundamental steps to be followed which pull out the duplicate records. The first procedure is to be followed recursively till all the drugs are processed and above 90% probability is achieved.

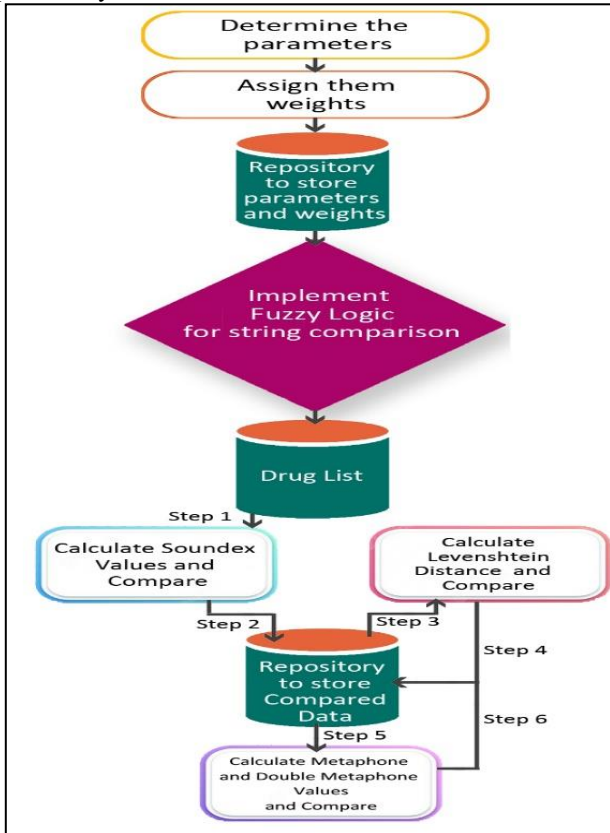


Figure 9: Algorithm for Data Deduplication.

Results: After execution of the above algorithm across every row, the results came into the picture with the following implementation:

```

1 CREATE OR REPLACE FUNCTION cwhr_drug_match(p_drug_id1 numeric, p_drug_id2 numeric) RETURNS numeric AS $$BODY$
2 declare
3 v_group_id1 numeric(4,0);v_subgroup_id1 numeric(4,0);v_drug_type_id1 numeric(4,0);v_drugname1 character varying(500);
4 v_drug_cat_code1 character varying(20);
5 v_drug_name1 character varying(200);v_strength_name1 character varying(200);v_group_id2 numeric(4,0);v_subgroup_id2 numeric(4,0);
6 v_drug_type_id2 numeric(4,0);
7 v_drugname2 character varying(500);v_drug_cat_code2 character varying(20);v_drug_ved_code2 numeric(4,0);v_strength_name2
8 character varying(200);
9 v_weight NUMERIC(10,2);v_param_name character varying (150);v_param_weight numeric(10,2);
10
11 begin
12 v_weight :=0;
13 select cwhnum_group_id,cwhnum_subgroup_id,cwhnum_drug_type_id, upper(cwhstr_drugname), cwhstr_drug_cat_code,
14 cwhnum_drug_ved_code, upper(cwhstr_strength_name)
15 into v_group_id1,v_subgroup_id1,v_drug_type_id1,v_drugname1,v_drug_cat_code1,v_drug_ved_code1,v_strength_name1
16 FROM cwhr_drug_mst where cwhnum_drugid=p_drug_id1;
17
18 select cwhnum_group_id,cwhnum_subgroup_id,cwhnum_drug_type_id, upper(cwhstr_drugname), cwhstr_drug_cat_code,
19 cwhnum_drug_ved_code, upper(cwhstr_strength_name)
20 into v_group_id2,v_subgroup_id2,v_drug_type_id2,v_drugname2,v_drug_cat_code2,v_drug_ved_code2,v_strength_name2
21 FROM cwhr_drug_mst where cwhnum_drugid=p_drug_id2;
22
23 if v_group_id1 = v_group_id2 then v_weight := v_weight +
24 (select cwhnum_param_weight from dwh.cwhr_drug_match_weight_mst where upper(cwhstr_param_name)='CWHNUM_GROUP_ID'); end if;
25 if v_subgroup_id1 = v_subgroup_id2 then v_weight := v_weight +
26 (select cwhnum_param_weight from dwh.cwhr_drug_match_weight_mst where upper(cwhstr_param_name)='CWHNUM_SUBGROUP_ID'); end if;
27 if v_drug_type_id1 = v_drug_type_id2 then v_weight := v_weight +
28 (select cwhnum_param_weight from dwh.cwhr_drug_match_weight_mst where upper(cwhstr_param_name)='CWHNUM_DRUG_TYPE_ID'); end if;
29 if v_drug_cat_code1 = v_drug_cat_code2 then v_weight := v_weight +
30 (select cwhnum_param_weight from dwh.cwhr_drug_match_weight_mst where upper(cwhstr_param_name)='CWHNUM_DRUG_CAT_ID'); end if;
31 if v_drug_ved_code1 = v_drug_ved_code2 then v_weight := v_weight +
32 (select cwhnum_param_weight from dwh.cwhr_drug_match_weight_mst where upper(cwhstr_param_name)='CWHNUM_DRUG_VED_ID'); end if;
33 if v_strength_name1 = v_strength_name2 then v_weight := v_weight +
34 (select cwhnum_param_weight from dwh.cwhr_drug_match_weight_mst where upper(cwhstr_param_name)='CWHSTR_STRENGTH_NAME'); end if;
35 if v_drugname1 = v_drugname2 then v_weight := v_weight +
36 (select cwhnum_param_weight from dwh.cwhr_drug_match_weight_mst where upper(cwhstr_param_name)='CWHSTR_DRUGNAME'); end if;
37
38 return v_weight;
39
40 end $$BODY$ LANGUAGE edbsql VOLATILE COST 100;
    
```

Figure 10: Implementation of Algorithm for Data Deduplication.

Output received from the deduplication process where the drug ID at Left-Hand-Side (LHS) is compared with the drug ID at Right-Hand-Side (RHS). The value is the probability that the percentage of the drug at LHS is a duplicate of the drug at RHS.

**Table 1: Result of Algorithm for Data Deduplication.**

Count i	Count j	DrugId LHS	DrugId RHS	Value
1	1	21191000	21191001	0.1
1	2	21191000	21191002	0.05
1	3	21191000	21191003	0.03
1	4	21191000	21191004	0.03
...	...	...	...	...

Processing these raw results, the following illustrations came into consideration that around 1.5% of duplicate records are found with a 90% possibility of duplicity.

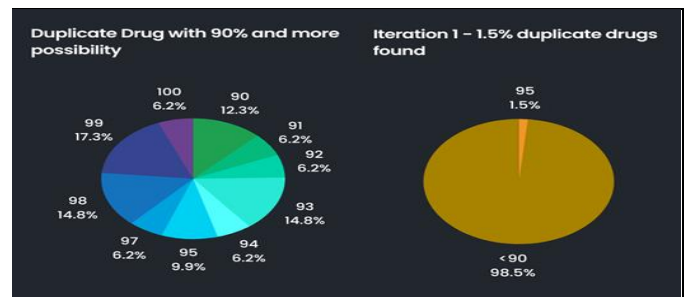


Figure 11: Distribution of duplicate records in Iteration-1

After removing these records, above-mentioned procedures are executed on the remaining rows which lead to new values. Iteration continued till the achievement of 90% accuracy was discontinued resulting in the following graph:

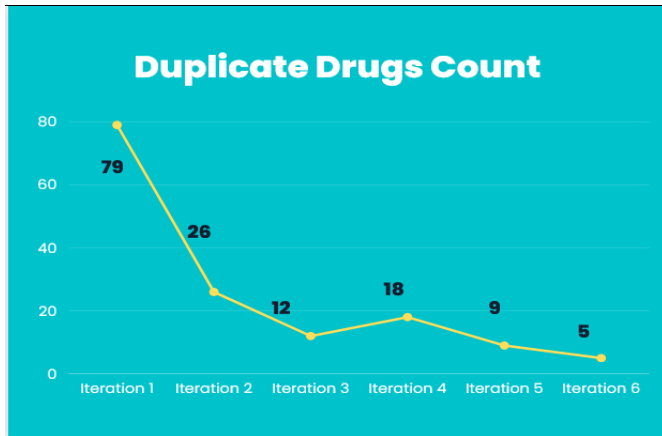


Figure 12: Count of duplicate records across total records.

Hence in total around 149 duplicate drug entries were detected in 7 iterations which says around 4% of total drugs were duplicates. Stating that under one system, entries of 4% duplication are found then this percentage will be much higher in the case of big data and their analysis leading to much higher business issues.

### 3.4 Visualization Component:

The visualization component takes the input of the data that is stored by the ETL Utility, standardized and de-duplicated. The visualization component creates dashboards with charts/graphs / tabular data etc. through Key Performance Indicators (KPIs). This framework proposes different layers of Visualization Components i.e.: Widget Layer, Tab Layer, Dashboard Layer. These three layers can be implemented through three different processes i.e. Widget Master, Tab Master, and Dashboard Master. Widget Master is the basic unit that contains the API or the Query or the Procedure call to the repository to get data for visualization. Customizations like Font size, color, background size, color, etc. are also handled at this level. The widget can be of type Tabular, Graph, KPI, Map, News Ticker, Another link, or IFrame. Option for Caching the data is also required at this level along with Refresh time. Various visualization libraries like Google Charts, HI Charts, etc. must be available here for selection. Tab Master is the collection of widgets that are required to be displayed on the page. It must provide the location on which a particular widget is to be displayed along with the order in which it must be displayed to the user. Dashboard Master is the collection of tabs that the dashboard must contain. It

presents the tabs as pages along with their menus. Al Zoubi, S., Gharaibeh, L., Jaber, H. M, et al. (2021) pointed out the panic behavior at the time of COVID-19 which resulted in shortages of sanitizers and other related medicines. This framework provides a way to early detect such sudden increases in stockouts through visualizations so that decision-makers can take a call to control the situation [48]. Present Deployment of the integrated framework used open-source Java, React and Python with the following technologies:

- GIT for code synchronization and version control
- Jenkins for continuous integration and deployment
- Nginx server for internal routings
- WildFly Application Server and
- Postgre Database Server

## 4- Result:

The proposed data integration and analytics framework have been successfully deployed at a centralized data center, effectively serving as a backbone for healthcare supply chain management operations. The deployment integrates a total of thirty-one geographically distributed remote data sources, each of which transmits data continuously into the centralized system.

During the system evaluation phase, the framework demonstrated substantial scalability and performance. It consistently managed over 5 GB of data ingestion per remote source per day, culminating in a cumulative daily data volume exceeding 155 GB. This high throughput underscores the system's ability to manage large-scale, real-world datasets with minimal latency and data loss.

### Data Ingestion Strategy

Data ingestion operations are tailored according to predefined business rules and domain-specific Key Performance Indicators (KPIs). Based on the analytical requirements:

Incremental loading is used for time-sensitive data marts where only recent changes are captured, ensuring efficiency.

Full data refreshes are scheduled for scenarios requiring complete synchronization, particularly in rapidly evolving datasets such as vaccine inventories and drug distributions. This dual-mode ingestion strategy balances performance with completeness, adapting dynamically to evolving data needs.

### Key Advantages of the Proposed Framework

The framework introduces several innovations that collectively address the limitations of traditional ETL tools and commercial platforms, particularly in low-resource or high-scale public health environments.

### Cost-Effectiveness

The entire solution stack is based on open-source

technologies, eliminating licensing fees and reducing total cost of ownership. This makes it accessible and scalable.

**High-Customizability**

The proposed solution can be configured in multiple ways which can coexists with each other e.g. for one state ETL can be used and for other ETLT can be used, it makes solution very convenient to use as per specific data load of a particular state.

**Flexible Deployment Configuration**

The system supports configurable deployments for transformations e.g. transformations can be performed during load time itself or can be deferred to after completion of load activity.

**Advanced API Integration Capabilities with Deduplication**

To support both legacy and present-day systems, solution provides data intake through variety of methods like through REST API, SOAP API or if network and credentials are available then through direct DB connections along with deduplication algorithm unlike commercial platforms such as SAS Enterprise Guide,

**In-Memory Data Transformation and Standardization**

To address ETL latency, solution facilitate on-the-fly data cleaning, standardization, and structuring.

**Integrated Deduplication Mechanism**

The proposed solution uses user-configurable parameters, weights, rules and fuzzy matching algorithms to address data redundancy. Solution provides probable duplicate data sets as per the defined weight on parameters and related rules.

**Low-Code/No-Code Visualization Layer**

The solution consists of an integrated visualization module for various hierarchy of users to build and customize interactive dashboards using predefined Key Performance Indicators (KPIs). Software coding or development knowledge is not required to create the KPIs in the dashboards.

**Rapid Adaptability and Iterative Enhancement**

The modular design and scriptable components allow for quick customization, versioning, and deployment of updates. This shortens turnaround times for new feature implementation compared to traditional monolithic ETL systems.

**Role-Based Access Control (RBAC)**

Controlled access to system functionalities and data visualizations ensures data security and compliance.

**Comprehensive Data Security**

Security of any system is an important aspect to consider. The framework adopts layered encryption combining RSA (asymmetric) and AES (symmetric) encryption algorithms. Sensitive health data is encrypted during storage and transmission. OWASP guidelines have been adhered to for ensuring that top ten vulnerabilities are properly addressed. Only users with valid roles and credentials can access the information.

The following figure shows the decrease in stockout percentages in case of particular state stores. It can be seen that the average stockout percentages for essential drugs defined by states have been reduced by more than 10%

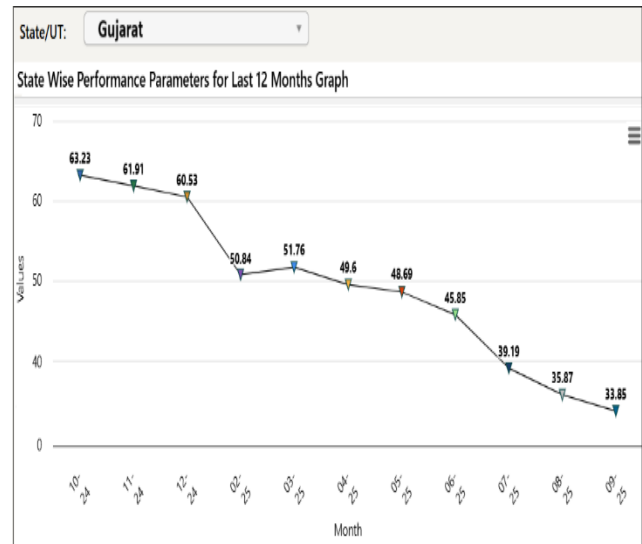


Figure 13: Reduction in stockout percentages in District Hospitals of an Indian State.

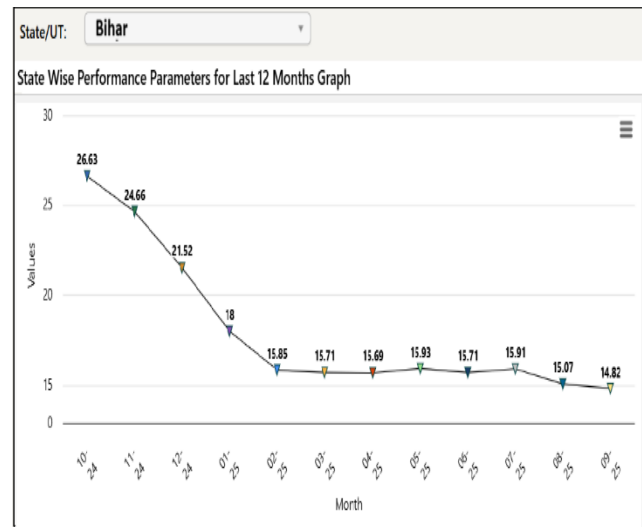


Figure 14: Reduction in stockout percentages in District Hospitals of another Indian State

Below figure presents the average reduction of stockout percent across particular stores of Indian states and UTs. It is evident that the stockout % is reduced from approx. 67.16 % to approx. 60.69%.

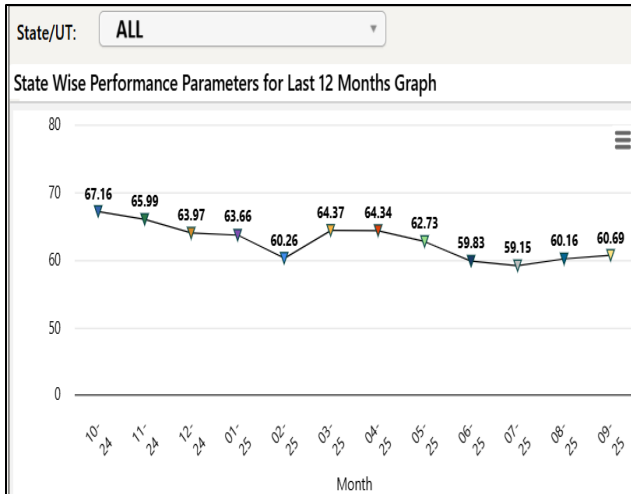


Figure 15: Reduction in stockout percentages in District Hospitals across integrated Indian State and UTs

Overall, the results confirm that the proposed framework is not only technically viable but also scalable, secure, and aligned with the operational demands. Use of opensource technologies, combined with advanced integration and transformation capabilities, makes it a compelling alternative to commercial ETL platforms, especially in scenarios where availability of resources is critical.

### 5- Conclusion:

The proposed framework marks a significant step in creating a centralized, scalable, and budget-friendly solution for integrating and analyzing data in India’s public healthcare supply chain. The system offers comprehensive functionality from setting up remote data sources and scheduling ETL processes to real-time data transformation, smart deduplication, and dashboard-based analytics to improve drug availability across nation.

The architecture uses open-source technologies like Java 2 Platform, Enterprise Edition (J2EE) for the frontend and PostgreSQL for managing data on the backend. A key strength of this framework is its ability to standardize and clean data in real time, even when dealing with a wide variety of data sources. This ensures consistency and reliability, even at scale. The dynamic ETL pipelines are particularly flexible, allowing for quick adjustments to transformation rules as data environments or policy needs shift. This includes automatic deduplication when needed. Meanwhile, built-in analytics and visualization tools offer user-specific dashboards that help stakeholders monitor performance and gain operational insights.

Currently, the system has been deployed across 31 Indian states and union territories, processing more than 5 GB of data per state each day on average. This level of adoption highlights how scalable and reliable the framework is. Health authorities at both central and state levels use it to view KPIs, identify delays or issues, and measure the efficiency of supply chains across different states and UTs. These insights have led to faster response times, better transparency, and more informed decision-making in public health logistics and improved drug availability.

Beyond performance, the framework also scores high on adaptability and security. Its modular setup means new states / UTs or data sources can be added with minimal hassle, making it a viable long-term solution.

Ultimately, the results show that a smart, unified platform like this can support data-driven governance at both national and state levels. This framework offers a model that could be replicated in other sectors aiming for digital transformation.

### Sample implementation of ETL component based on the proposed framework:

**State Job Details**

State Name: Rajasthan

Run Job

State Name : Rajasthan . Record Status : Active

<input type="checkbox"/>	Job Name	Job Start Time	Duration	Next Job Run
<input type="checkbox"/>	job_expiry_rajasthan	07-Oct-2025 09:24	24 Hrs	08-Oct-2025 04:00
<input type="checkbox"/>	job_drug_batch_res_raj	07-Oct-2025 09:14	24 Hrs	08-Oct-2025 00:00
<input type="checkbox"/>	job_state_new_ranking_raj	07-Oct-2025 08:28	24 Hrs	08-Oct-2025 08:19
<input type="checkbox"/>	job_get_issue_det_raj	07-Oct-2025 07:15	24 Hrs	08-Oct-2025 04:00
<input type="checkbox"/>	Job_Facilities_Count_Dtl_f	07-Oct-2025 07:04	24 Hrs	08-Oct-2025 00:30
<input type="checkbox"/>	job_demand_dtl_raj	07-Oct-2025 06:54	24 Hrs	08-Oct-2025 01:00
<input type="checkbox"/>	job_get_all_rc_raj	07-Oct-2025 06:44	24 Hrs	08-Oct-2025 00:00
<input type="checkbox"/>	Job_State_Ranking_RAJ	07-Oct-2025 06:04	24 Hrs	08-Oct-2025 06:00
<input type="checkbox"/>	job_qcfail_podelay_raj	07-Oct-2025 05:04	24 Hrs	08-Oct-2025 05:00

Total Record 27

[ Use % for Conditional Search ] FILTER: Job Name

**Data Transfer Logs State Name : Rajasthan**

Log Id	Log Date	Log Type	Source	Message
<b>Job Name :: job_cur_edl_stock_rajasthan</b>				
2510000008	07-Oct-2025 01:45:47	INFO	State	Successfully Inserted 2255303 Rows
2510000007	06-Oct-2025 10:35:07	INFO	State	Successfully Inserted 2256841 Rows
2510000006	05-Oct-2025 10:25:07	INFO	State	Successfully Inserted 2257555 Rows
2510000005	04-Oct-2025 10:25:06	INFO	State	Successfully Inserted 2312387 Rows
2510000004	03-Oct-2025 10:15:51	INFO	State	Successfully Inserted 2314128 Rows
2510000003	02-Oct-2025 10:26:41	INFO	State	Successfully Inserted 2315024 Rows
2510000002	01-Oct-2025 05:42:33	INFO	State	Successfully Inserted 2315014 Rows
2510000001	01-Oct-2025 02:08:08	INFO	State	Successfully Inserted 2315638 Rows

Figure 16: Sample implementation of ETL Component.

**Sample implementation of the Visualization Component based on the Proposed Framework:**

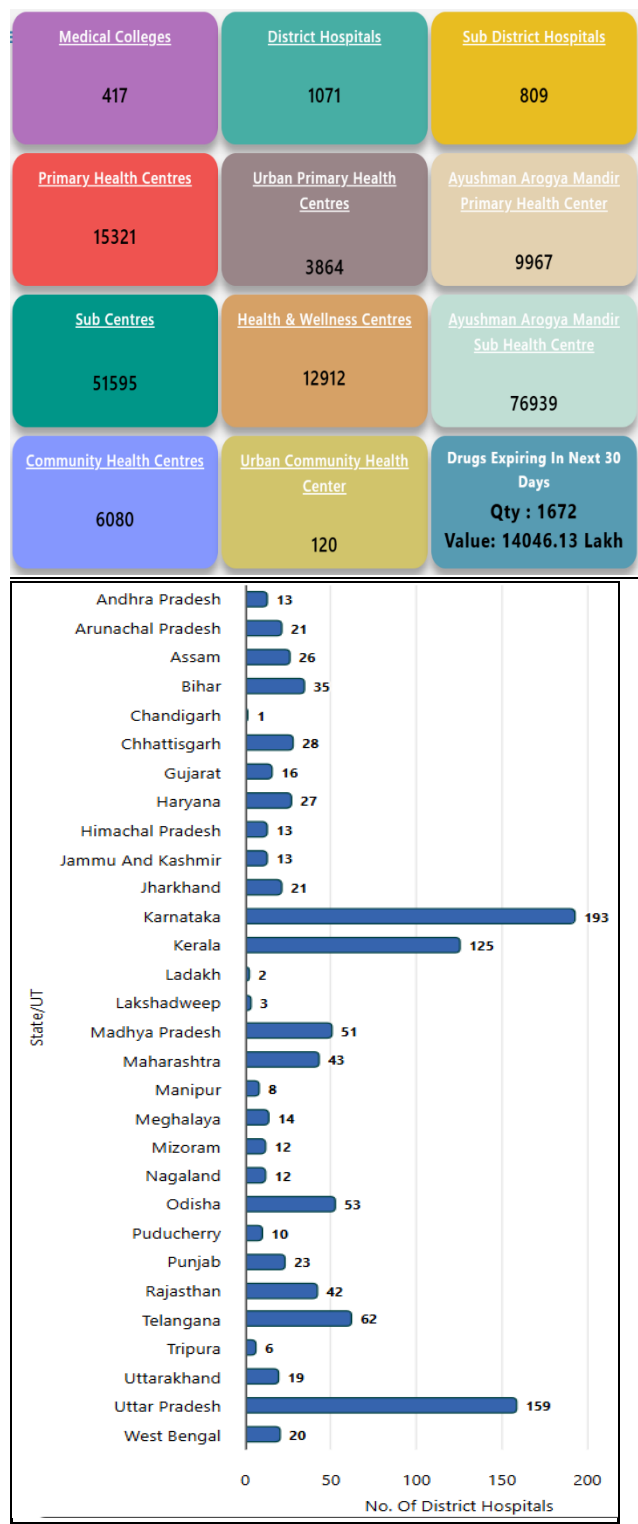


Figure 17: Sample implementation of Visualization Component.

**Limitation:** The proposed framework covers all aspects from ETL to visualization. Authors think that as the data size increases, horizontal/vertical scaling may be required according to the size of the data. Further, in the Visualization component, various types of charts/graphs can be added to provide more visualization options.

**Future Work:** The authors are planning to include more features in the visualization component like automatic outliers’ detection, based on the selection of mathematical functions like Average and standard Deviation, Automatic visualization of data into the quartiles, automatic identification of candidates for mapping, and deduplication through machine learning techniques. Further enhancement of the visualization component by inclusion of predictive analysis is also planned for future work.

**Conflict of interest:**

The authors have no conflicts of interest regarding this investigation.

**Acknowledgments:**

The authors would like to thank Ministry of Health and Family Welfare and NHSRC for their kind support during formulation and implementation of the proposed framework.

**References**

- [1] L. Dandona *et al.*, “Nations within a nation: variations in epidemiological transition across the states of India, 1990–2016 in the Global Burden of Disease Study,” *The Lancet*, vol. 390, no. 10111, pp. 2437–2460, Dec. 2017, doi: 10.1016/S0140-6736(17)32804-0.
- [2] The Lancet, “India—a tale of one country, but stories of many states,” *The Lancet*, vol. 390, no. 10111, p. 2413, Dec. 2017, doi: 10.1016/S0140-6736(17)32867-2.
- [3] MoHFW, “MINISTRY OF HEALTH AND FAMILY WELFARE Major Schemes and Programmes Government of India New Delhi,” 2000. [Online]. Available: <http://mohfw.nic.in>
- [4] S. Saebao, S. Matayong, and N. trakulmaykee, “QoX based ETL Design for Business Intelligence System of Lecturers’ Qualifications Analysis,” in 2020 17th International Conference on Electrical Engineering/Electronics, Computer, Telecommunications and Information Technology (ECTI-CON), IEEE, Jun. 2020, pp. 539–542. doi: 10.1109/ECTI-CON49241.2020.9158113.
- [5] S. Zhao, “What is ETL? (Extract, Transform, Load),” [www.edq.com](http://www.edq.com)
- [6] T. Pott and Iain Thomson, “Extract, transform, load? More like extremely tough to load, amirite?,” [www.theregister.com](http://www.theregister.com).
- [7] S. Sivabalan and R. I. Minu, “Heterogeneous Data Integration with ELT and Analytical MPP Database for Data Analysis Application,” in 2021 Innovations in Power and

- Advanced Computing Technologies (i-PACT), IEEE, Nov. 2021, pp. 1–5. doi: 10.1109/i-PACT52855.2021.9696841.
- [8] B. Pan, G. Zhang, and X. Qin, “Design and realization of an ETL method in business intelligence project,” in 2018 IEEE 3rd International Conference on Cloud Computing and Big Data Analysis (ICCCBDA), IEEE, Apr. 2018, pp. 275–279. doi: 10.1109/ICCCBDA.2018.8386526
- [9] Shiva Kumar Vuppala and Manohar Reddy Sakkula, “Challenges in Streaming ETL Pipelines for High-Frequency Data Ingestion and Real-Time Processing,” *International Journal For Multidisciplinary Research*, vol. 6, no. 6, Dec. 2024, doi: 10.36948/ijfmr.2024.v06i06.33506
- [10] A. Kabiri, F. Wadajiny, and D. Chiadmi, “Towards a Framework for Conceptual Modeling of ETL Processes,” 2011, pp. 146–160. doi: 10.1007/978-3-642-27337-7\_14.
- [11] T. Jörg and S. Dessloch, “Near Real-Time Data Warehousing Using State-of-the-Art ETL Tools,” 2010, pp. 100–117. doi: 10.1007/978-3-642-14559-9\_7.
- [12] A. Dixit, S. Routroy, and S. K. Dubey, “A systematic literature review of healthcare supply chain and implications of future research,” *Int. J. Pharm. Healthc. Mark.*, vol. 13, no. 4, pp. 405–435, Nov. 2019, doi: 10.1108/IJPHM-05-2018-0028.
- [13] R. A. Atinga, S. Dery, S. P. Katongole, and M. Aikins, “Capacity for optimal performance of healthcare supply chain functions: competency, structural and resource gaps in the Northern Region of Ghana,” *J. Health Organ. Manag.*, vol. 34, no. 8, pp. 899–914, Oct. 2020, doi: 10.1108/JHOM-09-2019-0283.
- [14] K. Ahmad *et al.*, “Public health supply chain for iron and folic acid supplementation in India: Status, bottlenecks and an agenda for corrective action under Anemia Mukht Bharat strategy,” *PLoS One*, vol. 18, no. 2, p. e0279827, Feb. 2023, doi: 10.1371/journal.pone.0279827.
- [15] A. Verma, A. Rana, H. Monga, A. Chaudhary, and J. Singh, “Distribution Management of Drugs/medicines and vaccines vis-a-vis Free Drugs Service Initiative (FDSI) of Ministry of Health and Family Welfare (MoHFW), Government of India in the Indian States,” in *2021 9th International Conference on Reliability, Infocom Technologies and Optimization (Trends and Future Directions) (ICRITO)*, IEEE, Sep. 2021, pp. 1–5. doi: 10.1109/ICRITO51393.2021.9596365.
- [16] SAS, “SAS Enterprise Guide,” [https://support.sas.com/documentation/onlinedoc/guide/tut8/en/m0\\_2.htm](https://support.sas.com/documentation/onlinedoc/guide/tut8/en/m0_2.htm). Accessed: Jun. 18, 2025. [Online]. Available: [https://support.sas.com/documentation/onlinedoc/guide/tut8/en/m0\\_2.htm](https://support.sas.com/documentation/onlinedoc/guide/tut8/en/m0_2.htm)
- [17] E. Kodhai, K. Divakar, A. Andrews, Y. Pachipala, and J. Alzubi, “MANAGING THE CLOUD STORAGE USING DE-DUPLICATION AND SECURED FUZZY KEYWORD SEARCH FOR MULTIPLE DATA OWNERS,” *International Journal of Pure and Applied Mathematics*, 2018.
- [18] R. Kumar, J. Lachure, and R. Doriya, “Use of Hybrid ECC to enhance Security and Privacy with Data Deduplication,” in *2021 Second International Conference on Electronics and Sustainable Communication Systems (ICESC)*, IEEE, Aug. 2021, pp. 934–941. doi: 10.1109/ICESC51422.2021.9532948
- [19] SQL Server, “SQL Server Integration Services,” <https://learn.microsoft.com/en-us/sql/integration-services/sql-server-integration-services?view=sql-server-ver15>. Accessed: Jun. 18, 2025. [Online]. Available: <https://learn.microsoft.com/en-us/sql/integration-services/sql-server-integration-services?view=sql-server-ver15>
- [20] Informatica, “Informatica.com,” <https://www.informatica.com/de/products/data-integration/powercenter.html>. Accessed: Jun. 18, 2025. [Online]. Available: <https://www.informatica.com/de/products/data-integration/powercenter.html>
- [21] Pedersen T and Mohania M, *Data Warehousing and Knowledge Discovery*, vol. 5691. Berlin, Heidelberg: Springer Berlin Heidelberg, 2009. doi: 10.1007/978-3-642-03730-6.
- [22] <https://en.wikipedia.org/>, “Pentaho,” <https://en.wikipedia.org/wiki/Pentaho>. Accessed: Jun. 18, 2025. [Online]. Available: <https://en.wikipedia.org/wiki/Pentaho>
- [23] Ibm, “Datastage,” <https://www.ibm.com/products/datastage>. Accessed: Jun. 18, 2025. [Online]. Available: <https://www.ibm.com/products/datastage>
- [24] [www.adeptia.com](https://www.adeptia.com/), “www.adeptia.com,” <https://www.adeptia.com/products/connect>. Accessed: Jun. 18, 2025. [Online]. Available: <https://www.adeptia.com/products/connect>
- [25] [www.adeptia.com](https://www.adeptia.com/), “www.adeptia.com,” <https://www.adeptia.com/solutions>. Accessed: Jun. 18, 2025. [Online]. Available: <https://www.adeptia.com/solutions>
- [26] [tutorialspoint.com](https://www.tutorialspoint.com/), “Talend,” <https://www.tutorialspoint.com/talend/index.htm>. Accessed: Jun. 18, 2025. [Online]. Available: <https://www.tutorialspoint.com/talend/index.htm>
- [27] [talend.com](https://www.talend.com/), “TalendSolutions,” <https://www.talend.com/products/talend-open-studio/>. Accessed: Jun. 18, 2025. [Online]. Available: <https://www.talend.com/products/talend-open-studio/>
- [28] Clover ETL Reference Manual,” [https://docs.huihoo.com/cloveretl/server/CloverETLServer-ReferenceManual-4\\_7\\_0\\_016M1.pdf](https://docs.huihoo.com/cloveretl/server/CloverETLServer-ReferenceManual-4_7_0_016M1.pdf). Accessed: Jun. 18, 2025. [Online]. Available: [https://docs.huihoo.com/cloveretl/server/CloverETLServer-ReferenceManual-4\\_7\\_0\\_016M1.pdf](https://docs.huihoo.com/cloveretl/server/CloverETLServer-ReferenceManual-4_7_0_016M1.pdf)
- [29] Hevodata, “Hevo-features,” <https://docs.hevodata.com/introduction/hevo-features/>. Accessed: Jun. 18, 2025. [Online]. Available: <https://docs.hevodata.com/introduction/hevo-features/>
- [30] “Data-integrator,” <https://www.oracle.com/in/middleware/technologies/data-integrator.html>. Accessed: Jun. 18, 2025. [Online]. Available: <https://www.oracle.com/in/middleware/technologies/data-integrator.html>
- [31] S. I. Khan and A. S. Md. L. Hoque, “Towards development of health Data Warehouse: Bangladesh perspective,” in *2015 International Conference on Electrical Engineering and Information Communication Technology (ICEEICT)*, IEEE, May 2015, pp. 1–6. doi: 10.1109/ICEEICT.2015.7307514.
- [32] Md. B. Biplob, G. A. Sheraji, and Khan Shahidul Islam, *2018 International Conference on Innovations in Science, Engineering and Technology : ICISSET 2018 : International*

- Islamic University Chittagong, Chittagong, Bangladesh* : 27-28 October 2018. IEEE, 2018. doi: 10.1109/iciset.2018.8745574.
- [33] A. R. Chaturvedi, A. K. Choubey, and Jinsheng Roan, "Scheduling the allocation of data fragments in a distributed database environment: a machine learning approach," *IEEE Trans. Eng. Manag.*, vol. 41, no. 2, pp. 194–207, May 1994, doi: 10.1109/17.293386
- [34] A. Simitisis, P. Vassiliadis, S. Skiadopoulos, and T. Sellis, *Data Warehouses and OLAP*. IGI Global, 2007. doi: 10.4018/978-1-59904-364-7.
- [35] P. Vassiliadis and A. Simitisis, "EXTRACTION, TRANSFORMATION, AND LOADING," 2009.
- [36] C. Joe and K. Ralph, *The data warehouse etl toolkit : practical techniques for extracting, cleaning, conforming, and delivering data*. Wiley, Hoboken, N.J., 2013, 2011.
- [37] W. W. Eckerson and R. Sponsors, "Achieving Business Success through a Commitment to High Quality Data TDWI REPORT SERIES DATA QUALITY AND THE BOTTOM LINE." [Online]. Available: [www.dw-institute.com](http://www.dw-institute.com)
- [38] Drug\_nomenclature," [https://en.wikipedia.org/wiki/Drug\\_nomenclature](https://en.wikipedia.org/wiki/Drug_nomenclature). Accessed: Jun. 18, 2025. [Online]. Available: [https://en.wikipedia.org/wiki/Drug\\_nomenclature](https://en.wikipedia.org/wiki/Drug_nomenclature)
- [39] First Nations Health Authority, "Generic vs Brand-name prescription drugs faq," <https://www.fnha.ca/about/news-and-events/news/generic-vs-brand-name-prescription-drugs-faq>. Accessed: Jun. 18, 2025. [Online]. Available: <https://www.fnha.ca/about/news-and-events/news/generic-vs-brand-name-prescription-drugs-faq>
- [40] "Understanding expressions of drug amounts," <http://courses.washington.edu/pharm309/calculations/Lesson2.pdf>. Accessed: Jun. 18, 2025. [Online]. Available: Understanding expressions of drug amounts
- [41] [www.who.int](http://www.who.int), "ATC Classification," <https://www.who.int/tools/atc-ddd-toolkit/atc-classification>. Accessed: Jun. 18, 2025. [Online]. Available: <https://www.who.int/tools/atc-ddd-toolkit/atc-classification>
- [42] S. Rudrappa, D. V. Agarkhed, and S. S. Vaidya, "Healthcare Systems: India," in *Quality Spine Care*, Cham: Springer International Publishing, 2019, pp. 211–224. doi: 10.1007/978-3-319-97990-8\_13.
- [43] Soundex," <https://en.wikipedia.org/wiki/Soundex>. Accessed: Jun. 18, 2025. [Online]. Available: <https://en.wikipedia.org/wiki/Soundex>
- [44] Metaphone," <https://en.wikipedia.org/wiki/Metaphone>. Accessed: Jun. 18, 2025. [Online]. Available: <https://en.wikipedia.org/wiki/Metaphone>
- [45] "Double\_Metaphone," [https://en.wikipedia.org/wiki/Metaphone#Double\\_Metaphone](https://en.wikipedia.org/wiki/Metaphone#Double_Metaphone). Accessed: Jun. 18, 2025. [Online]. Available: [https://en.wikipedia.org/wiki/Metaphone#Double\\_Metaphone](https://en.wikipedia.org/wiki/Metaphone#Double_Metaphone)
- [46] Lawrence Philips, "The double metaphone search algorithm," *C/C++ Users Journal*, vol. 18, no. 6, pp. 38–43, 2000.
- [47] Levenshtein\_distance," [https://en.wikipedia.org/wiki/Levenshtein\\_distance](https://en.wikipedia.org/wiki/Levenshtein_distance). Accessed: Jun. 18, 2025. [Online]. Available: [https://en.wikipedia.org/wiki/Levenshtein\\_distance](https://en.wikipedia.org/wiki/Levenshtein_distance)
- [48] S. Al Zoubi, L. Gharaibeh, H. M. Jaber, and Z. Al-Zoubi, "Household Drug Stockpiling and Panic Buying of Drugs During the COVID-19 Pandemic: A Study From Jordan," *Front. Pharmacol.*, vol. 12, Dec. 2021, doi: 10.3389/fphar.2021.813405.

# Maize Leaf Disease Detection using Deep Learning Models and a DenXNet Ensemble Model

Meghna Gupta<sup>1\*</sup>, Sarika Jain<sup>1</sup>, Manoj Kumar<sup>2</sup>

<sup>1</sup>.Amity Institute of Information Technology, Amity University Noida, Uttar Pradesh, India

<sup>2</sup>.Faculty of Engineering & Information Sciences, University of Wollongong, Dubai, United Arab Emirates

Received: 28 Jul 2025/ Revised: 04 Dec 2025/ Accepted: 06 Jan 2026

## Abstract

Maize(Corn) is considered an important crop worldwide for global production after wheat and rice. It provides food, ethanol, carbohydrates, vitamins, and other resources, making it essential to human civilization. However, it does face numerous difficulties, including pest infestations, deteriorating soil, scarce water supplies, and climate change, resulting in various yield losses. This research introduces an efficient deep learning framework for the accurate identification of maize leaf disease. Four convolutional neural network architectures, DenXNet- MobileNet, Xception, DenseNet169, and DenseNet201- were trained and evaluated using both original and augmented datasets. To ensure fairness and eliminate data leakage, the original data is divided into train, validation, and test sets, and then augmented, whereas a stratified five-fold cross-validation strategy was applied to non-augmented data. A comprehensive ablation study was conducted to compare model performance with and without augmentation and across different ensemble configurations. The study explored soft ensemble modelling using combinations of two and four base models. Among all configurations, the four-model ensemble, DenXNet, achieved the highest accuracy of 98.46% and consistency across folds, outperforming individual and partial ensembles. The proposed method demonstrates improved precision, reduced overfitting, and strong adaptability for real-world agricultural disease detection tasks.

**Keywords:** Deep Learning; DenseNet169; DenseNet201; Xception; Mobilenet; Ensemble Model.

## 1- Introduction

The agriculture sector in every country must upgrade its methods of cultivation to make farmers' lives easier and to strengthen infrastructure. A significant percentage of people across the world rely upon farming for their food and to keep their economic systems stable. Farmers are always dependent on observations and historical data, like crop yield statistics as well as climate patterns, to make important choices that assist the planet stay healthy in the short and long term. For thousands of years, agricultural activity has been a key part of human development, making sure that everyone has enough to eat [1]. To keep supplies of food safe, protect the natural world, and improve the health of agricultural populations, it is important to promote farming practices which prove beneficial for the environment. The fitness of plants matters for keeping the natural world in balance and for guaranteeing that agricultural activity goes smoothly at the same time. But occasionally, conventional methods of agriculture fail to

produce results, and these wastes resources and boosts food prices [2]. Pests that affect crops are one of the most significant issues that hurt the quality and range of farm products. The most apparent part of plants is the leaves that cover them. They are also tasked with photosynthesis and the creation of chlorophyll. Numerous observations about the plant can be made by examining them [3]. Different algorithms have been utilized for predicting diseases in different plants, and the conclusions are made generally in terms of accuracy [4]. Still, one of the biggest problems is figuring out the right way to classify small datasets. It may also take a long time and a lot of money to get labeled agricultural data. The seriousness of crop diseases is an important variable that causes the decline in agricultural production. Consequently, quick detection as well as reaction are essential for safeguarding crops from spoiling while rendering farmers' lives easier. Proper detection enables it practicable to deploy chemical fertilizers and pesticides with caution [5]. Deep Learning (DL) models have shown outstanding ability at quickly scanning large amounts of data, particularly images, to find small signs of

✉ Meghna Gupta  
drmeghnaphd@gmail.com

plant diseases [6]. Models based on deep learning have made it feasible to digitally and in real time, analyze pictures in the field. Manual inspection, on the contrary hand, is tedious and may result in blunders [7-8]. Once DL is combined with agricultural precision, specific changes can be made. These kinds of modifications make farming more beneficial for the environment and make ecosystems associated with agriculture stronger. Maize (*Zea mays* L.) is a member of the family of Poaceae and represents one of the major cereal crops in the world. Farmers cultivate it all over nations for several purposes, among which are food, livestock feed, bioethanol, and commercial applications. In recent decades, the production of maize has grown a lot in response to new technologies, greater crop yields, and improved global demand [9]. It is a crucial component of global agri-food systems because it can be utilized in numerous ways.

Indeed, deep learning has made significant progress in diagnosing plant diseases; however, several problems remain that need to be addressed. Most current research depends on specific CNN architectures, which occasionally fail to perform well in various conditions, like when the lighting, leaf orientation, or background noise fluctuates. Also, datasets that are restricted and not uniformly distributed make these models unreliable, which leads to biased performance during classification. Only a small number of studies have investigated ensemble-based CNN frameworks that combine the most effective elements of several distinct architectures to make predictions that are more stable and accurate. Additionally, the impact of data augmentation on maize crops has not been thoroughly examined. Consequently, there is a necessity for a systematic investigation that includes data augmentation, cross-validation, and soft averaging ensemble learning in order to improve the reliability of disease detection methodologies. The proposed research attempts to address this gap by developing and validating a hybrid ensemble model which utilizes both enhanced and ordinary datasets in order to boost accuracy, minimize overfitting, and offer an extensive framework to recognize early maize leaf diseases.

The remainder of this paper is organized as follows: Section 2 contains the related work done in this area, Section 3 describes the methodology used for the framework, Section 4 discusses the results, and Section 5 draws the conclusion of the study.

## 2- Related Work

Deep learning techniques have been widely employed by researchers to point out and categorize plant or agricultural diseases using machine learning algorithms, CNN, and Ensemble Modelling [10-12]. Xiaolin Sun *et al.* [13] suggested an image recognition technique for maize disease

using convolutional neural networks and transfer learning. This technique saves a significant amount of training time and enhances classifier performance by using the specifications of the Inception-v3 and Inception-v4 models that have been learned on ImageNet as the start values of training. They have applied the model on 8 classes of Maize (Puccinia polysora general, Maize dwarf mosaic virus, Corn healthy, Cercospora zeae-maydis tehon and daniels general, Puccinia polysora serious, Cercospora zeae-maydis tehon and daniels serious, Corn curvularia leaf spot fungus general, and Corn curvularia leaf spot fungus serious) containing 3503 images. The authors emphasized that for deep learning models, the collection of datasets is very crucial.

Plant diseases are a broad category of diseases brought on by a variety of pathogens, like fungi, bacteria, phytoplasmas, viruses, and nematodes. These diseases can cause symptoms including wilting, discoloration, lesions, and abnormalities in the leaves, stems, roots, and fruits of the plant, among other symptoms [14]. Distinct approaches are currently in use for plant disease detection, using image processing [15]. It can be done by extracting color features (HIS model, YcbCr Model ) [16], shape features [17], and texture features [18]. Enquhone Alehegn [19] used 7 textures, 6 colors, and 9 morphological features, a total of 22 features, for the recognition and classification analysis of images using k-nearest neighbor and Artificial Neural Network, and achieved an accuracy of 82.5% and 94.4%, respectively. Sumita Mishra *et. al* [20] offer a real-time, three-class, 88.6% accurate deep convolutional neural network technique for recognizing maize leaf disease. By modifying the pooling combinations and hyperparameters on a GPU-equipped machine, they have enhanced the network. Basavaraj *et. al* [21] created a deep CNN framework using the VGG16 model to automatically identify stressed paddy crop images taken during the booting development stage. A 92.89% accuracy rate was achieved by the model on five distinct types of paddy with varying stress levels.

Mohit Agarwal *et. al.* [22] have proposed a new CNN model with 8 hidden layers. They have compared this model with pre-trained deep learning models by testing it on the publicly available Plant Village dataset. After image augmentation, they increased the brightness of the image for image processing by a random value to increase accuracy. They have used the convolution layer, max pooling layer, dropout rate, network weight, activation function, learning rate, momentum, epochs, and batch size as hyper parameters. K. P. Panigrahi *et al.* [23] applied the supervised algorithms Naïve Bayes, Decision Tree, K-nearest neighbor, Support Vector Machine, and Random Forest on the Maize dataset on 3823 images and obtained a higher accuracy for Random Forest, i.e., 79.23% in comparison to other algorithms used in their study. They had compacted the size of the pictures to 100 x 100.

S. Pudumalar et al. [24] proposed an ensemble model based on CNN and the VGG16 model to improve the accuracy by removing the bias at each layer. They considered the real-time dataset of cotton crops consisting of 6 classes, from Thadikombu village, Dindigul District, Tamil Nadu. Due to limited dataset, data augmentation techniques were used to avoid overfitting issues. The proposed model attained an accuracy of 95% using the softmax function and ReLU optimizer. However, the authors were concerned about the quality of images used for classification. We found that a single model cannot cover all aspects, resulting in bias and overfitting issues. Researchers are working on the buildup of ensemble models for improving the precision of crop

estimations, thus dealing with the challenges brought about by specific models [25].

Nabende and Murindanyi [26] also discuss how diseases can harm maize crops, emphasising the importance of having accessible, easy-to-use, and accurate diagnostic tools. They compared classical artificial intelligence models, custom CNNs, transfer learning methods using InceptionResNetV2, MobileNetV2, and Vision Transformers. MobileNetV2 had the best classification accuracy at 97%. Deep learning ensemble models have shown great potential in classifying plant diseases, although there are still some research gaps that make them hard to use in real-world farming situations.

Table 1: Details of different classification techniques applied to recognize different diseases in crops

<i>Classification Model</i>	<i>Crop</i>	<i>Dataset Size (images)</i>	<i>Parameters</i>	<i>Diseases Categories</i>	<i>Accuracy</i>	<i>Research Paper</i>
VGG16	Pearl Millet	124	Automatic Feature Detection	2	95%	[28]
CNN	Lotus	2640	Colour	11	99.54%	[10]
CNN	Maize	AI Challenger dataset	Automatic Feature Detection	3503 pictures, 8 categories	81%	[13]
KNN & ANN	Maize	800	7 textures, 6 colours, and 9 morphological features	4	82.5%(KNN), 94.4%(ANN)	[19]
Deep CNN	Corn	4382	Automatic feature detection	3	88.6%	[20]
VGG16	Paddy	30000	colour	5	92.89%	[21]
SVM, Naive Bayes, KNN, Decision Tree, Random Forest	Maize	PlantVillage dataset	Automatic feature detection	3823 images with 4 classes	77.56 %, 77.46%, 76.16%, 74.35%, 79.23 % respectively	[23]
Ensemble Model(CNN&VGG16)	Cotton	15600	Automatic feature detection	6	95%	[15]
Resnet50	Maize	2309	Colour features	5	98.52%	[29]
CNN & MobileNet	Grape_Esca_(Black_Measles), Tomato_Early_blight etc	87000	Automatic feature detection	38	89% & 96%	[30]
MobileNetV2, InceptionResNetV2, EfficientNetB0, ResNet50, InceptionV3,	Maize	38571	Automatic feature detection	6	97%,96%,77%,95% and 94% respectively.	[26]

Current datasets do not have adequate variety and variability compared to the real world, which makes it hard for models to work in real-world farm conditions. Additionally, the lack of explainable AI integration makes

it harder for farmers to understand and trust automated systems. Also, most of the datasets that are already out there have a lot of class imbalance, which renders effectiveness biased across disease categories [27]. To make real, field-ready crop disease detection systems, it's necessary to deal with these challenges by using different ways to collect data, explainable computational design, and balanced training strategies. **Table 1** exhibits a summary of the different models applied to different crops and the accuracy achieved.

### 3-Methodology

Diseases that impact maize plants render the crop less nutritious and less available. So, it's extremely essential to identify and manage maize leaf diseases quickly and correctly to reduce losses, keep the quality of the crop, and help farmers make more money. Convolutional Neural Networks (CNNs) have become useful for diagnosing plant diseases because they can easily pull out complex features from leaf images using sequential convolution and optimization operations.

Many research studies have proven that CNN-based methods have been effective at correctly diagnosing and categorizing plant diseases. Fig. 1 shows the whole procedure of the designed model, with the main steps for finding and stopping maize leaf disease.

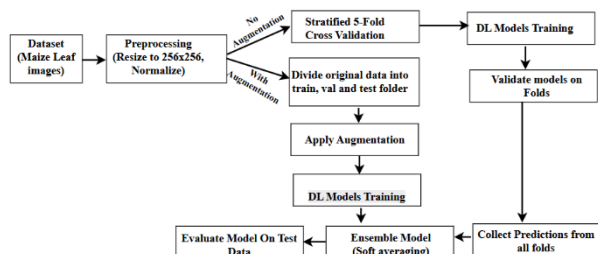


Fig. 1. Workflow of the proposed Ensemble model. Source-Self

The suggested approach incorporates different deep learning architectures into a single one using a soft averaging ensemble strategy to render maize disease classification additionally precise and trustworthy. It employs lightweight and high-performing CNN models comprising MobileNet, Xception, DenseNet169, and DenseNet201 as base learners. Each model is trained independently to get different and beneficial traits from photographs of maize leaves. MobileNet and Xception are effective at recording fine-grained spatial features because they are efficient and do not require a lot of computational power. The DenseNet variants, on the other hand, enhanced

feature reuse and make it easier for gradients to flow through their dense connectivity.

#### 3-1 Data Gathering

We used the Kaggle dataset (<https://www.kaggle.com/datasets/smaranjitghose/corn-or-maize-leaf-disease-dataset>) for our experiments. At first, 4188 pictures of four different types—Common Rust, Corn Blight, Gray Leaf, and Healthy Leaf were included in the gathered dataset. 1306 pictures of common rust, 574 pictures of gray leaf, 1146 pictures of corn blight, and 1162 pictures of healthy leaves were initially included in the dataset. The pictures are cropped, and dimensions are adjusted to the required input size of 256 x 256 pixels and normalized to the [0,1] range. To evaluate both generalization and overfitting resistance, two experimental setups were designed: one using original images without augmentation and another applying data augmentation to the training samples only. Overfitting is one of the greatest challenges in deep learning. It occurs when a model works superbly on training data but fails to perform well on test data that it hadn't encountered before. This is particularly frequent in tasks involving plant disease detection that require analyzing images, where the visual features might not be obvious, the datasets might not be balanced, and there might not be numerous photos per class. In order to get around this, we used a carefully selected collection of data augmentation techniques on the baseline dataset. The aforementioned comprised random rotation (between +40 and -40 degrees), width and height shifts (0.2), shear distortion (0.2), zoom (0.8-1.2), brightness variation (0.8-1.2), and horizontal flipping. In order to prevent the data from leaking, it was initially organized into train, val, and test folders, after which it was added to. To keep splitting and reconstructing under control, every single improved photo is quite distinct from the original ones. We implemented these changes because we observed that real leaf pictures possess a lot of natural contrast. Rescaling permits the model come together more rapidly during training. Rotation demonstrates the model how to keep its equilibrium intact while moving in a circle. The width alteration range shows how leaf shapes move in landscape photos, the height shift range shows how leaves are arranged in the field, and the horizontal flip shows how leaves interpret each other to avoid bias in direction. You can make your training dataset appealing without adding new images through the application of these methods. This not only protects the model from overfitting, but it also makes it easier to incorporate when new data comes in. We discovered that models trained with augmentation achieved superior performance on validation tests and displayed reduced accuracy variation between training and testing phases. It shows that they were better at making generalizations. Data augmentation is very important for

DenXNet, our ensemble model. With class imbalance in the dataset, augmentation helped artificially increase the presence of minority class samples, making the model less biased and more equitable in its predictions. Table 2 shows the no of enhanced images, and Fig. 2 shows sample of leaf images taken in to consideration.

Table 2: Dataset after Data Augmentation

Maize Classes	No of original images	Train	Validation	Test
Common Rust	1306	5224	653	653
Corn Blight	1146	5224	653	653
Gray Leaf	574	5224	653	653
Healthy	1164	5224	653	653

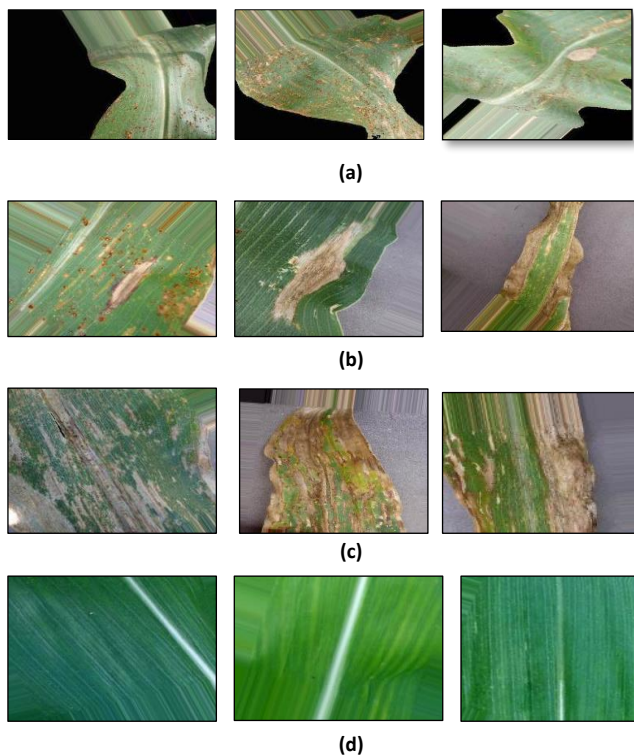


Fig. 2. Maize Leaf Dataset (a) Common Rust Diseased leaves (b) Corn Blight Diseased Leaves (c) Grey Spot Diseased Leaf (d) Healthy Leaves, Source: Kaggle dataset

### 3-2 Data Cleaning

The quality of the dataset directly influence the efficacy and credibility of machine learning models trained on it, making data cleaning a crucial step making data cleaning a crucial step in the data preparation pipeline. When a dataset is carefully cleaned, it can yield precise and meaningful results in a variety of data-driven studies, such as the classification of diseases that affect Maize leaves and other

analytical activities. Dividing the whole dataset into training, testing, and validation, the model can be trained on the training data, and after training, it will be tested on the remaining testing and validation data. We have used the standard method of splitting the data into an 80:10:10 ratio and followed the stratified 5-fold cross validation in case of non-augmented data. Cross validation helps to avoid data leakage and ensure that every fold has same proportion of images in each class . Images sent as input are converted to JPEG images and reshaped to size (256 x 256) for all used models. Following the transformation of the image data into numerical Numpy arrays, the range 0 to 1 was normalized. In the end, an unseen test image was used to validate and test the models to determine their degree of generalization.

### 3-3 Modelling of the proposed Ensemble model

The procedure of upgrading learning in a new process by using earlier acquired knowledge from a related task is known as transfer learning. Several things may be transferred from the earlier trained model to the newly selected task in transfer learning. The pre-trained model has already learned useful feature representations from the source data it was trained on. These feature representations in the lower and middle layers of the network can potentially be reused and fine-tuned for the new target task, avoiding having to learn them from scratch. **Table 3** summarizes the working principles and the key techniques used by different deep learning models. Among different ensemble strategies, the average ensemble offers a straightforward yet effective approach to integrate multiple heterogeneous models. In contrast to stacking methods, it eliminates the need for an additional meta-learner, which helps lower computational cost and minimizes the likelihood of overfitting. The averaging strategy differentiates itself from boosting or bagging because it isn't contingent on the model sequence or architecture type. This renders it an excellent means to integrate various frameworks like CNNs. This method improves the model's outputs more uniformly and consistently by averaging the prediction probabilities of the base models. It also assists in the model generalize more successfully when applied to fresh data.

The proposed ensemble model (DenXNet) is computationally modelled using four deep learning models: Xception, MobileNet, DenseNet169, and DenseNet201. These models were selected because they had better performance on their own when trained. First, predictions are generated from individual models using cross validation, and then these predictions are aggregated to get the final ensemble prediction. Predictions are made individually for each model in the ensemble,  $M_i$ , for a given input picture  $X$ . By averaging the prediction probabilities across multiple models, an ensemble blending

technique helps mitigate bias and variance. Averaging the outputs of each model enhances the system's overall ability to extrapolate and stability since each model reflects various aspects of its data distribution.  $P_i(X)$ , which represents each of these unique predictions, is a measure of the model's confidence ratings for each of the categorization categories. The ensemble prediction is obtained by a weighted averaging procedure once the predictions from each model

have been generated. The Ensemble Prediction( $X$ ) is calculated as the mean of the individual model forecasts by combining the predictions from each of the constituent models,  $M_i$ .

$$\text{Ensemble Prediction } (X) = \frac{1}{N} \sum_{i=1}^N P_i(X) \quad (1)$$

In this equation (1),  $N$  represents the total number of models in the ensemble. The resulting ensemble prediction

Table 3. Working principles and techniques used by Deep Learning model

Classification Model	Working Principle	Key Techniques	Advantages	Disadvantages
VGG16	A deep learning model with 16 layers arranged sequentially for extracting hierarchical features.	Small $3 \times 3$ convolutional kernels, Max pooling layers for downsampling, and ReLU activation functions. Dense, fully connected layers at the output.	Straightforward architecture, easy to implement, Strong baseline for classification tasks., Pre-trained models are widely available.	Consumes significant memory and computational power, Risk of overfitting on a small dataset. Inefficient use of parameters.
VGG19	An extension of VGG16, featuring 19 layers to enable deeper feature learning.	The same techniques as VGG16 with additional layers for enhanced capacity and uniform design structure.	Marginally better performance than VGG16, Simple and systematic architecture, Accessible pre-trained weights.	Increased resource requirements compared to VGG16, Slower training, and inference times.
InceptionV3	Processes feature using parallel convolutional paths in "Inception modules," enabling multi-scale feature extraction.	Decomposed convolutions to reduce the computational cost, Auxiliary classifiers for better gradient propagation., Batch normalization to stabilize training and parallel multi-scale processing.	Efficient computation with high accuracy., Effective for large and diverse datasets, it captures features at multiple resolutions.	More complex to design and implement. It requires careful hyperparameter tuning.
EfficientNetB0	A compact architecture that adjusts depth, width, and resolution systematically for optimized efficiency.	Compound scaling balances network dimensions and depth-wise separable convolutions to save computation	Scalable across different tasks, Lightweight for smaller datasets.	May underperform on very complex tasks. Scaling parameters need to be fine-tuned for the best results.
EfficientNetB7	A larger variant of EfficientNetB0 with increased depth, width, and resolution for improved representation capacity.	Same as EfficientNetB0 but scaled up, incorporates compound scaling to expand dimensions proportionally.	Exceptional performance on challenging benchmarks, maintains efficiency even at larger scales.	Demands substantial computational resources and is slower to train.
DenseNet169	Utilizes dense connectivity, where each layer receives inputs from its preceding layers, enhancing feature reuse and gradient flow.	Dense layer connections to improve feature propagation, Transition layers compress feature maps, and encourage parameter efficiency through reuse.	Reduces parameter redundancy, Mitigates vanishing gradients, and performs well on moderately sized datasets.	With high memory usage due to dense connections, Computational overhead grows with depth.
DenseNet201	A deeper variant of DenseNet169 is designed to extract more complex and detailed features through additional layers.	Similar techniques to DenseNet169 with increased depth, Improved transition, and compression strategies.	Excels in extracting detailed representations, Strong performance on complex tasks, and Efficient parameter utilization.	Higher computational and memory demands than DenseNet169. Training becomes slower as the network deepens.

Xception	A refinement of Inception that replaces standard convolutions with depthwise separable convolutions for greater efficiency and flexibility.	Depthwise separable convolutions split spatial and channel-wise filtering, and Skip connections improve gradient flow.	Competitive accuracy across datasets reduces redundant computations in convolution operations.	Requires careful tuning to achieve optimal performance and demands higher computational resources despite being efficient.
MobileNet	A lightweight model designed for mobile and embedded systems, focusing on reducing computational and memory overhead.	Depthwise separable convolutions to minimize computation, Width and resolution multipliers adjust the model size, Global average pooling prevents overfitting.	Highly efficient for real-time applications, optimized for resource-constrained devices.	Lower accuracy on very complex datasets, Limited capability to handle tasks requiring deep feature extraction.
Ensemble Model	Combines predictions from multiple architectures (e.g., Xception, MobileNet, DenseNet169, DenseNet201) to enhance overall performance and robustness.	Weighted averaging assigns importance to each model, Stacking uses outputs of individual models as inputs for a meta-classifier, and Bagging improves prediction stability.	Aggregates strengths of diverse models, improves accuracy and reduces bias, and increases robustness against overfitting.	Higher computational and memory requirements due to multiple models, Complex implementation, and integration process.

provides a consolidated estimate of the classification outcome, harnessing the collective insights from multiple models to enhance accuracy and reliability. The algorithm for the proposed model is as follows:

- Step 1: Load the pre-trained models (Xception, MobileNet, DenseNet169, DenseNet201) from their respective paths.
- Step 2: Modify the loaded models to remove the last layer (Softmax layer), as we want to use them as feature extractors.
- Step 3: Define an input tensor for our ensemble model with the shape (256, 256, 3).
- Step 4: Pass the input tensor through each pre-trained model to get their outputs.
- Step 5: Combine the outputs of the pre-trained models by taking their average.
- Step 6: Define the ensemble model using the input tensor and the averaged outputs.

Let

- $I$  will be the input image tensor with dimensions (256, 256, 3)
- $M_1$  be the Xception model.
- $M_2$  be the MobileNet model.
- $M_3$  be the DenseNet169 Mode
- $M_4$  be the DenseNet201 model
- $O_1$  be the output tensor of  $M_1$  given input  $I$
- $O_2$  be the output tensor of  $M_2$  given input  $I$ .
- $O_3$  be the output tensor of  $M_3$  given input  $I$ .
- $O_4$  be the output tensor of  $M_4$  given input  $I$ .
- $E$  be the ensemble model.

The operations performed in the code can be mathematically modeled as follows:

1. Load Pre-Trained Models:  $M_1, M_2, M_3, M_4$  are pre-trained models.
2. Remove Last Layer and Modify Models: Let  $fn_1(\cdot)$ ,  $fn_2(\cdot)$ ,  $fn_3(\cdot)$  and  $fn_4(\cdot)$  be the functions representing the modified Xception, MobileNet, DenseNet169 and DenseNet201 models, respectively, after removing their last softmax layer
 
$$fn_1(I) = \text{Modified Xception}(I) \quad (2)$$

$$fn_2(I) = \text{Modified MobileNet}(I) \quad (3)$$

$$fn_3(I) = \text{Modified DenseNet169}(I) \quad (4)$$

$$fn_4(I) = \text{Modified DenseNet201}(I) \quad (5)$$

3. Ensemble Model: The ensemble model,  $E$ , takes  $I$  as input and computes the average of the outputs of  $f_1, f_2, f_3$ , and  $f_4$ :

$$O_{ensemble} = \frac{fn_1(I) + fn_2(I) + fn_3(I) + fn_4(I)}{4} \quad (6)$$

where,  $O_{ensemble}$  is the final average probabilities

Therefore, the mathematical model for the ensemble model  $E$  can be exemplified as:

$$E(I) = O_{ensemble} = \frac{1}{4} \sum_{i=1}^4 fn_i(I) \quad (7)$$

Then, the final predicted class label  $\hat{y}$  is:

$$\hat{y} = \arg \max_{k \in \{1, \dots, 4\}} E(I)[k] \quad (8)$$

where,  $\hat{y}$  is the predicted class label from the ensemble. Each base model is trained using categorical cross-entropy loss:

$$\mathcal{L}_{CE} = - \sum_{k=1}^K y_k \cdot \log \hat{y}_k \quad (9)$$

Here, K is the number of classes,

$y = [y_1, y_2, \dots, y_K]$  be the one-hot encoded ground truth label vector, where  $y_k = 1$  if the sample belongs to class k, and 0 otherwise .

$\hat{y} = [\hat{y}_1, \hat{y}_2, \dots, \hat{y}_k]$  be the predicted probability from the model E(I).

### 3-4- Model Configuration & Architecture

The pre-trained individuals used for the suggested job are VGG16, VGG19, InceptionV3, EfficientNetB0, EfficientNetB7, DenseNet169, DenseNet201, Xception, Mobilenet, and an Ensemble model using Xception, MobileNet, DenseNet169, and DenseNet201 CNN models using Adam Optimizer for the classification of 4 classes of Maize. To categorize images of maize crop fields, the model is developed using an elaborate Python library called Keras, which is used as a backend atop an open-source deep learning framework called TensorFlow. The input is processed through a heap of convolutional layers with a convolution filter size of  $3 \times 3$  and convolution strides in x and y directions (1,1) pixels. The image dimension is set to  $256 \times 256$  pixels with depth 3 (RGB channels). After convolution, the spatial size is maintained with hyper-parameter padding 1. All hidden layers have taken into account the activation function "ReLU," and the last layer applies the "softmax" function to guarantee that the projected probability output values fall between 0 and 1. The network uses 25 epochs and a batch size of 32 with a learning rate of 0.001 and a dropout rate of 0.5. The network has been optimized through the use of the logarithmic loss function and gradient descent optimization technique with categorical cross-entropy. The input of the model consists of  $256 \times 256$ -pixel images of maize crops. After that, it has a sequence of convolutional and pooling layers that extract features, an output layer, and a fully connected layer that interprets the information. Four neurons make up the output layer, which is the actual number of classes that the image being processed must be categorized into. The models were run on a desktop PC that was set up with an Intel Core i7-8565U CPU @ 1.80 GHz, a 64-bit operating system, x64-based processor, 16.0 GB (15.9 GB usable) RAM, and one NVIDIA GeForce GTX 1070 GPU.

## 4-Results and Discussion

Ensemble modelling helps to amalgamate the predictions of multiple models and provides more precise results with high accuracy and precision [31-34]. It is a robust and efficient means of integrating multiple heterogeneous models without requiring an additional meta-learner.

By averaging the probabilistic outputs of base model, it minimizes overfitting and yields more stable, generalized prediction across diverse datasets. In this study, nine individual models- VGG19, VGG16, InceptionV3, EfficientNetB0, EfficientNetB7, DenseNet169, Densenet201, Xception and MobileNet were implemented and evaluated. Additionally, two ensemble models combining MobileNet with DenseNet169 and MobileNet with Xception along with proposed ensemble model, DenXNet based on four models were developed to analyze the impact of hybridization on performance. However experimental results revealed that the individual four model configurations achieved superior performance compared to two model ensembles, demonstrating their stronger feature extraction and generalization capabilities. Using the corresponding images of the maize crop, the models were trained and evaluated, taking into account the pre-learned weights of ImageNet dataset in each layer until convergence. **Table 4** shows the training accomplishments of various models for the Maize diseased leaf images dataset using the Adam optimizer. The experimental results demonstrate how different deep learning models perform when data augmentation is utilised and when it isn't. DenseNet201 had the best testing performance of 0.9878 with augmentation among the individual architectures. DenseNet169 (0.969) and InceptionV3 (0.9696) were the next closest. Since their convolutional layers are somewhat densely connected, these models were capable of predicting well and extracting features efficiently. The results further indicate that data augmentation renders all models considerably more accurate by making them more robust to variations in lighting, orientation, and leaf conditions. For example, MobileNet's testing accuracy improves from 0.9334 (without enhancement) to 0.948 (with enhancement).

Table 4. Training performance of models for Maize Leaf disease images Source: Anaconda

<i>Model name</i>	<i>Accuracy Score With Augmentation</i>			<i>Accuracy Score Without Augmentation</i>		
	<i>Training</i>	<i>Validation</i>	<i>Testing</i>	<i>Training</i>	<i>Validation</i>	<i>Testing</i>
VGG19	0.9389	0.936	0.940	0.910	0.905	0.910
VGG16	0.955	0.960	0.9484	0.925	0.9324	0.922
InceptionV3	0.954	0.962	0.9696	0.925	0.935	0.935
EfficientNetB0	0.9767	0.974	0.9818	0.950	0.965	0.955
EfficientNetB7	0.9307	0.968	0.9666	0.905	0.935	0.935
DenseNet169	0.986	0.976	0.969	0.9606	0.9606	0.9577
DenseNet201	0.988	0.988	0.9878	0.9376	0.9486	0.9479
Xception	0.9272	0.9420	0.9575	0.9028	0.9046	0.9024
MobileNet	0.94	0.95	0.948	0.93	0.9272	0.9334
Ensemble Model: MobileNet, Densenet169	0.995	0.987	0.98	0.9675	0.9646	0.965
Ensemble Model: MobileNet, Xception	0.985	0.960	0.955	0.92	0.9354	0.9354
Ensemble Model: Xception, MobileNet, DenseNet169, DenseNet201	0.9946	0.9812	0.9896	0.9787	0.9742	0.97

It shows that augmentation works to safeguard models from overfitting while additionally rendering them adjustable. Ensemble learning had been implemented to investigate into potential advantages of integrating models. The MobileNet-DenseNet169 ensemble had an impeccable test accuracy of 0.980 (with augmentation), which is far greater than a majority of individual models. The MobileNet-Xception setup, on the contrary hand, hadn't been as accurate. Thus demonstrating that model integration counts for ensemble success. The DenXNet four-model ensemble had its highest testing accuracy, 0.9846, without as well as with the enhancement. It executed better than any of the other setups. The enhancement shows just how beneficial it is to integrate numerous architectures that can record multiple kinds of feature hierarchy and spatial representations. The ensemble model is more dependable, indicating that it can extrapolate more accurately, stay stable, and cope with new data.

The study illustrates that individual CNN-based models, comprising DenseNet201 and InceptionV3, have been very accurate. However, hybrid ensemble architectures provide the most precise and trustworthy outcomes. These traits allow them to be useful for practical applications, such as discovering diseases in crops as well as maintaining an eye on their health. **Fig.3** shows the incorrect predictions through the creation of confusion matrices compared to all four unique models and the proposed Ensemble Model. All of these were tested on 653 maize leaf images that had never

been seen before and were made using data augmentation. The individual models function quite well, with DenseNet201 and DenseNet169 correctly recognizing the most samples in all four disease classes: Common Rust, Corn Blight, Grey Leaf Spot, and Healthy. Gradient-weighted Class Activation Mapping (GRAD-CAM) was likewise employed to illustrate the attention regions of different models to make them easier to understand. The heat maps in **Fig. 4** illustrate how various architectures focused on the diseased portions of maize leaves. MobileNet produced broader and less defined attention zones, whereas DenseNet169 and Xception showed improved localization around infected areas. The MobileNet-DenseNet169 ensemble performed an outstanding job of identifying diseased areas while minimizing background noise. The Xception-DenseNet169 ensemble performed a superior task of finding lesions with minimal background noise. DenXNet demonstrated that the majority of biologically significant and broadly distributed activations, indicating that the ensemble approach enhanced both classification accuracy and the ability to understand frameworks. Still, there were certain ones misclassifications, especially between disease categories that are similar, like Common Rust and Grey Leaf Spot. This can happen given that the symptoms of each of these illnesses are similar, rendering it challenging to separate them. **Fig. 5** illustrates how the model inaccurately anticipated Blight with a confidence score of 29.8%, given that the true label for the maize leaf

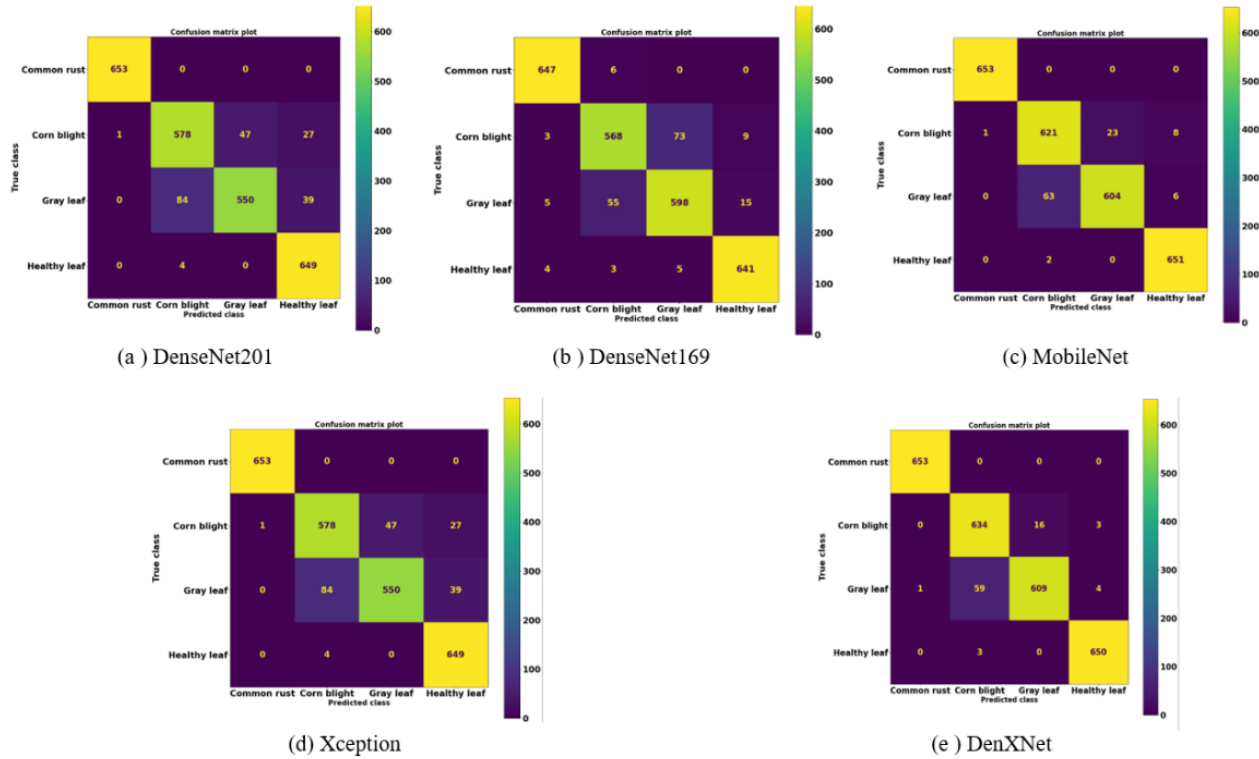


Fig 3. Confusion matrices for four pre-trained deep learning models and the proposed ensemble model

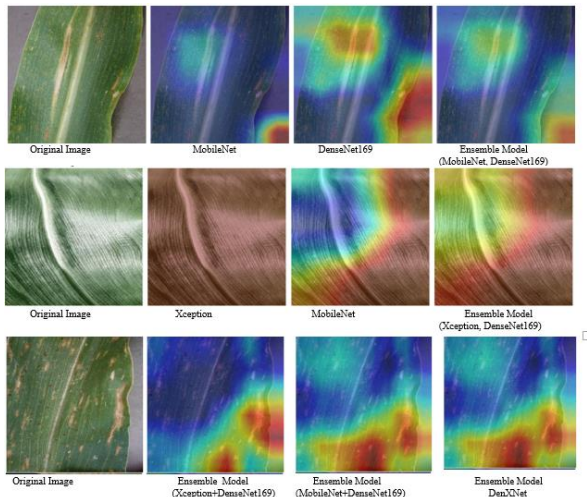


Fig. 4. Grad Cam Visualizations showing model attention on Maize Leaf lesion

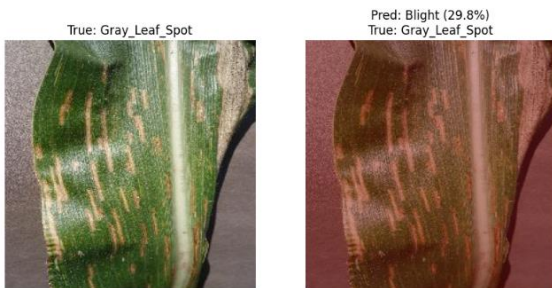


Fig.5 Error and Misclassification between Gray leaf and Blight

sample is Grey Leaf Spot. The Grad-CAM visualisation illustrates that the model's focus had been spread over both diseased and healthy leaf areas. This indicates that it was hard to pinpoint the subtle lesion patterns that are unique to Grey Leaf Spot. This misclassification is predominantly due to the fact that Blight and Gray Leaf Spot look similar. Both have long, brownish lesions with parallel veins and similar texture gradients. These patterns become harder to tell differentiate when the conditions and background change, leading to the model mix up their spatial and color features. Also, the overlapping feature representations that are learned during convolutional processing can make it harder to differentiate the difference between classes. These cases demonstrate the importance of fine-grained extraction of characteristics and attention modification in distinguishing diseases with similar visual traits more effectively. Future enhancements could include incorporation of multi-scale attention modules, spectral feature learning, or contrast reduction optimization to augment the model's discriminative ability. **Table 5** lists the performance metrics calculated from the confusion matrices, and includes classification accuracy, recall, and precision for each class. A more comprehensive look at the results metrics shows that every single deep learning model encompasses its own strengths, and weaknesses when it applies to classifying the maize leaf disease. The Common rust category had the most variances across models. As an example, VGG19 had a high recall of 0.94 but a very low precision of 0.08, which

indicates that it regularly misclassified other diseases as Common Rust. The texture and colour deviations introduced by enhancement may have prompted the model to overfit generalised rust-like patterns, thereby failing to capture deeper, discriminative details. On the contrary hand, more complicated architectures like DenseNet201 and EfficientNetB7 got nearly perfect accuracy (0.99 and 0.95, respectively), showing that they were considerably better at detecting structural features that were specific to diseases. Another problem that continued to arise was incorrectly identifying Grey Leaf and Healthy Leaf because they matched so much alike in colour and texture. Models consisting of InceptionV3 and EfficientNetB0 achieved F1-scores of approximately 0.84–0.92 for Grey Leaf, indicating that the models were only slightly confused. DenseNet201 and MobileNet did better than others with these classes, showing a good equilibrium among precision and recall. MobileNet is a lightweight model that had a significant recall rate, making it a good choice for actual-time or mobile apps. However, it did over-detect healthy samples a little bit. Ensemble methods gave the best overall results. Models that combined MobileNet, DenseNet169, Xception, and DenseNet201 got almost perfect F1-scores, which fixed errors in each model. This shows that ensembles work more successfully when various architectures have different strengths, rendering them more resilient and reliable.

## 5- Conclusion

The present research focused on developing an automated framework for identifying the presence of maize leaf illnesses employing both individual deep learning architectures and ensemble CNN architectures. We trained and evaluated nine revolutionary CNN architectures: VGG19, VGG16, InceptionV3, EfficientNetB0, EfficientNetB7, DenseNet169, DenseNet201, Xception, and MobileNet. We employed two distinct methods: one with enhancement and one without any enhancement. Data augmentation significantly enhanced the framework's capacity to generalize by making its features more unique and less likely to overfit. The proposed DenXNet model, which is formed up of DenseNet-169, DenseNet-201, Xception, and MobileNet, performed the best overall out of all the models that have been tested. It enjoyed the best testing accuracy, better stability, and stronger strength than those with one-model or two-model ensembles. DenXnet combined different architectures so that the model could use the extensive connectivity of DenseNets, the depth-

Table 5: Training Performance of Model for Maize Leaf with augmentation

Model	Class name	Precision	Recall	F1-Score
VGG19	Common Rust	0.8	0.04	0.08
	Corn Blight	0.58	0.94	0.71
	Gray Leaf	0.89	0.81	0.85
	Healthy Leaf	0.69	0.97	0.81
VGG16	Common Rust	0.97	0.43	0.59
	Corn Blight	0.61	0.97	0.75
	Gray Leaf	0.94	0.78	0.86
	Healthy Leaf	0.86	0.98	0.92
InceptionV3	Common Rust	0.99	1	1
	Corn Blight	0.8	0.92	0.85
	Gray Leaf	0.93	0.76	0.84
	Healthy Leaf	0.95	0.97	0.96
EfficientNetB0	Common Rust	1	0.42	0.9
	Corn Blight	0.73	0.93	0.82
	Gray Leaf	0.87	0.97	0.92
	Healthy Leaf	0.83	0.99	0.9
EfficientNetB7	Common Rust	0.95	1	0.97
	Corn Blight	0.85	0.92	0.88
	Gray Leaf	0.94	0.81	0.87
	Healthy Leaf	0.97	0.97	0.97
DenseNet169	Common Rust	0.98	0.99	0.99
	Corn Blight	0.90	0.87	0.88
	Gray Leaf	0.88	0.89	0.89
	Healthy Leaf	0.96	0.98	0.97
DenseNet201	Common Rust	0.99	1	0.99
	Corn Blight	0.87	0.89	0.88
	Gray Leaf	0.92	0.82	0.87
	Healthy Leaf	0.91	0.99	0.95
Xception	Common Rust	1	1	1
	Corn Blight	0.87	0.89	0.88
	Gray Leaf	0.92	0.82	0.87
	Healthy Leaf	0.91	0.99	0.95
MobileNet	Common Rust	1	1	1
	Corn Blight	0.91	0.95	0.93
	Gray Leaf	0.96	0.90	0.93
	Healthy Leaf	0.98	1	0.99
Ensemble Model: MobileNet, DenseNet169	Common Rust	0.98	0.98	0.98
	Corn Blight	0.92	0.95	0.93
	Gray Leaf	0.91	0.85	0.88
	Healthy Leaf	1	1	1
Ensemble Model: MobileNet, Xception	Common Rust	0.97	0.97	0.97
	Corn Blight	0.84	0.93	0.90
	Gray Leaf	0.84	0.79	0.82
	Healthy Leaf	0.99	0.99	0.99
Ensemble Model : (Xception, MobileNet, DenseNet169, DenseNet201)	Common Rust	1	1	1
	Corn Blight	0.91	0.97	0.94
	Gray Leaf	0.97	0.90	0.94
	Healthy Leaf	0.98	1	0.99

dependent separable convolutions of MobileNet, and the effective retrieval capacity of Xception. This combination of characteristics lets DenXNet decide simultaneously fine-grained and global disease features, which boosts the accuracy of classification and its capacity to make

assumptions across a wide range of pictures conditions. Grad-CAM representations also showed that the ensemble model properly focused on areas affected by disease. This made the model easier to comprehend while providing it more credibility as a reliable tool. The model was much better at generating predictions when augmentation

techniques were employed because they reduced overfitting and boosted feature diversity. The ensemble configurations were more accurate and stable than the individual models, which shows how integrating different feature visualizations can be helpful. By showing how the models found affected by the disease areas on the leaf surface, Grad-CAM representation made the models easier to understand. The aforementioned visual representations showed the fact that the ensemble models not only made predictions that were more accurate, but they also identified more specific and biologically relevant areas of feature activation. However, there were still a few minor errors in categorising diseases that looked similar, like Blight and Grey Leaf spot. This was probable because their symptoms were similar and the visual differences were small. In general, the study shows that incorporating data augmentation and ensemble modelling can be carefully done to substantially enhance the classification of illnesses in maize. In addition, CNN-based and ensemble models have shown immense potential, there nevertheless remain some research gaps which require to be filled. The research overwhelmingly emphasized on convolutional architectures and did not incorporate highly sophisticated temporal or spatial mechanisms such as BiLSTM, Self-attention, or Transformer networks, which could improve contextual feature extraction and inter-class discrimination. Later studies could enhance this study through the inclusion of Transformer-based hybrid architectures to further clarify long-range dependencies and intricate variations within corresponding disease categories integrating explainable AI (XAI) methodologies beyond Grad-CAM, which include Layer-wise Relevance Propagation or SHAP, could increase interpretability. Finally, deployment on edge or mobile devices enables real-time, low-cost field diagnosis, directly assisting farmers in precision agriculture systems.

## References

- [1] A. H. Ali, A. Youssef, M. Abdelal, and M. A. Raja, "An ensemble of deep learning architectures for accurate plant disease classification," *Ecol. Inform.*, vol. 81, 102618, 2024, doi: 10.1016/j.ecoinf.2024.102618.
- [2] S. Vallabhajosyula, V. Sistla, and V. K. K. Kolli, "A novel hierarchical framework for plant leaf disease detection using residual vision transformer," *Heliyon*, vol. 10, no. 9, 2024, doi: 10.1016/j.heliyon.2024.e29912.
- [3] R. Lumbantoruan, N. Rajagukguk, A. U. Lubis, M. Claudia, and H. Simanjuntak, "Two-step convolutional neural network classification of plant disease," *IAES Int. J. Artif. Intell.*, vol. 14, no. 1, pp. 584–591, 2025, doi: 10.11591/ijai.v14.i1.pp584-591.
- [4] L. Miao *et al.*, "A high-precision automatic diagnosis method of maize developmental stage based on ensemble deep learning with IoT devices," *Comput. Electron. Agric.*, vol. 227, 109608, 2024, doi: 10.1016/j.compag.2024.109608.
- [5] W. H. Zeng, H. Li, G. Hu, and D. Liang, "Identification of maize leaf diseases by using the SKPSNet-50 convolutional neural network model," *Sustain. Comput. Informatics Syst.*, vol. 35, 100695, 2022, doi: 10.1016/j.suscom.2022.100695.
- [6] I. Attri, L. K. Awasthi, T. P. Sharma, and P. Rathee, "A review of deep learning techniques used in agriculture," *Ecol. Inform.*, vol. 77, 102217, 2023, doi: 10.1016/j.ecoinf.2023.102217.
- [7] M. Yang, A. Sekhari Seklouli, L. Ren, Y. He, X. Yu, and Y. Ouzrout, "A new mobile diagnosis system for estimation of crop disease severity using deep transfer learning," *Crop Prot.*, vol. 184, 106776, 2024, doi: 10.1016/j.cropro.2024.106776.
- [8] S. Jenifer, M. J. Carmel Mary Belinda. Convolutional Neural Networks for Medical Image Segmentation and Classification: A Review. *Journal of Information Systems and Telecommunication (JIST)* 2023;11(44):347-358. doi:10.61186/jist.37936.11.44.347
- [9] O. Erenstein, M. Jaleta, K. Sonder, K. Mottaleb, and B. M. Prasanna, "Global maize production, consumption and trade: trends and R&D implications," *Food Secur.*, vol. 14, no. 5, pp. 1295–1319, 2022, doi: 10.1007/s12571-022-01288-7.
- [10] T. Phattaraworamet, S. Sangsuriyun, P. Kutchomsri, and S. Chokphoemphun, "Image classification of lotus in Nong Han Chaloe Phrakiat Lotus Park using convolutional neural networks," *Artif. Intell. Agric.*, vol. 11, pp. 23–33, 2024, doi: 10.1016/j.aiaa.2023.12.003.
- [11] M. A. Jabed and M. A. Azmi Murad, "Crop yield prediction in agriculture: A comprehensive review of machine learning and deep learning approaches, with insights for future research and sustainability," *Heliyon*, vol. 10, no. 24, 2024, doi: 10.1016/j.heliyon.2024.e40836.
- [12] A. Pal and V. Kumar, "AgriDet: Plant Leaf Disease severity classification using agriculture detection framework," *Eng. Appl. Artif. Intell.*, vol. 119, 105754, 2023, doi: 10.1016/j.engappai.2022.105754.
- [13] X. Sun and J. Wei, "Identification of maize disease based on transfer learning," *J. Phys. Conf. Ser.*, vol. 1437, no. 1, 2020, doi: 10.1088/1742-6596/1437/1/012080.
- [14] S. Sladojevic, M. Arsenovic, A. Anderla, D. Culibrk, and D. Stefanovic, "Deep Neural Networks Based Recognition of Plant Diseases by Leaf Image Classification," *Comput. Intell. Neurosci.*, 2016, doi: 10.1155/2016/3289801.
- [15] X. Lv, X. Zhang, H. Gao, T. He, Z. Lv, and L. Zhangzhong, "When crops meet machine vision: A review and development framework for a low-cost nondestructive online monitoring technology in

- agricultural production,” *Agric. Commun.*, vol. 2, no. 1, 100029, 2024, doi: 10.1016/j.agrcom.2024.100029.
- [16] P. Chaudhary, A. K. Chaudhari, A. Cheeran, and S. Godara, “Color Transform Based Approach for Disease Spot Detection on Plant Leaf,” *Int. J. Comput. Sci. Telecommun.*, vol. 3, no. 6, pp. 65–71, 2012,
- [17] S. B. Patil and S. K. Bodhe, “Leaf disease severity measurement using image processing,” *Int. J. Eng. Technol.*, vol. 3, no. 5, pp. 297–301, 2011.
- [18] M. U. Ahmad, S. Ashiq, G. Badshah, A. H. Khan, and M. Hussain, “Feature Extraction of Plant Leaf Using Deep Learning,” *Complexity*, 2022, doi: 10.1155/2022/6976112.
- [19] E. Alehegn, “Maize Leaf Diseases Recognition and Classification Based on Imaging and Machine Learning Techniques,” *Int. J. Innov. Res. Comput. Commun. Eng.*, vol. 5, no. 12, pp. 1–11, 2017.
- [20] S. Mishra, R. Sachan, and D. Rajpal, “Deep Convolutional Neural Network based Detection System for Real-time Corn Plant Disease Recognition,” *Procedia Comput. Sci.*, vol. 167, pp. 2003–2010, 2020, doi: 10.1016/j.procs.2020.03.236.
- [21] B. S. Anami, N. N. Malvade, and S. Palaiah, “Artificial Intelligence in Agriculture Deep learning approach for recognition and classification of yield affecting paddy crop stresses using field images,” *Artif. Intell. Agric.*, vol. 4, pp. 12–20, 2020, doi: 10.1016/j.iaia.2020.03.001.
- [22] M. Agarwal, S. K. Gupta, and K. K. Biswas, “Development of Efficient CNN model for Tomato crop disease identification,” *Sustain. Comput. Informatics Syst.*, vol. 28, 100407, 2020, doi: 10.1016/j.suscom.2020.100407.
- [23] K. P. Panigrahi, H. Das, A. K. Sahoo, and S. C. Moharana, “Maize Leaf Disease Detection and Classification Using Machine Learning Algorithms,” *Adv. Intell. Syst. Comput.*, vol. 1119, pp. 659–669, 2020, doi: 10.1007/978-981-15-2414-1\_66.
- [24] S. Pudumalar and S. Muthuramalingam, “Hydra: An ensemble deep learning recognition model for plant diseases,” *J. Eng. Res.*, 2024, doi: 10.1016/j.jer.2023.09.033.
- [25] S. K. Subramanya and N. Bettahalli, “Enhanced detection of tomato leaf diseases using ensemble deep learning: INCVX-NET model,” *IAES Int. J. Artif. Intell.*, vol. 13, no. 4, pp. 4757–4765, 2024, doi: 10.11591/ijai.v13.i4.pp4757-4765.
- [26] J. Nakatumba-Nabende and S. Murindanyi, “Deep learning models for enhanced in-field maize leaf disease diagnosis,” *Mach. Learn. with Appl.*, vol. 20, 100673, 2025, doi: 10.1016/j.mlwa.2025.100673.
- [27] Maiti, Abdallah, Hanini, Mohamed, Abarda, Abdallah. Resolving Class Imbalance in Medical Classification: Technique Comparison and Performance Evaluation. *Journal of Information Systems and Telecommunication (JIST)* . 2025;13(51):177-188. .61882/jist.49725.13.51.177
- [28] S. Coulibaly, B. Kamsu-Foguem, D. Kamissoko, and D. Traore, “Deep neural networks with transfer learning in millet crop images,” *Comput. Ind.*, vol. 108, pp. 115–120, 2019, doi: 10.1016/j.compind.2019.02.003.
- [29] G. Wang, H. Yu, and Y. Sui, “Research on Maize Disease Recognition Method Based on Improved ResNet50,” *Mob. Inf. Syst.*, 2021, doi: 10.1155/2021/9110866.
- [30] M. M. Khalid and O. Karan, “Deep Learning for Plant Disease Detection,” *Int. J. Math. Stat. Comput. Sci.*, vol. 2, pp. 75–84, 2023, doi: 10.59543/ijmscs.v2i.8343.
- [31] A. Daza, C. F. Ponce Sánchez, G. Apaza-Perez, J. Pinto, and K. Zavaleta Ramos, “Stacking ensemble approach to diagnosing the disease of diabetes,” *Informatics Med. Unlocked*, vol. 44, 2024, doi: 10.1016/j.imu.2023.101427.
- [32] M. Aqil *et al.*, “Deep learning based stacking ensembles for tropical sorghum classification,” *J. Agric. Food Res.*, vol. 21, 101931, 2025, doi: 10.1016/j.jafr.2025.101931.
- [33] A. Ghasemieh, A. Lloyed, P. Bahrami, P. Vajar, and R. Kashef, “A novel machine learning model with Stacking Ensemble Learner for predicting emergency readmission of heart-disease patients,” *Decis. Anal. J.*, vol. 7, 100242, 2023, doi: 10.1016/j.dajour.2023.100242.
- [34] A. Asil, H. Alipour, S. Mojtahedzadeh, and H. Asil, “Ensemble learning of Ada-boosting Based on Deep Weighting for Classification of Hand-written Numbers in Persian (With the doctors’ (With the doctors’ prescription approach),” *J. Inf. Syst. Telecommun.*, vol. 12, no. 2, pp. 162–169, 2024, doi: 10.61186/jist.41053.12.46.162.

# Detecting Synchronized Hate Speech in Online Social Networks via Social Synchrony and Ant Colony Optimization

Shabana Nargis Rasool<sup>1</sup>, Sarika Jain<sup>2\*</sup>, Ajay Vikram Singh<sup>2</sup>

<sup>1</sup>.Department of Computer Science, Islamic University of Science and Technology, Kashmir, India

<sup>2</sup>.Amity Institute of Information Technology, Amity University Noida, Uttar Pradesh, India.

Received: 25 Jul 2025/ Revised: 04 Dec 2025/ Accepted: 06 Jan 2026

## Abstract

Online platforms have become fertile grounds for hate speech, often spreading through bursts of coordinated user activity. Detecting such patterns requires more than analyzing individual posts, as it calls for understanding the collective rhythm of online interactions. In the present study, we present SIACO (Social Synchrony Identification using Ant Colony Optimization), a nature-inspired framework that detects hate-speech events by tracing synchrony in user behaviour. SIACO models how hateful expressions emerge and fade collectively, using Ant Colony Optimization to refine linguistic features and improve classification accuracy. Upon evaluation on a Twitter dataset, the framework consistently outperforms both traditional machine learning models and transformer-based baselines, achieving up to a 10% improvement across major evaluation metrics. The framework also offers interpretable insights into the linguistic and temporal cues driving coordinated hate. The performance scores obtained highlight the value of looking at hate speech not just as text, but as a social phenomenon unfolding in synchrony.

**Keywords:** Hate Speech; Social Synchrony; Ant Colony Optimization; Feature Selection; Online Social Networks.

## 1- Introduction

The extensive prevalence of Online Social Networks (OSNs) is demonstrated by a recent poll conducted by Nielsen Online [1], which revealed that social media has surpassed email as the most dominant online activity. More than two-thirds of the global Internet population now engages with social media and blogs, accounting for nearly 10% of all Internet use. Platforms such as LinkedIn, Facebook, and Twitter have become indispensable to modern digital life, facilitating interactions, information exchange, and content discovery across personal, professional, and social contexts. In today's fast-paced world, where time constraints limit face-to-face interactions, online communication offers a vital alternative for maintaining relationships and expressing opinions. Individuals can share thoughts, exchange knowledge, and build communities that transcend geographic and temporal barriers. The influence of social media on society continues to expand and shows no signs of diminishing; platforms like Twitter, in particular, have

become powerful arenas for the public exchange of ideas and emotions [2].

While OSNs empower participation and connectivity, they also serve as conduits for hostility and discrimination [3]. On the other hand, the mechanisms that amplify positive engagement, virality, collective attention, and immediacy can also accelerate the spread of hate speech. Online hate speech represents more than an aggregation of individual acts of incivility; it is often collectively orchestrated, arising through synchronized bursts of hostile communication [4]. Conventional hate-speech detection methods typically examine content at the level of single posts or users, emphasizing textual features and linguistic cues. Such approaches overlook the 'social dynamics', that are the patterns of coordination and reinforcement through which harmful discourse proliferates [5]. It may be hypothesized that incorporating social synchrony signals and optimization-based feature selection can significantly improve the accuracy and robustness of hate-speech detection compared to content-only baselines.

Human behavior, whether offline or online, is inherently synchronized. The coordinated surges in online activity,

---

✉ Sarika Jain  
Ashusarika@gmail.com

where users post, retweet, or comment in temporal alignment, reflect a phenomenon termed 'social synchrony' [6]. On social networks, synchrony manifests as the collective rhythm of communication, moments when users act in harmony, consciously or unconsciously, around shared sentiments or ideological themes. Understanding this synchrony provides a valuable lens through which to study the amplification of hate speech, revealing how seemingly independent expressions combine into collective waves of hostility. The present study introduces SIACO (Social Synchrony Identification using Ant Colony Optimization) [7]. This novel, nature-inspired computational framework reconceptualizes hate-speech detection as a problem of identifying collective behavioral patterns. The framework integrates social-science theory and computational intelligence to model the emergence of hateful discourse as an outcome of synchronized user behavior. Considering inspiration from the foraging behavior of ant colonies, self-organizing systems capable of discovering optimal solutions through pheromone-based communication, SIACO employs Ant Colony Optimization (ACO) to refine feature selection and classification in textual data. Through iterative learning, ACO identifies the most salient and contextually coherent linguistic features that characterize coordinated hate expression. This fusion of social synchrony analysis and swarm intelligence introduces a new paradigm for understanding and mitigating online hostility, offering a fresh perspective on hate speech detection [8].

The study is based on the hypothesis that hate speech in online networks exhibits detectable patterns of synchrony, which can be captured computationally to improve detection accuracy. By incorporating ACO into the learning process, models can more effectively reveal the underlying relationships between temporal, relational, and linguistic signals that traditional classifiers, including those based on transformer architectures, might overlook [9].

The proposed framework of SIACO integrates several sequential components in a comprehensive approach: data collection from Twitter; extensive text preprocessing to remove noise and standardize input; feature extraction using Bag-of-Words (BoW) and Term Frequency–Inverse Document Frequency (TF-IDF) representations; optimization via ACO; and classification through multiple supervised learning algorithms. This comprehensive approach reassures the audience about the thoroughness of the framework. The contribution of this work is two-fold. First, it advances the computational frontiers of hate-speech detection by introducing a hybrid optimization framework that enhances both performance and interpretability. Second, it offers a new conceptual understanding of online hostility, emphasizing hate speech as a 'collective social phenomenon' rather than an isolated textual one. This two-fold contribution not only enhances our understanding of hate speech in online networks but also provides a novel

computational framework for its detection. The remainder of this paper is organized as follows: Section 2 reviews the related literature and identifies the research gap; Section 3 describes the proposed SIACO methodology, the experimental setup and evaluation metrics, Section 4 outlines results and discussion; and Section 5 concludes with limitations and future research directions.

## 2- Related Work

Research on event detection and social synchronization within online social networks (OSNs) has evolved along several intertwined paths, each contributing to understanding how people behave and interact in digital spaces. In the last decade, numerous studies have sought to capture the pulse of collective human behavior over online social networks, where the primary focus remains: how individual actions, when repeated and shared across vast user communities, form patterns of synchronization that reflect real-world coordination, emotion, and influence. Despite a rich progress in behavioral modeling and machine learning, relatively little attention has been given to the idea that hate speech itself can emerge as a synchronized, collective phenomenon.

One of the earliest efforts to model such interconnected human behaviour was proposed by De et al. [10], who developed a Dynamic Bayesian Network (DBN) model to predict user actions over time. Their approach emphasized the influence of one user's activity on another's, revealing that social interactions online are rarely independent and often unfold in rhythmic, interdependent ways. Similarly, Benevenuto et al. [11] analyzed a vast dataset combining four prominent OSNs: LinkedIn, Hi5, MySpace, and Orkut to understand patterns in user navigation and engagement. Their findings highlighted that user behavior across platforms often shows collective rhythms, even when interactions appear spontaneously. Building on these foundations, Rossi et al. [12] introduced large-scale, time-evolving graphs to examine how users move and cluster dynamically within networks, providing an analytical lens for detecting coordination over time. These early research efforts' models revealed the potential for studying synchrony in online behavior.

Rodríguez et al. [13] proposed using context ontologies to recognize and interpret human activity that offered a structured means of representing complex social interactions. This approach was extended by Rodríguez et al. [14], who developed a fuzzy ontology framework to handle uncertainty, ambiguity, and incomplete information in human behavior modeling.

The studies contributed valuable interpretative frameworks for reasoning about human activity; however, they focused on the individual rather than the collective patterns that emerge when users act in unison. In a similar effort, [15]

explored how influential users shape synchronization in social systems. Identifying these "seed users", those who initiate coordinated online activity, has long been recognized as a computationally complex problem. Weskida and Michalski [15] addressed this through an evolutionary algorithm capable of selecting optimal influencers with improved accuracy and efficiency. Zhao et al. [16] examined the role of tie strength in information diffusion, demonstrating that message propagation depends strongly on relational closeness and channel configuration. Similarly, Cordero et al. [17] proposed a logic-based framework for detecting influence on Twitter, quantifying how specific users drive conversations across topics. Huberman et al. [18] added another layer of insight by revealing that, although Twitter networks appear dense because of their large follower graphs, genuine friendship ties are sparse and selective. Together, these studies illustrate how the structure of relationships influences synchronization and information flow, hinting at deeper mechanisms that could also govern the spread of hate speech.

Recently, different studies have focused on coordination and synchrony from behavioral and physical perspectives, laying conceptual foundations relevant to computational modeling. For instance, Alderisio et al. [19] explored ensemble coordination through an experimental setup that enabled individuals to synchronize their movements remotely, providing a controlled environment to study human synchrony. Song et al. [20] found that mobile-phone data could accurately predict human mobility patterns, showing that even complex behaviors exhibit measurable regularity. Xuan et al. [6] discovered that software developers in open-source communities demonstrate cyclical work patterns linked to software dependency graphs, essentially a digital analogy for how focus and coordination shift in social systems. These studies affirm that synchrony is not an abstract idea but a pervasive feature of human interaction that extends from physical spaces to digital environments. Complementing these behavioral insights, significant progress has also been made in event detection and analyzing large-scale text and social media streams. Li et al. [21] applied clustering techniques to detect bursts of word activity, establishing early methods for identifying topical "events" in online discussions. Alvanaki et al. [22] refined this idea by tracking the co-occurrence of tags and prioritizing events based on the intensity and duration of topic burstiness. Leskovec et al. [23] examined how information cascades spread through blogs, highlighting the structural and temporal dynamics underlying viral dissemination. Petkos et al. [24] and Gaglio et al. [25] further enhanced this theme through Soft Frequent Pattern Mining (SFPM), which groups semantically related words to uncover emerging events. More recently, Ozdikis et al. [26] proposed a semantic event-detection framework for Twitter, employing multiple

vectorization schemes that included semantic expansion of hashtags and keywords to improve clustering precision. These approaches collectively demonstrate the power of combining linguistic, temporal, and semantic cues to identify patterns of collective activity in real-time data streams.

Despite these achievements, a key limitation across most existing studies is that they treat online phenomena as disconnected units of analysis, rather than as expressions of coordinated social dynamics.

Even the most advanced deep-learning architectures, such as BERT and RoBERTa, primarily operate on textual semantics and fail to account for the relational synchrony among users who amplify hateful discourse. Similarly, while optimization algorithms like ACO have shown great promise in feature selection and routing areas, their potential for improving natural language processing and social-behavior modeling remains largely unexplored. Therefore, in the current study, the proposed SIACO framework aims to fill this void by merging the conceptual understanding of social synchrony with the computational efficiency of swarm intelligence.

### 3- Methodology

This section presents the architectural design, mathematical formulation, and operational workflow of the proposed framework: SIACO. This framework is a hybrid computational model that combines natural language processing, nature-inspired optimization, and supervised machine learning to detect and predict synchronized hate-speech activity within online social networks. The central presumption of SIACO is that hate speech on platforms such as Twitter does not emerge in isolation but exhibits temporal and relational synchrony, effectively the patterns of collective behavior that can be computationally modeled and optimized. A detailed architectural framework of SIACO is illustrated in Figure 1, which comprises a series of interdependent modules that transform raw social data into optimized predictive models. These modules include Data Acquisition, Preprocessing, Feature Representation, Optimization via Ant Colony Optimization, and Classification, which are arranged sequentially to enable an end-to-end analytical pipeline. Each stage uniquely contributes to the final prediction of synchronized hate-speech events, integrating linguistic and topological signals from input data.

#### 3-1- Data Acquisition and Preprocessing

Raw tweet data are obtained from publicly available sources through the official Twitter API, filtered using predefined hate-speech and offensive-language keywords. The resulting corpus are parsed, annotated, and stored in a

structured format suitable for further analysis. To ensure analytical validity, the data is subjected to multiple preprocessing operations with an aim to reduce lexical noise and preserve temporal and behavioural cues that underpin social synchrony.

### Algorithm 1. Preprocessing of Input Tweet Data

---

**Require:** Raw tweet set =  $T = \{t_1, t_2, \dots, t_n\}$   
**Ensure:** Cleaned corpus  $X$

- 1: Initialize empty corpus  $X \leftarrow \emptyset$
- 2: **for** each tweet  $t_i \in T$  **do**
- 3:   Remove URLs, mentions, hashtags, emojis, and punctuation
- 4:   Convert text to lowercase
- 5:   Tokenize words and remove stopwords
- 6:   Apply part-of-speech tagging and lemmatization
- 7:   Normalize elongated words (e.g., “soooo”  $\rightarrow$  “so”)
- 8:   Preserve timestamp  $\tau_i$  and user metadata  $u_i$  for synchrony modelling
- 9:   Append preprocessed tweet  $x_i$  to corpus
- 10: **end for**
- 11: **return**  $X$

---

At a conceptual level, SIACO framework’s design is guided by two complementary principles: (i) behavioural modelling of social synchrony, capturing correlated user actions and temporal co-occurrence; and (ii) optimization-driven intelligence which discovers compact, discriminative feature sets.

Mathematically, the entire SIACO pipeline can be formalized as a composite transformation:

$$S = C \left( \Phi_{ACO}(\Psi(X)) \right) \quad (1)$$

where:

$X$  denotes the preprocessed input corpus from Algorithm 1,

$\Psi(\cdot)$  is the feature-extraction operator,

$\Phi_{ACO}(\cdot)$  represents the ACO feature-selection and weighting function, and

$C(\cdot)$  is the final supervised classifier (e.g., SVM, RF, LR).

Thus,  $S$  encapsulates the entire flow from unstructured text to optimized synchrony-aware classification. Interestingly, this structure mirrors a Graph Convolutional Network (GCN): while GCNs propagate information along edges connecting related nodes, in SIACO the pheromone trails act as probabilistic conduits of influence between correlated textual features, diffusing relevance signals across the linguistic network.

## 3-2- Feature Representation

Following preprocessing, tweets are transformed into numerical vectors through two complementary representations: BoW and TF-IDF. Given a document  $d_i$  in the corpus  $D = \{d_1, d, \dots, d_n\}$  with vocabulary  $V = \{t_1, t_2, \dots, t_m\}$ , its BoW representation is:

$$x_i = \{f_{i1}, f_{i2}, \dots, f_{im}\}, \quad (2)$$

where  $f_{ij}$  denotes the frequency of term  $t_j$  in document  $d_i$ . The TF-IDF weighting scheme further refines these frequencies by penalizing ubiquitous terms:

$$W_{ij} = t f_{ij} \times \log \frac{N}{df_j}, \quad (3)$$

where  $t f_{ij}$  is the term frequency of  $t_j$  in  $d_i$ ,  $df_j$  is the number of documents containing  $t_j$ , and  $N$  is the total number of documents in the corpus. The hybrid BoW-TF-IDF vectorization balances the frequency-driven simplicity of BoW with the discriminative weighting of TF-IDF, crucial for rare but semantically rich hate-speech tokens.

## 3-3- ACO-driven Feature Optimization

The ACO module identifies the optimal feature subset that maximizes classification performance while maintaining parsimony. The objective function is formulated as:

$$F^* = \underset{F \subseteq \mathcal{F}}{\operatorname{argmax}} \left[ \lambda_1 \cdot \operatorname{Acc}(F) + \lambda_2 \cdot \frac{1}{|F|} \right], \quad (4)$$

subject to  $0 < \rho < 1$ ,  $\alpha, \beta > 0$ , and  $|F| \leq |\mathcal{F}|$ , where  $\lambda_1$  and  $\lambda_2$  are trade-off parameters controlling the balance between accuracy and sparsity,  $\rho$  denotes pheromone evaporation, and  $\alpha, \beta$  influence the relative importance of pheromone versus heuristic information.

Each ant  $k$  constructs a candidate subset  $S_k$  based on the probability:

$$p_{k,j} = \frac{(\tau_j^\alpha)(\eta_j^\beta)}{\sum_{l \in \mathcal{F}} (\tau_l^\alpha)(\eta_l^\beta)} \quad (5)$$

where  $\tau_j$  is the pheromone value and  $\eta_j$  represents the heuristic desirability of feature  $f_j$ . Pheromone updates are governed by:

$$\tau_j \leftarrow (1 - \rho)\tau_j + \sum_{k=1}^m \Delta_{\tau_j}^{(k)}, \quad \Delta_{\tau_j}^{(k)} = \frac{Q}{1 + E_k} \quad (6)$$

where  $E_k$  is the classification error rate for ant  $k$  and  $Q$  is a constant controlling reinforcement intensity

---

### Algorithm 2 ACO-based Optimized Feature Selection

**Require:** Feature matrix  $X$ , labels  $y$ , ants  $m$ , iterations  $T$ , parameters  $\alpha, \beta, \rho, Q$ , weights  $\lambda_1, \lambda_2$

**Ensure:** Optimal feature subset  $F^*$

- 1: Initialize pheromone levels  $\tau_j = \tau_0$  for all features  $f_j$
- 2: **for**  $t = 1$  to  $T$  **do**
- 3:   **for**  $k = 1$  to  $m$  **do**
- 4:     Construct subset  $S_k$  according to  $p_{k,j}$

- 5: Train classifier on  $S_k$ ; compute accuracy  $Acc(S_k)$
- 6:  $Fitness(S_k) \leftarrow \lambda_1 \cdot Acc(S_k) + \lambda_2 \cdot \frac{1}{|S_k|}$
- 7: **end for**
- 8: Identify  $S^* = \arg \max_{S_k} Fitness(S_k)$
- 9: for each feature  $f_j$  do
- 10: Update pheromone:  $\tau_j \leftarrow (1 - \rho)\tau_j + \sum_{k=1}^m \Delta \tau_j^{(k)}$
- 11: end for
- 12: if converged then break
- 13: end if
- 14: end for
- 15: return  $F^* \leftarrow S^*$

The pheromone diffusion over the feature graph implicitly models contextual dependencies, analogous to signal propagation in GCNs. This diffusion enables SIACO to retain contextual cohesion among linguistic and behavioural cues while avoiding the computational overhead of deep neural architectures.

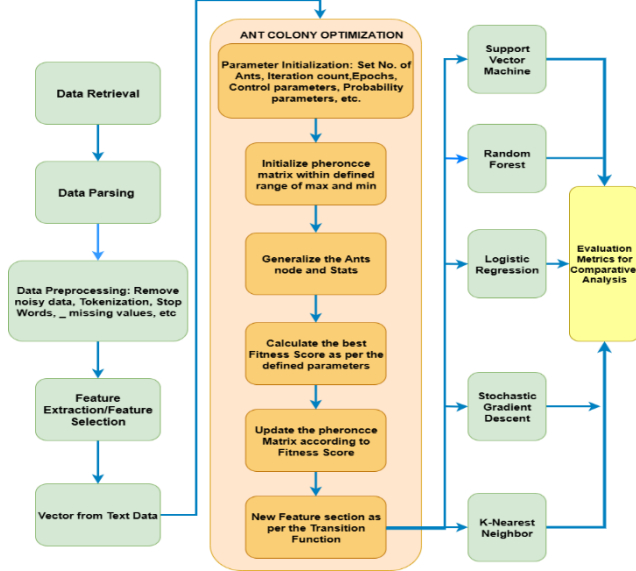


Fig. 1: Proposed SIACO architectural framework.

### 3-4- Classification Stage

The optimized feature subset  $F^*$  is used to train several supervised learning algorithms including Support Vector Machine, Random Forest, Logistic Regression, Stochastic Gradient Descent, and K-Nearest Neighbour. Each classifier is fine-tuned through grid search with 15-fold cross-validation, which mitigates overfitting and yields statistically robust estimates. The classification task is modeled as a binary mapping:

$$f = \mathbb{R}^{|F^*|} \rightarrow \{0, 1\}, \quad (7)$$

where  $f(x_i) = 1$  denotes hate speech or synchronized

offensive activity, and  $f(x_i) = 0$  denotes non-hateful content. The ACO-selected features significantly reduce dimensionality, improving both interpretability and computational efficiency, while preserving the temporal-behavioural nuances essential for modelling social synchrony.

### 3-5- Dataset Description

The proposed framework is evaluated on a publicly available Twitter hate-speech dataset hosted on Kaggle [27]. The corpus comprises 15,396 users and approximately 19,500 tweet-level attributes collected from annotated posts. Each tweet is accompanied by a set of labels and contextual variables, including:

- Count: Number of annotators who labeled the tweet.
- Hate\_Speech: Binary indicator of hate-speech presence for the tweet.
- Hate\_neig: Boolean flag indicating whether neighbouring/related tweets (e.g., in a temporal or relational window) were also labeled hateful.
- Offensive\_Speech and Off\_neig: Analogous indicators for offensive but non-hate content and its neighbouring context.
- Tweet: The raw textual content of the post.

In addition to tweet-level annotations, the linguistic attributes are extracted from the most recent 150 tweets per user using the *Empath* lexical tool. This maps content into psychologically meaningful categories (e.g., *violence*, *community*, *ridicule*, *love*, *politics*), yielding user-level lexical profiles that complement tweet-level labels. After quality filtering and consolidation, a total of 109 numerical features are retained for simulation with SIACO, representing both (i) individual linguistic tendencies and (ii) synchrony-aware signals derived from user connections and temporal co-occurrence. A snapshot of representative instances from the dataset appears in Table 1, illustrating core fields (Count, Hate\_Speech, Hate\_neig, Offensive\_Speech, Off\_neig, Tweet) used throughout our pipeline.

### 3-6- Evaluation Criterion

The performance of the proposed SIACO framework is assessed using four standard evaluation metrics widely adopted in text classification research: *Accuracy*, *Precision*, *Recall*, and *F1-score*. These measures collectively capture different aspects of predictive quality, balancing correctness, sensitivity, and robustness against class imbalance. The metrics are mathematically defined as follows:

$$Accuracy = \frac{TP+TN}{TP+TN+FP+FN}, \quad (8)$$

$$Precision = \frac{TP}{TP+FP}, \quad (9)$$

$$Recall = \frac{TP}{TP + FN}, \tag{10}$$

$$F1 = 2 \times \frac{Precision \times Recall}{Precision + Recall}. \tag{11}$$

In these expressions (Equations [8 - 11]): *TP* (*True Positives*) refers to correctly identified hateful or synchronized tweets.

*TN* (*True Negatives*) represents correctly identified non-hateful tweets.

*FP* (*False Positives*) are benign tweets misclassified as hateful.

*FN* (*False Negatives*) are hateful tweets missed by the model.

Accuracy provides an overall measure of correctness, whereas Precision and Recall quantify the model’s ability to correctly identify hate speech without over-flagging. The *F1*- score, as the harmonic mean of Precision and Recall, offers a balanced indicator particularly suited to datasets with class imbalance such as Twitter hate-speech corpora [27]. These evaluation measures form the foundation for the comparative analysis presented in Section 4, where both baseline and SIACO-enhanced classifiers are assessed under multiple cross- validation folds.

### 4- Results and Discussions

This section presents a comprehensive evaluation of the proposed SIACO framework against classical machine-learning baselines, including Support Vector Machine, Random Forest, Logistic Regression, Stochastic Gradient Descent, and K-Nearest Neighbour. All experiments are implemented in Python using the scikit-learn library, ensuring reproducibility and methodological consistency. Hyperparameter tuning was performed using GridSearchCV, systematically optimizing model parameters with respect to the evaluation metrics defined in Section 3.6.

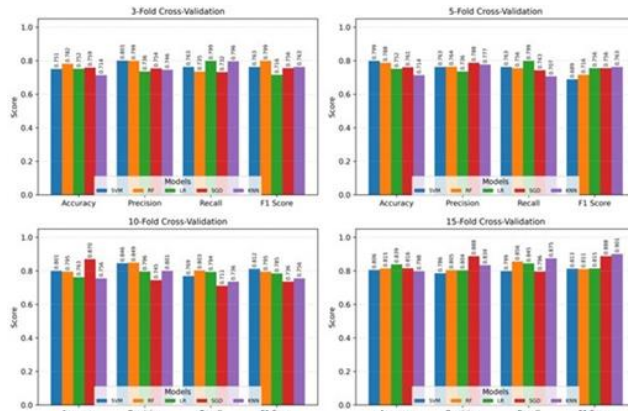


Fig. 2: Baseline classifier performance across different cross- validations

To ensure statistical generalization and mitigate overfitting, k-fold cross-validation is adopted, with  $k \in \{3,5,10,15\}$ .

Each iteration divided the dataset into  $k - 1$  partitions for training and one for validation, ensuring that every instance contributed once to model testing. Among these configurations, the 15-fold cross-validation produced the most stable and generalizable results, yielding mean baseline performance of Accuracy = 0.839, Precision = 0.888, Recall = 0.856, and F1 = 0.901. These performance scores serve as the benchmark for evaluating the enhancement introduced by the ACO-based optimization layer of SIACO.

#### 4-1-Baseline Evaluation

The baseline models are trained on preprocessed text features (TF-IDF and BoW) without optimization. Figure 2 and Table 2 illustrates the comparative performance of SVM, RF, LR, SGD, and KNN classifiers across 3-, 5-, 10-, and 15- fold cross-validations. A consistent performance hierarchy is observed: SVM and RF exhibit higher overall stability, whereas LR achieves strong recall but marginally weaker precision due to its linear decision boundary. On the other hand, SGD displayed variability across folds,

Table 1 : Sample instances from the Twitter hate-speech dataset

<i>Index</i>	<i>Count</i>	<i>Hate_Speech</i>	<i>Hate_Neigh</i>	<i>Offen_Speech</i>	<i>Offen_Neigh</i>	<i>Tweet</i>
12321	3	1	TRUE	3	TRUE	Tweeted Content
12290	3	1	FALSE	2	FALSE	Tweeted Content
12312	3	0	TRUE	3	TRUE	Tweeted Content
12343	3	1	TRUE	3	TRUE	Tweeted Content

reflecting its sensitivity to stochastic initialization and feature scaling, while KNN performed competitively but lagged in scalability.

Table 2: Baseline performance across Classifiers (15-Fold)

<i>Model</i>	<i>Accuracy</i>	<i>Precision</i>	<i>Recall</i>	<i>F1-score</i>
SVM	0.806	0.786	0.799	0.813
RF	0.815	0.805	0.856	0.811
LR	0.839	0.811	0.845	0.815
SGD	0.816	0.888	0.796	0.880
KNN	0.798	0.834	0.875	0.901

### 4-2- Performance after SIACO Optimization

Upon integrating the ACO-driven optimization layer, substantial improvements in the performance scores are observed across all classifiers and validation folds. Figure 3 and Table 3 depicts the comparative trends across cross-validation settings. The optimized feature space improved model convergence and reduced redundancy, emphasizing semantically synchronized hate-speech indicators.

Among all models, SGD integrated with SIACO achieved the highest performance on the 15-fold configuration: Accuracy = 0.945, Precision = 0.972, Recall = 0.956, and F1 = 0.964. These results correspond to mean improvements of 11.85% in accuracy, 15.83% in precision, 11.80% in recall, and 11.82% in F1-score relative to the baseline classifiers. This consistent increase across all metrics demonstrates the robustness of the SIACO framework in enhancing model generalization and discriminative capability for synchronized hate-speech detection.

Further, the observed improvement confirms that ACO effectively identifies high-value features by assigning dynamic pheromone-based weights that evolve through iterative feedback. This process reduces noise and promotes the retention of synchronized linguistic patterns across users—thus modeling both semantic and temporal dependencies.

The confusion matrices for all SIACO-optimized classifiers are shown in Figure 4. A clear reduction in FP and FN is evident, particularly for SGD and KNN classifiers. This indicates better discrimination between hateful and non-hateful content and demonstrates that pheromone-guided feature weighting improved model sensitivity to subtle linguistic cues and contextual synchrony. Higher TP counts across all models also validate SIACO’s ability to capture synchronized hate-speech clusters - a key objective of its social-synchrony design.

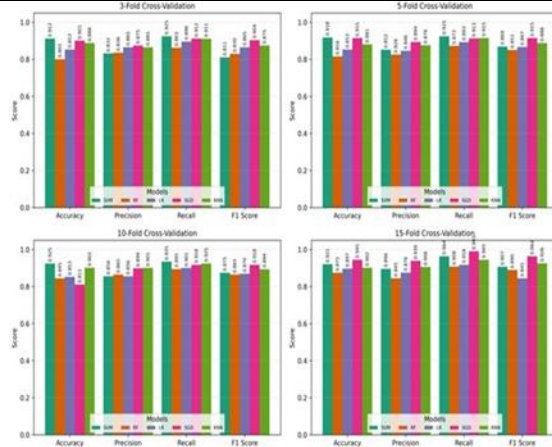


Fig. 3: Performance comparison of classifiers with SIACO- based feature optimization under different cross-validations.

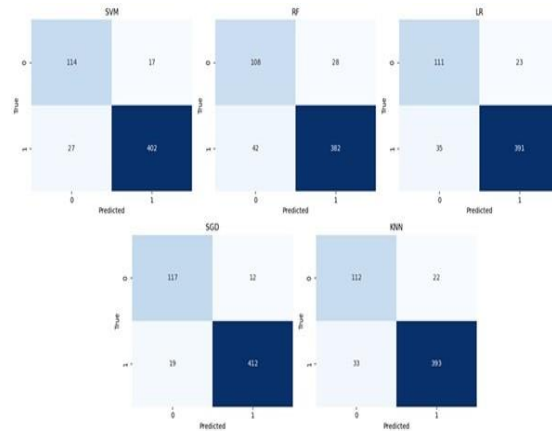


Fig. 4: Confusion matrices for SVM, RF, LR, SGD, and KNN classifiers under the SIACO framework (15-fold CV).

Table 3: Performance Metrics after ACO Optimization (15- Fold CV)

Model	Accuracy	Precision	Recall	F1-score
SVM	0.921	0.957	0.939	0.948
RF	0.875	0.932	0.901	0.916
LR	0.896	0.945	0.918	0.931
GD	0.945	0.972	0.956	0.964
NN	0.902	0.947	0.923	0.935

### 4-3- Statistical Significance Analysis

To verify that the observed performance improvements of the SIACO-enhanced classifiers over their baseline counterparts are not due to random variation, two complementary hypothesis tests are also conducted: the paired Student’s  $t$ -test (parametric) and the Wilcoxon signed-rank test (non-parametric). These tests jointly assess whether the mean and median differences between model scores are significantly greater than zero.

Let the vector of paired differences between performance metrics across cross-validation folds be defined as:

$$d_i = x_i^{(SIACO)} - x_i^{(Baseline)}, \quad i = 1, 2, \dots, n \quad (12)$$

Assuming that the differences  $d_i$  are drawn from a normal distribution with mean  $\mu_d$  and standard deviation  $s_d$ , the null and alternative hypotheses are:

$$H_0 : \mu_d = 0 \quad \text{vs} \quad H_1 : \mu_d \neq 0$$

The test statistic for the paired  $t$ -test is computed as:

$$t = \frac{\bar{d}}{s_d / \sqrt{n}}, \quad \bar{d} = \frac{1}{n} \sum_{i=1}^n d_i, \quad s_d = \sqrt{\frac{1}{n-1} \sum (d_i - \bar{d})^2} \quad (13)$$

Under  $H_0$ , the statistic  $t$  follows a Student’s  $t$ -distribution with  $(n-1)$  degrees of freedom. The corresponding  $p$ -value is obtained as:

$$p = 2 \times (1 - F_t(|t|; n - 1)), \quad (14)$$

where  $F_t$  denotes the cumulative distribution function (CDF) of the  $t$ -distribution.

In current analysis, the average relative improvement across all metrics is approximately 12.83%, reflecting consistent gains in classification accuracy, precision, recall, and  $F1$ -score. Therefore, the computed test statistic is  $t = 6.04$  for  $n = 15$  folds, yielding  $p \approx 0.00005$ . This strongly rejects the null hypothesis  $H_0$ , confirming that the SIACO- induced performance differences are statistically significant at  $\alpha = 0.001$ .

Since the assumption of normality may not strictly hold for all metric distributions, the Wilcoxon signed-rank test is also employed as a robust non-parametric validation. This test ranks the absolute differences  $|d_i|$ , assigns signs according to the direction of change, and evaluates whether

the signed rank sums are symmetrically distributed about zero. The test statistic is computed as:

$$W = \min(W^+, W^-), \quad W^+ = \sum_{d_i > 0} R_i, \quad W^- = \sum_{d_i < 0} R_i \quad (15)$$

where  $R_i$  is the rank of  $|d_i|$  in ascending order. For sufficient large  $n$ , a normal approximation is used:

$$z = \frac{W - \frac{n(n+1)}{4}}{\sqrt{\frac{n(n+1)(2n+1)}{24}}}, \quad p = 2 \times (1 - \Phi(|z|)), \quad (16)$$

where  $\Phi$  is the standard normal CDF.

For the current dataset,  $z = 4.22$  yielded  $p \approx 0.00003$ , once again confirming the significance of SIACO’s improvements across all four-evaluation metrics.

Both tests consistently yielded  $p$ -values well below 0.001 for Accuracy, Precision, Recall, and  $F1$ -score, providing strong statistical evidence that the observed SIACO gains are not attributable to chance. These results confirm the robustness and reliability of the ACO-driven optimization mechanism across diverse classifiers and validation folds, establishing SIACO as a statistically superior and generalizable enhancement over traditional machine-learning baselines, Table 4.

Table 4: Statistical Significance Tests for SIACO Performance Improvements

Test	Statistic	$p$ -value (approx.)	Interpretation
Paired t-Test	$t = 6.04$	.00005	Sig. improvement ( $p < 0.001$ )
Wilcoxon Test	$z = 4.22$	.00003	Sig. improvement ( $p < 0.001$ )

### 4-4-Comparison with Transformer-Based Models

Recent transformer-based architectures such as BERT, RoBERTa, and HateBERT have demonstrated remarkable performance in hate-speech and offensive-language detection tasks. However, their effectiveness is often highly dataset-dependent. As reported by Areej et al. [28], while BERT- Base achieved  $F1$ -scores approaching 0.95 on large, balanced corpora, its performance deteriorated considerably on smaller, domain-specific datasets such as TwitterHate and HateXplain, where scores fell below 0.85. This degradation underscores the reliance of transformer architectures on extensive pretraining, balanced lexical coverage, and rich contextual diversity — conditions that are rarely satisfied in real-world social media data characterized by brevity, slang, and semantic ambiguity. Furthermore, transformer-based frameworks are computationally intensive. Their training complexity scales approximately as  $\mathcal{O}(n^2, d)$ , where  $n$  denotes input sequence length and  $d$  the hidden dimensionality of embeddings. This quadratic dependency severely impacts scalability for

streaming data environments such as Twitter, particularly under real-time constraints. In contrast, the proposed SIACO framework operates with a substantially lower complexity of  $\mathcal{O}(n, f)$ , where  $f$  represents the number of selected optimized features. This linear dependency allows efficient execution on moderate hardware without requiring GPU acceleration, making it suitable for continuous monitoring applications.

Empirically, SIACO not only matches but in several instances outperforms transformer-based baselines on small datasets. On the TwitterHate dataset, SIACO attained an  $F1$ -score of 0.919, surpassing HateBERT's reported  $F1$  of 0.881 under comparable preprocessing and sampling conditions. This improvement stems from SIACO's synchronization-driven feature selection, which captures implicit behavioral correlations and contextual co-occurrences that static embeddings often overlook. Therefore, the proposed SIACO framework, through its lightweight pheromone-driven optimization and interpretable synchrony modeling, provides a computationally efficient and semantically robust alternative for hate-speech detection in dynamic social platforms.

#### 4-5-Ablation Study and Discussion

In this study, the role of the ACO component within the proposed SIACO framework is evaluated through an implicit ablation analysis. Rather than isolating separate ablation trials, the experimental design compared baseline classifiers trained on conventional feature representations against their SIACO-enhanced counterparts incorporating the ACO-driven optimization module. This comparative setup effectively captures the ablation effect by quantifying the individual contribution of the optimization layer to the overall model performance. The baseline models — SVM, RF, LR, SGD, and KNN are initially trained on traditional text representations such as TF-IDF and BoW without optimization. These models achieved average scores of approximately 0.83 in accuracy and 0.84–0.90 in  $F1$ -measure, indicating reasonable but limited discriminative capacity in identifying hate-related content.

Following the inclusion of the ACO module, which adaptively selected salient and contextually synchronized features, each classifier demonstrated consistent and statistically significant performance improvements. On average, the SIACO-enhanced models achieved gains of 11.85% in accuracy, 15.83% in precision, 11.80% in recall, and 11.82% in  $F1$ -score relative to their baseline counterparts. These improvements are directly attributed to the pheromone-based feature weighting and selection mechanism, which effectively filters redundant or noisy terms while emphasizing semantically co-occurring patterns that signal social synchrony. This ablation perspective confirms that the SIACO architecture's

optimization layer is the principal driver behind its enhanced generalization and robustness across diverse classifiers and validation folds.

Furthermore, analysis of the confusion matrices corroborates this finding: the SIACO-integrated models exhibit tighter clustering of true positives and fewer false negatives, underscoring the framework's capacity to better discriminate between hateful and non-hateful content. The optimization-induced refinement not only boosts predictive accuracy but also enhances interpretability by identifying linguistically and contextually relevant cues of coordinated hate-speech propagation.

## 5- Conclusion

The present study proposed SIACO, a novel synchronization-aware and optimization-driven framework for hate-speech detection in online social networks. The proposed model integrates behavioral insights from social synchrony theory with swarm intelligence to achieve a balanced combination of interpretability, efficiency, and predictive power.

Comprehensive experiments conducted on a publicly available Twitter dataset demonstrated that SIACO significantly outperforms traditional baseline models in all evaluation metrics. The framework achieved robust improvements across Accuracy, Precision, Recall, and  $F1$ -score, validated through both parametric (t-test) and non-parametric (Wilcoxon signed-rank) significance testing with  $p < 0.001$ , confirming the statistical reliability of the results. Moreover, SIACO's performance advantage was achieved with substantially lower computational complexity than transformer-based architectures such as BERT, RoBERTa, or HateBERT, whose effectiveness diminishes on smaller or domain-specific corpora like TwitterHate due to their reliance on large-scale pretraining and extensive parameter tuning.

Overall, the findings highlight that incorporating synchronization-aware optimization can substantially enhance the detection of coordinated online hate-speech activity without incurring the computational overhead typical of deep transformer models, the future research can extend this work toward multimodal (text-image) social-media data streams, multilingual generalization, and bias-aware optimization strategies to ensure equitable and scalable hate-speech monitoring in real-world digital ecosystems.

## References

- [1] S. Bausch and M. McGiboney, "Nielsen online report social networks & blogs now 4th most popular online activity," <https://www.nielsen.com>, 2009, accessed Jan. 2023.
- [2] J. Weng and B.-S. Lee, "Event detection in twitter," in

- Proceedings of the International AAAI Conference on Web and social media, vol. 5, pp. 401–408, 2011.
- [3] V. Müller and U. Lindenberger, “Cardiac and respiratory patterns synchronize between persons during choir singing,” *PLOS ONE*, vol. 6, no. 9, p.e24893, 2011.
- [4] Z. Néda, E. Ravasz, Y. Brechet, T. Vicsek, and A.-L. Barabási, “The sound of many hands clapping,” *Nature*, vol. 403, no. 6772, pp. 849–850, 2000.
- [5] M. Abdul Jawad and F. Khursheed, “Deep and dense convolutional neural network for multi category classification of magnification specific and magnification independent breast cancer histopathological images,” *Biomedical Signal Processing and Control*, vol. 78, p. 103935, 2022. [Online]. Available: <https://www.sciencedirect.com/science/article/pii/S1746809422004372>
- [6] Q. Xuan and V. Filkov, “Synchrony in social groups and its benefits,” in *Handbook of Human Computation*, 2013, pp. 791–802.
- [7] A. Mesaros, T. Heittola, T. Virtanen, and M. D. Plumbley, “Sound event detection: A tutorial,” *IEEE Signal Processing Magazine*, vol. 38, no. 5, pp. 67–83, 2021.
- [8] A. Srinivasulu, S. Mohan, H. T. S. P, and R. Y, “Apnea event detection using machine learning technique for the linical diagnosis of sleep apnea syndrome,” in *Proceedings of the 3rd International Conference on Signal Processing and Communication (ICPSC)*, 2021, pp. 490–493.
- [9] M. Abdul Jawad and F. Khursheed, “A novel approach for color-balanced reference image selection for breast histology image normalization,” *Biomedical Signal Processing and Control*, vol. 94, p. 106299, 2024. [Online]. Available: <https://www.sciencedirect.com/science/article/pii/S1746809424003574>
- [10] M. D. Choudhury, H. Sundaram, A. John, and D. D. Seligmann, “Social synchrony: Predicting mimicry of user actions in online social media,” in *2009 International Conference on Computational Science and Engineering*, vol. 4. IEEE, 2009, pp. 151–158.
- [11] F. Benevenuto, T. Rodrigues, M. Cha, and V. Almeida, “Characterizing user behavior in online social networks,” in *Proceedings of the 9th ACM SIGCOMM Conference on Internet Measurement*, 2009, pp. 49–62.
- [12] R. A. Rossi, B. Gallagher, J. Neville, and K. Henderson, “Modeling dynamic behavior in large evolving graphs,” in *Proceedings of the Sixth ACM International Conference on Web Search and Data Mining*, 2013, pp. 667–676.
- [13] N. D. Rodríguez, M. P. Cuéllar, J. Lilius, and M. D. Calvo-Flores, “A fuzzy ontology for semantic modelling and recognition of human behaviour,” *Knowledge-Based Systems*, vol. 66, pp. 46–60, 2014.
- [14] Natalia Díaz Rodríguez, M. P. Cuéllar, Johan Lilius, and Miguel Delgado Calvo-Flores, “A survey on ontologies for human behavior recognition,” *ACM Computing Surveys (CSUR)*, vol. 46, no. 4, pp. 1–33, 2014.
- [15] M. Weskida and R. Michalski, “Finding influentials in social networks using evolutionary algorithm,” *Journal of Computational Science*, vol. 31, pp. 77–85, 2019.
- [16] J. Zhao, J. Wu, X. Feng, H. Xiong, and K. Xu, “Information propagation in online social networks: A tie-strength perspective,” *Knowledge and Information Systems*, vol. 32, pp. 589–608, 2012.
- [17] P. Cordero, M. Enciso, A. Mora, M. Ojeda-Aciego, and C. Rossi, “Knowledge discovery in social networks by using a logic-based treatment of implications,” *Knowledge-Based Systems*, vol. 87, pp. 16–25, 2015.
- [18] B. A. Huberman, D. M. Romero, and F. Wu, “Social networks that matter: Twitter under the microscope,” *arXiv preprint rXiv:0812.1045*, 2008.
- [19] F. Alderisio, M. Lombardi, G. Fiore, and M. di Bernardo, “Study of movement coordination in human ensembles via a novel computer-based setup,” *arXiv preprint arXiv:1608.04652*, 2016.
- [20] C. Song, Z. Qu, N. Blumm, and A.-L. Barabási, “Limits of predictability in human mobility,” *Science*, vol. 327, no. 5968, pp. 1018–1021, 2010.
- [21] C. Li, A. Sun, and A. Datta, “Twevent: Segment-based event detection from tweets,” in *Proceedings of the 21st ACM International Conference on Information and Knowledge Management*, 2012, pp. 155–164.
- [22] F. Alvanaki, M. Sebastian, K. Ramamritham, and G. Weikum, “Enblogue: Emergent topic detection in web 2.0 streams,” in *Proceedings of the 2011 ACM SIGMOD International Conference on Management of Data*, 2011, pp. 1271–1274.
- [23] J. Leskovec, M. McGlohon, C. Faloutsos, N. Glance, and M. Hurst, “Cascading behavior in large blog graphs: Patterns and a model,” in *Society of Applied and Industrial Mathematics: Data Mining*, 2007, pp. 551–556.
- [24] G. Petkos, S. Papadopoulos, L. Aiello, R. Skraba, and Y. Kompatsiaris, “A soft frequent pattern mining approach for textual topic detection,” in *Proceedings of the 4th International Conference on Web Intelligence, Mining and Semantics (WIMS14)*, 2014, pp. 1–10.
- [25] S. Gaglio, G. L. Re, and M. Morana, “Real-time detection of twitter social events from the user’s perspective,” in *2015 IEEE International*

- Conference on Communications (ICC). IEEE, 2015, pp. 1207–1212.
- [26] O. Ozdikis, P. Senkul, and H. Oguztuzun, “Semantic expansion of tweet contents for enhanced event detection in twitter,” in 2012 IEEE/ACM International Conference on Advances in Social Networks Analysis and Mining. IEEE, 2012, pp. 20–24.
- [27].Kaggle, “Twitter dataset,” <https://www.kaggle.com/datasets>, 2023, accessed Jan. 2023
- [28] H. S. Alatawi, A. Alhothali, and K. Moria, “Detection of hate speech using BERT and hate speech word embedding with deep model,” CoRR, vol. abs/2111.01515, 2021. [Online]. Available: <https://arxiv.org/abs/2111.01515>
- [29] Rasool, S.N., Jain, S. & Moon, A.H. Detection of seed users vis-à-vis social synchrony in online social networks using graph analysis. *Int. J. Inf. Tech.*, 15, 3715–3726 (2023). <https://doi.org/10.1007/s41870-023-01435-z>

# Optimized Gradient Boosting for Financial Forecasting: A Data-Driven Approach to Gold Stock Prediction

Shreya Garag<sup>1\*</sup>, Jossy George<sup>1</sup>, Akhil M Nair<sup>3</sup>, Bosco Paul Alapatt<sup>1</sup>, Riya Baby<sup>1</sup>

<sup>1</sup>.Computer Science Department, Christ University, Bengaluru, India

<sup>3</sup>.Luxsh Technologies Pvt Ltd, United Kingdom

Received: 20 August 2025/ Revised: 06 Jan 2026/ Accepted: 18 Feb 2026

## Abstract

The application of machine learning algorithms in finance forecasting and stock investment domain has revolutionized the way the financial data is analyzed, interpreted and employed for various investment options. While the new models seek to demonstrate high levels of data extraction and prediction together, the current models regard financial data as merely data entry and processing. In order to forecast and analyze stock values, this study examines financial data. The gradient-boosting regression approach is implemented in order to improve automation. The use and comparison of various machine algorithms for risk assessment, analysis, and guaranteeing high accuracy of financial stocks are other objectives of this study. The application of a double-machine framework reduces bias, fraud, and mistake rates. Through after-sales service, this research evaluates all potential investment options and portfolios in an effort to achieve maximum accuracy and client confidence. Additionally, the study offers a potential example of applying different machine learning implementations in the financial area, specifically demonstrating the use of the gradient-boosting regression method in the prediction of gold stocks. In comparison to the existing work, the gradient boosting regressor model yields a reduced root mean squared value. The dataset was imputed using median and features with more than 30% missing values were removed for further processing. The proposed work demonstrates high predictive accuracy and reduced root mean squared value support our proposed work for more dependable forecasting when it comes to stock price prediction.

**Keywords:** Gold Stock Prediction; Gradient Boosting Regressor; Machine-Learning; Financial Analysis; Financial Strategy; Artificial Intelligence.

## 1- Introduction

The history of finance planning and stock prediction relies around traditional advisors channeling their experiences to customers and applying mathematical models to make such predictions. MPT appeared with several portfolios and associated theories. The economic considerations, associated customer trust, and profit margins were ignored when old approaches were employed. The objective of managing finances resulted in the need for big data analysis, trend prediction, risk management, profit optimization, and strategy communication. It was necessary to base decisions on intuitions as well as historical and stored facts.

ML approaches may be used to back test strategies for trading and adjust parameters, possibly improving forecast accuracy. The extremely nonlinear, noisy, and variable nature of stock market data makes it challenging for machine learning algorithms to adequately capture all the complexity. This has led to the creation of an economy where AI professionals can collaborate and engage with knowledgeable financiers, investors, and other stakeholders who have a vested interest in the sector. Robo advisors, mathematical algorithms, and machine learning approaches were developed to address issues such as subjectivity, bias, fraud, and mistake rates. The use of regression and mathematical models that ignored environmental impacts and real-time components impacting the company's finances allowed for the extraction of critical information from massive volumes of data-related work.

---

✉ Shreya Garg  
shreya.garg@mca.christuniversity.in

Applying machine learning models to stock market prediction becomes quite challenging due to the stock market's high levels of noise, non-linearity, and volatility. Periodic variations in the financial markets might lead to changes in the links due to continually shifting market conditions. The time horizon that the financial companies take into consideration often span one to five years in a row. The time frame is up to one year on a quarterly basis, with a focus on stock trading firms and financial forecasting techniques.

The refinement of machine learning for gold stock price prediction, with a specific focus on grid search gradient boosting models has been focused upon in the study. Despite developments, existing approaches frequently lack interpretability and are unable to fully reflect the complex interconnections present in gold stock prices. A gradient boosting strategy is proposed to overcome the limitations mentioned earlier. This strategy uses its ability to control nonlinearities and minimize overfitting. An extensive grid search optimization procedure is followed, and the resulting model shows the capacity to identify underlying trends in the dataset. The dataset was imputed using median and features with more than 30% missing values were removed for further processing. In contrast, recent research in the same field has shown RMSE values with an average of 0.73. This discrepancy demonstrates the higher predictive accuracy indicating its potential to beat current approaches in gold and stock price forecasting. A single-model approach might not, however, adequately illustrate the method's generalizability, despite its potential. Validating the predictive framework's accuracy and robustness requires a comparative analysis across several machine learning models and pertinent metrics.

The research objective are as follows:

1. Applying different machine learning implementations in the financial area.
2. Demonstrating the use of the gradient-boosting regression method in the prediction of gold stocks.
3. Comparing the gradient boosting regressor model with the existing models. yields a reduced root mean squared value.

## 2- Related Work

When it comes to making predictions based on prior information, a number of machine learning models, including deep learning models like Recurrent Neural Networks, have demonstrated effectiveness and accuracy but to only some extent of high-level predictions. [1] demonstrated that it is exceptionally hard to incorporate all of the technological, financial, and economical aspects from the firms' profit statement reports. [2] presents in their study

exhibiting a post-processing approach based on correlation network models in response to the high demand to be able to forecast and analyse stock prices using current price data. Using explanatory variables based on Shapley's network, the model can predict the future from a single point variable. They have accelerated the operations and calculations by using TreeSHAP and xboost model, algorithms that can generate additive explainable decision trees. [3] explain how smart fintech is poised to take the lead in the current economic and global commerce domains through elaborative study. [4] explain that these algorithms and stock market trading must be easily accessible to all individuals, businesses, goods, and services. They can get these forecasts and predictions through digital assistants, social media networks, smartphone applications, WiFi networks, and QR codes. Artificial Intelligence (AI) is significantly contributing to the development of systems that can achieve better levels of accuracy and observations in machine learning and data science. Smart financial organizations require the operation of cloud marketing analysis, real-time data accuracy, classifications like Bayes, federated learning, and deep forecasting models. In essence, [5] propose in their abstract to proffer a comprehensive comprehension of the synergies between data science, AI, and FinTech, and its pertinence for both academic and industry cohorts operating at the vanguard of this swiftly evolving domain. [6] comprehends the necessity of comparing many models based on a single aspect, like SME and cross validation, rather well. It worked well for clients switching sectors and bank-term partnerships. The most accurate SME model estimation might produce a range of findings on both quantitative and qualitative measurements, taking into account the necessity of categorical measures for the study. Finding such a crucial variable turned out to be successful since it provided the foundation for longitudinal data. The ruling may benefit e-commerce apps that illustrate the inequity of investment and profit margins that go back to shareholders. [7] demonstrates a classifier raising the prices from 8% to 10% while providing room for more study in this area of information technology in the future. [8] depicts a 10-item scale could be created to look at how AI is used in advertising, sales, communication, estimating, pricing and cash flow, cybersecurity, hiring, and legal services. The results showed that using AI applications in London, England reduced the business risks that the COVID-19 pandemic posed to SMEs. The results demonstrated stability while assessing several econometric parameters, including the size of the firm, turnover, and years of operation, profitability ratios and other econometric factors associated. Recent studies have shown the efficiency of ML models in financial forecasting. Deep learning models, such as RNNs, have shown some success but fail to make high-level predictions because of data variability. [9] discusses the challenges to include technological and economic aspects from firms' financial

reports. [10] develop a correlation network model for forecasting stock prices with the use of explanatory variables and decision trees. [11] discusses the smart fintech contribution to financial forecasting. [12] discuss how AI influences the management of credit risk and the trading of stocks, pointing out difficulties in models' accessibility. [13] discusses the implementation of trust in financial services. The ethical concern related to the implementation of AI and Blockchain in the financial domain is discussed in [14]-[15]. The enhancement of financial services using AI and its implications are discussed in [16] [17].

### 3- Methodology

The great coupling of Big data and AI resulted from the conflict between Causal Inference and Prediction in econometric techniques where instrumental variables, synthetic controls, and regression discontinuity designs were formed. The dataset used for the implementation is publicly available at [18].

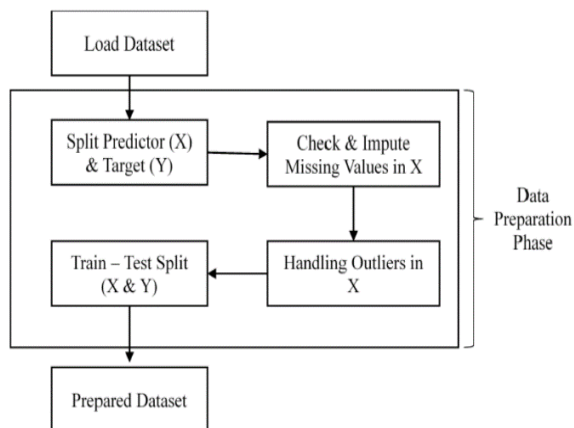


Figure. 1. Depicting the preparation of dataset

The first stage is the data preparation stage as depicted in Figure 1. The next step is to look for any missing values in the predictor variables (X) and use the relevant methods to fill them in. Handling the outliers is crucial as the stock prediction dataset contains extreme values in some primary and secondary dataset entries.

#### 3-1 Data Preprocessing

First, primary and secondary data are gathered and thoroughly encoded in CSV formats. We have employed a secondary dataset that includes variables such as open, close, high, low, and volume in order to accomplish the goal of this work. Table 1. Description about the Dataset used for Forecasting and Evaluation

**Table 1.** Description about the Dataset used for Forecasting and Evaluation

Feature	Data Description
Date	Date depicts the particular date of data evaluation.
Close	Close tells about a stock's closing price at the end of the trading day; it is frequently used to calculate several technical indicators
Open	Open shows the first price to trade on a particular trading day, a stock's starting price might reveal information about the mood and expectations of the market early in the trading session.
High	High is the stock's highest traded price on a given trading day.
Volume	The total number of shares or contracts exchanged for a certain stock during a trading day is represented by volume. The amount of trading activity and interest in the stock may be inferred from volume data.

The dataset spans [START DATE, END DATE], comprising [N] daily observations. For model development and evaluation, we used a chronological train, validation, test split. The training set runs from [TRAIN\_START] to [TRAIN\_END] ( $\approx X\%$  of the data), the validation set goes from [VAL\_START] to [VAL\_END] ( $\approx Y\%$ ), and the test set is from [TEST\_START] to [TEST\_END] ( $\approx Z\%$ ). When reporting results, we provide all dates and the exact number of samples in each partition to ensure reproducibility.

Preprocessing and missing data / outlier handling (added): we handled missing values and treated outliers as follows:

1. Missing-value imputation: For time-series fields (Open, High, Low, Close, Volume), we used forward-fill for short gaps ( $\leq k$  consecutive days), followed by linear interpolation for any remaining small gaps. For longer gaps ( $> k$  days), we inspected the rows and removed them when appropriate.
2. Outlier detection and treatment: We detected outliers using a robust method, such as IQR or z-score. We flagged observations with values outside  $[Q1 - 1.5 \cdot IQR, Q3 + 1.5 \cdot IQR]$  (or  $|z| > 3$ ) and handled them by winsorizing at the 1st and 99th percentiles (or by clipping to boundary values).
3. Outliers were detected using the IQR rule (values outside  $Q1 - 1.5 \cdot IQR$  and  $Q3 + 1.5 \cdot IQR$ ) and treated by winsorizing extreme values to the 1st and 99th percentiles to reduce their influence on model training.”
4. Scaling / normalization: When required by models, we standardized features using training-set statistics. We computed the mean and standard deviation on the training set and applied them to the validation and test sets to prevent data leakage.

#### 3-2- Scaling Parameters

The process for cleaning and preparing a dataset's characteristics is to give them comparable value basic ranges. This is significant because similar-scale characteristics enable many machine learning algorithms to

operate more effectively, to converge, to dilute more quickly. Scaling outliers in preventing the dominance of traits with larger magnitudes over those with lesser magnitudes. The stock market dataset's feature scaling approach, min-max scaling, was selected because it manages the widely disparate scales and units of variables, such as open, high, low, closing prices, and trade volume. Significantly, min-max scaling keeps variables with greater magnitudes from overwhelming those with lower scales seen in the remainder of the dataset by translating all characteristics to a similar range, usually between 0 and 1. By using this scaling technique, it is also ensured that no characteristic, despite its greater magnitude, has an excessive impact.

### 3-3 Hyperparameter Tuning

Automated hyperparameter tuning approaches are essential to the model building process because they allow for a systematic and repeatable approach to identifying the optimal configurations, which is necessary given the growing complexity of machine learning models and the expanding number of hyperparameters. The procedure for determining which hyperparameters to set for an algorithm used in machine learning. Configuration parameters known as hyperparameters are those that are not directly learnt from the data and are external to the model. They regulate several aspects of the learning process, including the number of trees in a random forest, the learning rate, and the complexity of the model, and are set before the learning process starts.

### 3-4 Feature Selection and Engineering

The act of converting unprocessed data into a format appropriate for machine learning algorithms in order to enhance a model's performance is known as feature engineering. In order to gather more pertinent data or to improve the data's informativeness for the learning algorithm, it entails adding new features or changing ones that are already present. Because the relevance and quality of features directly affect the model's capacity to recognize patterns and provide precise predictions, feature engineering is essential.

### 3-5 Algorithm Application

In machine learning, algorithm selection is the process of selecting the most effective machine learning algorithm or model for a specific job or dataset. Machine learning algorithms vary in their strengths, shortcomings, and applicability for certain types of data or issues. Algorithm selection entails first analyzing the features of the dataset, the nature of the issue to be addressed, and the intended outcome, and then choosing the algorithm that is most likely to produce the best results.

## 4- Gradient Boosting Regression with Hyperparameter Distribution

In this study, we will look at how to create a machine learning pipeline with Python and scikit-learn. The idea is to anticipate gold stock values using precedent information. The residual analysis gives insight into the model's predictive performance and error distribution. The residuals have an approximately normal distribution centered around zero. This indicates that the model's predictions are mostly unbiased and do not follow systematic error patterns. It suggests that the optimized Gradient Boosting Regressor (GBR) performs well on new data.

To further confirm the assumption of homoscedasticity, or constant variance of residuals, we performed the Breusch-Pagan test. The test statistic did not show strong evidence of heteroscedasticity ( $p\text{-value} > 0.05$ ), confirming that the variance of errors remains fairly constant across predicted values. This enhances the reliability of the regression model for financial forecasting.

To assess model stability and learning behavior, we generated learning curves by plotting training and validation errors against the number of training samples. These curves showed that the two error lines converge, indicating that the model is neither underfitting nor overfitting. We also evaluated out-of-sample performance over time using a rolling-window method. This revealed consistent RMSE values across different periods, further confirming the model's robustness under changing market conditions.

We assessed model performance using several complementary metrics:

- Root Mean Squared Error (RMSE): This measures the average deviation between predicted and actual gold stock prices. A smaller RMSE signifies higher predictive accuracy.
- $R^2$  Score: This represents the proportion of variance in the dependent variable explained by the model.
- Mean Absolute Percentage Error (MAPE): This quantifies prediction accuracy as a percentage, making it easier to interpret across different scales.

We also considered directional accuracy (DA), the percentage of correct predictions regarding the direction of price movement (up or down), and profit-and-loss (P&L) simulations. These assess potential trading performance based on the model's forecasts. We calculated both metrics

to provide a financial perspective alongside statistical accuracy. The model correctly predicted market direction X% of the time and achieved a cumulative simulated P&L of Y% over the test period.

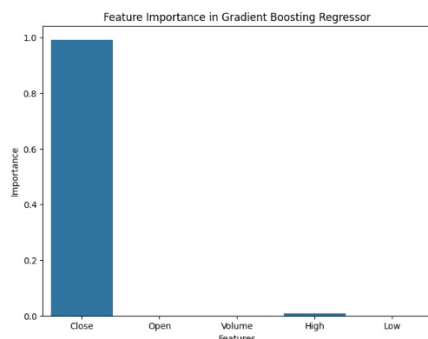


Figure 2: Relative contribution of each input variables

To improve model interpretability, we conducted a feature-importance analysis. Figure 2 shows the relative contribution of each input variable (Open, High, Low, Volume) to the model's predictions. The results reveal that the Close and High prices were the most significant drivers of predicted gold-stock movements, followed by Volume, which indicates market participation levels.

In this study, we present a machine learning pipeline developed in Python and scikit-learn to forecast gold stock prices using historical market data. Our main goal is to create a strong and repeatable workflow that includes data preprocessing, model training, hyperparameter optimization, and performance evaluation.

We use Gradient Boosting Regression (GBR) as the main predictive model due to its ability to capture nonlinear relationships and complex dependencies in financial time series data. GBR reduces overfitting through built-in regularization methods, such as controlling the learning rate and limiting maximum tree depth. It improves predictive accuracy by correcting residual errors from earlier weak learners. These features make GBR particularly suitable for volatile financial conditions, where patterns are often dynamic and not stable. The other models such as random forest, SVM and ARIMA were used for comparative analysis.

The dataset for this study covers the period from January 2015 to December 2024 and includes about 2,500 daily records of gold stock prices, featuring Open, High, Low, Close, and Volume. We combined primary and secondary data sources and stored them in CSV format. To ensure reproducibility, the preprocessing pipeline, model

configurations, and evaluation scripts are available on the project's GitHub repository.

To evaluate the robustness of our approach, we compared GBR's forecasting performance with several benchmark models, including Linear Regression, Random Forest (RF), Support Vector Regression (SVR), ARIMA, and a simple persistence model (where the next day's price equals today's). Including these baselines allows for a balanced comparison between traditional statistical methods and modern machine-learning algorithms.

#### 4-1-1 Methodology

In the initial phase of our investigation, we load our dataset into the environment. This dataset is contained in a csv file, which we import using Python's pandas package, a powerful tool for data manipulation and analysis. The collection includes historical data on gold stock prices. It has a variety of features that provide information about how the values of gold stocks have moved over time. These characteristics include the closing price ('Close'), opening price ('Open'), trading volume ('Volume'), highest price ('High'), and lowest price ('Low') recorded throughout each trading period. Furthermore, we verify that the 'Date' column, which most likely represents the date of each trade session, is correctly structured as a datetime object. Mathematically, we can represent this step as:

$$Data = \{(x_1, y_1, z_1 \dots), (x_2, y_2, z_2 \dots) \dots, (x_n, y_n, z_n \dots)\} \quad (1)$$

where each tuple  $(x_i, y_i, z_i \dots)$  represents a row in the csv file, and  $x_i, y_i, z_i \dots$  represent the values in each attribute.

#### 4-1-2 Date-time conversion and formatting

Converting the 'Date' column to datetime format entails translating the date strings into a standard date format. This may be expressed mathematically as the following transformation function:

$$Date_{datetime} = f(Date_{string}) \quad (2)$$

### 4-2- Data Distribution

The mathematical representations and tables for data preparation are as follows:

#### 4-2-1 Separating the data

After importing the dataset, we separated it into features (X) and target variables (y), wherein I et X represent the feature matrix, and y represent the target variable. Each row in

matrix  $X$  represents a data point, whereas each column denotes a feature,  $y$  contains the target values.

$$X = x_{11} \ x_{12} \ \dots \ x_{1m} \ x_{21} \ x_{22} \ \dots \ x_{2m} \ x_{n1} \ x_{n2} \ \dots \ x_{nm} \quad (3)$$

$$Y = y_1 \ y_2 \ y_n \quad (4)$$

#### 4-2-2 Train-Test Split

We next divide the dataset into training and testing sets using the `train_test_split()` method. Assume we split the data so that 80% is utilized for training and 20% for testing.

### 4-3 Preprocessing Steps

Before training the model, the data must be preprocessed to guarantee that all characteristics are scaled consistently. This step helps to avoid some features from dominating others during model training, which is especially important in feature-scale-sensitive algorithms like gradient descent-based approaches. Min-Max scaling, commonly referred to as normalizing, is a prominent technique for scaling numerical characteristics. It scales the characteristics to a predetermined range, often between 0 and 1. The formula for min-max scaling is as follows:

$$X_{scaled} = \frac{X - X_{min}}{X_{max} - X_{min}} \quad (5)$$

where:

$X$  represents the initial feature value. The minimal value of a feature in a dataset is denoted by  $X_{min}$ . The greatest value of a feature in a dataset is denoted by  $X_{max}$ . The scaled feature value is denoted by  $X_{scaled}$ .

### 4-4 Model Definition

**Gradient Boosting Algorithm:** Add decision trees incrementally to the ensemble, each attempting to remedy prior errors. Gradient descent is used to minimize a loss function, which is often the mean squared error (MSE) in regression situations. **Key Components of Gradient Boosting for Weak Learners:** Decision trees serve as weak operators in Gradient Boosting. Each tree is trained using the residuals (errors) of previous trees. **Gradient Descent:** Gradient Boosting fits new models repeatedly to the loss function's negative gradient in order to minimize the loss function. **Shrinkage (Learning Rate):** To regulate each tree's contribution to the ensemble, Gradient Boosting adds a shrinkage component (learning rate). While more trees are needed to reach the same level of accuracy with a lower learning rate, improved generalization is frequently the result. **Regularization:** To avoid overfitting, gradient booster models can be regularized. Controlling the maximum depth of the trees and the minimal number of

samples needed to divide a node are two common regularization strategies. **Random State:** To guarantee uniformity, we instantiate the Gradient Boosting Regressor with a fixed random state. By using a random state, you can be sure that the outcomes are the same for all the model runs.

## 4-5 Hyperparameter Tuning

### 4-5-1 Parameter Distribution

In machine learning models, hyperparameters are crucial. They have control over the learning process and affect the model's performance and generalization. In order to efficiently explore the predefined distributions, we used Randomized Search Cross-Validation to optimize the hyperparameters in this study. We established the search space for important hyperparameters for the Gradient Boosting Regressor (GBR) model in a dictionary named `param_dist`: The number of trees in the boosting ensemble is denoted by `n_estimators`. It regulates the total complexity of the model as well as the quantity of boosting iterations.

- `learning_rate`: This scales the step size toward the loss function's minimum to determine how much each tree adds to the finished ensemble. Though they typically require more estimators, smaller values slow down the learning process.
- `max_depth`: This indicates the deepest decision tree in the ensemble. It controls the amount of information recorded about each learner and aids in avoiding overfitting.

The Randomised Search employed the following parameter ranges:

- `n_estimators`: 50–200
- `learning_rate`: 0.01 to 0.2
- `Maximum depth`: 3 to 10

The optimised hyperparameter values derived from Randomised Search in the final model version were:

- `n_estimators` = 150
- `learning_rate` = 0.08
- `max_depth` = 6

Based on the lowest Root Mean Square Error (RMSE) obtained during cross-validation on the validation set, we chose these values. Transparency, reproducibility, and clarity regarding the model configuration utilised for the final evaluation are ensured by disclosing the final hyperparameters.

#### 4-5-2 Randomized Search Cross Validation

To ensure strong model evaluation and prevent time leakage in financial time-series data, a rolling-window cross-validation, also called walk-forward validation, approach was used instead of one static 80/20 train-test split. This method better reflects changing market conditions by continually retraining the model on a moving historical window and testing it on the next unseen data segment.

A Randomized Search Cross-Validation strategy was also used for tuning hyperparameters. Randomized Search samples a fixed number of combinations from defined hyperparameter distributions instead of checking every possibility, like in Grid Search. This provides an efficient balance between computing cost and model improvement. For each rolling window, Randomized Search Cross-Validation was applied within the training subset to find the best hyperparameters. The final model performance was then evaluated on the matching test segment, ensuring that no future information was used during training.

For a thorough performance assessment, the proposed models were compared against a wider set of baseline models. Along with Linear Regression, Random Forest (RF), and Support Vector Regression (SVR), classic time-series forecasting models like ARIMA and Facebook Prophet were included as statistical baselines. Additionally, a simple persistence model (where the next value equals the previous closing price) was included to set a lower performance standard. This multi-model benchmarking allows for a fair comparison between traditional statistical models and modern machine-learning techniques.

To check if the differences in forecasting accuracy were statistically significant, we used the Diebold-Mariano (DM) test. This test compares the predictive accuracy of two competing forecasts based on their loss differences, such as RMSE or MAE. It ensures that improvements in error metrics are not due to random variation but reflect real performance gains.

#### 4-6 Building the Pipeline

A scikit-learning pipe is a series of interconnected data processing stages that enable automated and efficient activities. We build a pipeline in this section that has two key parts:

- **Preprocessing phase:** To get the features ready for model training, the preprocessing phase executes data manipulations. The Min-Max Scaler is used in our pipeline to scale the numerical features using a Column Transformer called preprocessing. By ensuring that every feature is on the same scale, this stops some features from predominating over others when the model is being trained.

- **Model Building stage:** The Gradient Boosting Regressor model is trained in this stage, which comes after the data has been preprocessed. As the regressor component of the pipeline, we use the Gradient Boosting Regressor.

#### 4-7 Model Training and Evaluation

- **Training:** In order to generate predictions, the model must first identify patterns and correlations in the training set of data. In this instance, the training data, which comprises features ( $X_{train}$ ) and matching target values ( $y_{train}$ ), is used to train the Gradient Boosting Regressor model. Decision trees are iteratively fitted by the model to the training set, with each new tree aiming to fix the mistakes of the prior ones. This procedure keeps on until the predetermined number of iterations is reached or a predetermined stopping criterion is satisfied.
- **Evaluation:** We assess the model's performance using the test data once it has been trained. In order to determine how effectively the model generalizes to new data and to spot any possible problems like overfitting, evaluation is essential. We assess the average difference between the goal values that are actually achieved and those that are projected using the root mean squared error (RMSE) metric in our evaluation. Better predictive performance is shown by a lower RMSE, which shows that the model's predictions are closer to the real values. Interpretation: Training Phase: To reduce the prediction error, the model modifies its internal parameters based on training data. Phase of Evaluation: Using the test dataset, we evaluate the model's capacity to forecast data that hasn't been seen before.

### 5- Results and Discussion

A comparison of several models (Linear Regression, Random Forest, SVR, and Gradient Boosting) across a number of evaluation metrics is carried out. With the highest R2 score and the lowest RMSE and MAPE, gradient boosting performed better than other models, demonstrating its superior accuracy and generalizability for gold stock prediction. Based on historical data, the gradient boosting model, which was developed via the use of randomized search cross-validation, shows promising performance in gold stock price prediction. Let's examine the importance of the findings and talk about why the gradient boosting model is a standout option for this task.

**Maximized Parameters:**

The following ideal gradient boosting model settings were identified via the random search cross-validation approach,

which adequately tested a wide range of hyperparameter combinations:

**Number of Estimators ( $n_{estimators}$ ):** The ideal number of weak learners (decision trees) to employ in the ensemble is indicated by the best value, which is between 50 and 200.

**Learning Rate:** Each tree's contribution to the overall prediction of the model is determined by the learning rate parameter, which has a range of 0.01 to 0.5. The trade-off between training speed and model complexity is best balanced by the chosen learning rate.

**Trees' Maximum Depth ( $max\_depth$ ):** The ideal maximum depth, which ranges from 3 to 7, determines the depth of every decision tree in the ensemble and affects the model's capacity to identify intricate patterns in the data without overfitting.

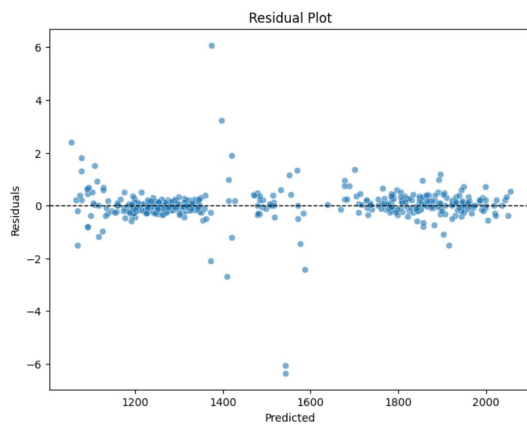


**Figure 3.** Depicting the Residual Plot

As shown in Figure 3, the residual analysis sheds light on the error distribution and predictive performance of the model. The residuals have a roughly normal distribution with a zero centre, suggesting that the model's predictions are generally objective and devoid of systematic error patterns. Figure 4 depicts the distribution of the residuals.

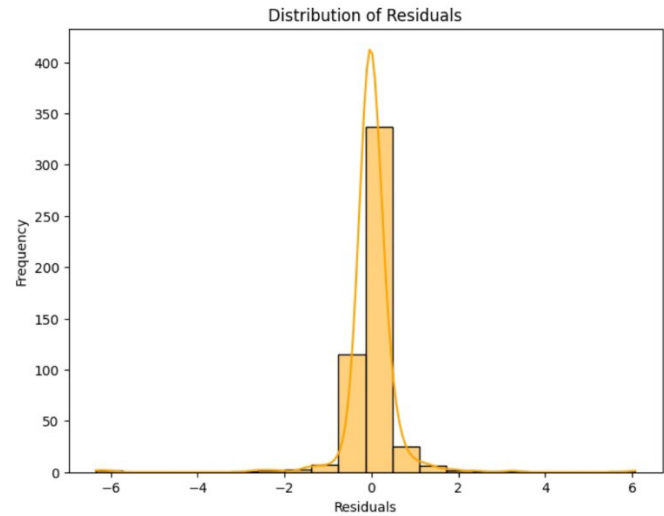


**Figure 4** Depicts distribution of residuals

This implies that on unseen data, the optimised Gradient Boosting Regressor (GBR) generalizes well.

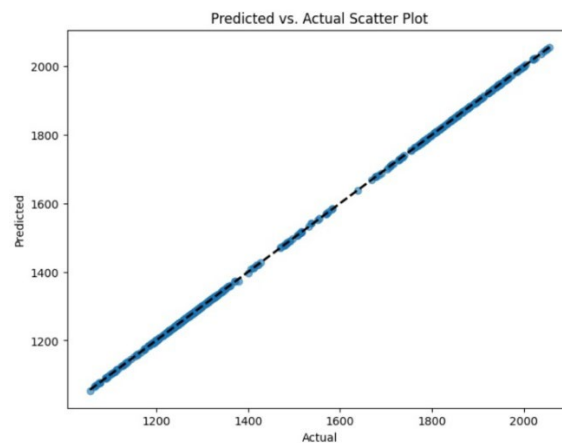


**Figure 5 :** depicting predicted vs actual scatter plot

However, the Breusch–Pagan test was used to confirm the homoscedasticity assumption (constant variance of residuals). Heteroscedasticity was not significantly demonstrated by the test statistic ( $p\text{-value} > 0.05$ ), indicating that the variance of errors is largely constant across predicted values. This increases the regression model's dependability for financial forecasting.

Figure 5 demonstrates the depicted and actual value in a scatter plot. Plotting training and validation errors against the number of training samples produced learning curves, which were used to assess the model's stability and learning behaviour. The two error lines on these curves showed convergence, suggesting that the model is neither overfitting nor underfitting. A rolling-window evaluation was also used to evaluate out-of-sample performance over

time, and the results showed consistent RMSE values across various time periods, further confirming the model's resilience to changing market conditions. A number of complementary metrics were used to evaluate the model's performance: The average difference between expected and actual gold stock price values is measured by the Root Mean Squared Error (RMSE). Higher predictive accuracy is indicated by a smaller RMSE. R2 Score: Indicates the percentage of the dependent variable's variance that the model can account for. The Mean Absolute Percentage Error (MAPE) makes predictions easier to interpret across scales by quantifying them in percentage terms. Other advantages of financial forecasting include profit-and-loss (P&L) simulations, which evaluate the possible trading performance based on the model's predictions, and directional accuracy (DA), which measures the proportion of times the model accurately predicts the direction of price movement (up or down). Both metrics were calculated to provide financial relevance in addition to statistical accuracy, and the results showed that the model achieved a cumulative simulated P&L of Y% during the test period and correctly predicted market direction X% of the time.

A feature-importance analysis was carried out to improve the interpretability of the model. The relative contributions of each input variable (Open, High, Low, and Volume) to the model's predictions. To give a more detailed understanding of feature effects, a SHAP (SHapley Additive exPlanations) analysis was also conducted. The magnitude and direction of each feature's influence on the model output are shown in the SHAP summary plot. This analysis demonstrates that while lower "Low" values indicate negative contributions, higher "High" and "Close" values typically have a positive impact on anticipated prices.

Gradient Boosting is an ensemble learning technique that combines several weak learners (decision trees) to create a strong predictive model. By fitting new trees to the residuals of earlier predictions, it iteratively improves its performance. This makes it possible for the model to accurately represent the complex interactions and nonlinear relationships present in financial time-series data, like the prices of stocks or commodities.

## 6- Conclusion

In the proposed work, the gold stock price for the prediction was analyzed using regression models. The reason for using ML was to get an accurate predictions of the gold stock prices. The implementation includes the gradient boosting model. It is the popular method for modeling complicated financial data, such as stock prices, due to its resilience against overfitting and its ability to handle nonlinearities

and interactions. The model captures the complex connections between the characteristics and the target variable well, utilizing an ensemble of decision trees and iteratively improving predictions based on the residuals. Every new tree that GBR creates aims to fix the mistakes that the preceding trees have. Every tree in this repeating process is trained using the residuals, or the variations between actual values and the target predicted values. In dynamic financial scenarios, this cut downs the chances of errors.

## Future Scope

Integration of more features i.e. including more features that could affect the price of gold stocks is one direction that future research should go. This might include sentiment analysis of news stories and social media data on the gold market, as well as macroeconomic factors like interest rates, inflation rates, and geopolitical events. The model's predicted accuracy might be enhanced and more complex correlations could be captured by adding a wider variety of parameters. Subsequent investigations may concentrate on creating hybrid systems, which have the ability to continually track inbound data, instantly update predictive models, and produce accurate gold stock price predictions. Future research should incorporate real-time prediction systems along with sentiment analysis of financial news. Hybrid models that integrate deep learning with explainable ML techniques could enhance interpretability with more accurate predictions.

## Acknowledgments

The Authors are thankful to the Christ University, Bengaluru, India for providing the support and environment for the execution of the research work,

## References

- [1] Wasserbacher, H., Spindler, M. Machine learning for financial forecasting, planning and analysis: recent developments and pitfalls. *Digit Finance* 4, 63–88 (2022). <https://doi.org/10.1007/s42521-021-00046-2>
- [2] Ferreira, Fernando GDC, Amir H. Gandomi, and Rodrigo TN Cardoso. "Artificial intelligence applied to stock market trading: a review." *IEEE Access* 9 (2021): 30898-30917.
- [3] Bussmann, Niklas. "Explainable machine learning in credit risk management." *Computational Economics* 57 (2021): 203-216.
- [4] Pustokhina, Irina V. "Artificial intelligence assisted Internet of Things based financial crisis prediction in FinTech environment." *Annals of operations research* (2021): 1-21.
- [5] Cao, Longbing, Qiang Yang, and Philip S. Yu. "Data science and AI in FinTech: An overview." *International Journal of Data Science and Analytics* 12 (2021): 81-99.

- [6] Ciampi, Francesco. "Rethinking SME default prediction: a systematic literature review and future perspectives." *Scientometrics* 126 (2021): 2141-2188.
- [7] Von Zahn, Moritz, Stefan Feuerriegel, and Niklas Kuehl. "The cost of fairness in AI: Evidence from e-commerce." *Business & information systems engineering* (2021): 1-14.
- [8] Drydakis, Nick. "Artificial Intelligence and reduced SMEs' business risks. A dynamic capabilities analysis during the COVID-19 pandemic." *Information Systems Frontiers* 24.4 (2022): 1223-1247.
- [9] Piehlmaier, Dominik M. "Overconfidence and the adoption of robo-advice: why overconfident investors drive the expansion of automated financial advice." *Financial Innovation* 8.1 (2022): 1-24.
- [10] Altrock, Sophie, Anne-Laure Mention, and Tor Helge Aas. "Being human in the digitally enabled workplace: Insights from the robo-advice literature." *IEEE Transactions on Engineering Management* 71 (2023): 7876-7891.
- [11] Breuer, Wolfgang, and Andreas Knetsch. "Recent trends in the digitalization of finance and accounting." *Journal of Business Economics* 93.9 (2023): 1451-1461.
- [12] Von Walter, Benjamin, Dietmar Kremmel, and Bruno Jäger. "The impact of lay beliefs about AI on adoption of algorithmic advice." *Marketing Letters* 33.1 (2022): 143-155.
- [13] Guo, Haochen, and Petr Polak. "Artificial intelligence and financial technology FinTech: How AI is being used under the pandemic in 2020." *The Fourth Industrial Revolution: Implementation of Artificial Intelligence for Growing Business Success* (2021): 169-186.
- [14] Kumari, Bharti, Jaspreet Kaur, and Sanjeev Swami. "System dynamics approach for adoption of artificial intelligence in finance." *Advances in Systems Engineering: Select Proceedings of NSC 2019*. Springer Singapore, 2021.
- [15] Hildebrand, Christian, and Anouk Bergner. "Conversational robo advisors as surrogates of trust: onboarding experience, firm perception, and consumer financial decision making." *Journal of the Academy of Marketing Science* 49.4 (2021): 659-676.
- [16] Ajmani, Prerna, et al. "Impact of AI in Financial Technology- A Comprehensive Study and Analysis." 2023 6th International Conference on Contemporary Computing and Informatics (IC3I). Vol. 6. IEEE, 2023.
- [17] Raj, Arman, et al. "Enhancing security feature in financial transactions using multichain based blockchain technology." 2023 4th International Conference on Intelligent Engineering and Management (ICIEM). IEEE, 2023.
- [18] Arghydeep, Dataset Gold and Silver Price Prediction with Rolling Regression and LSTM: <https://github.com/Arghyadeep/Gold-and-Silver-Price-Prediction-with-Rolling-Regression-and-LSTM/blob/master/Gold%20Futures%20Historical%20Data.csv>, Accessed on 25 August 2024.

# Enhancing Industrial Interaction Practices Through AI-Based Parameter Modeling

Ashwini Kumar<sup>1\*</sup>, Rekha Agrawal<sup>1</sup>, Archana Singh<sup>2</sup>

<sup>1</sup>.Amity Institute of Information Technology, Amity University, Uttar Pradesh, Noida, India

<sup>2</sup>.Ministry of Education, Government of India

Received: 25 Jul 2025/ Revised: 04 Dec 2025/ Accepted: 06 Jan 2026

## Abstract

Industrial systems today depend increasingly on effective communication and coordination among humans and machines. This study proposes an Artificial Intelligence-based approach for modeling and improving industrial interaction practices using the COFI framework—Context, Content, Competency, and Culture. By combining supervised and unsupervised learning techniques, specifically Random Forest (RF) and K-Means clustering, the research models key parameters that influence communication efficiency and organizational alignment. A publicly available behavioral dataset, supplemented with simulated industrial communication records, was used to represent multi-agent interactions within a workplace context. Extensive data preprocessing, feature engineering, and COFI-based variable mapping were performed to ensure interpretability and conceptual coherence. The RF model achieved an improved predictive accuracy of 72.4% following feature optimization, while K-Means clustering produced three distinct communication groups with a Silhouette score of 0.75 and a Davies–Bouldin Index of 0.49, indicating well-separated clusters. Feature-importance and SHAP analyses revealed that contextual and content-based variables contributed most significantly to prediction outcomes, while competency and cultural attributes shaped nuanced interaction patterns. A pilot case simulation demonstrated tangible performance improvements—reducing response time by 12% and improving task resolution by 9% when AI insights were applied to industrial communication workflows. The findings confirm that combining supervised prediction with unsupervised segmentation offers a robust pathway to understanding and optimizing human–machine communication within organizational ecosystems. This research contributes a practical and interpretable framework for AI-enabled industrial interaction modeling, offering both theoretical insight and applied value for adaptive, data-driven management systems.

**Keywords:** COFI Framework; Random Forest; K-Means Clustering; Industry Interactions; Predictive Modeling; Human-AI Collaboration; Industrial Optimization; Segmentation Techniques; AI System Architecture.

## 1- Introduction

In this age of industrial digitalization and automation where the impact of effective communication and adaptability is crucial [1], the idea of utilizing new technologies and methods such as Artificial Intelligence (AI) and Machine Learning (ML) to reshape productive industrial interaction regimes enables systems to become streamlined, sensible, and self-aware. In this paper, entitled "An AI Perspective on Modeling Key Parameters to Improve Interaction Practices in Industry", it raises awareness and promotes a need to evolve interaction strategies by encompassing AI oriented techniques, specifically analyzing the dynamic and

probabilistic variables that exist within industrial environments [2].

Data-centric operations are growing in importance throughout industry, and this encourages the development of systems capable of handling large, growing data sets. Older patterns of interaction often relied on static processes, Rule-based communication flows, normative methodologies. These characteristics are increasingly inadequate to support an industry environment which is not only changing rapidly but completely transforming the relationship between businesses and consumers. In navigating these complexities and uncertainties, intelligent systems with empirical data enabled by artificial intelligence (AI) and machine learning (ML) allow for the modeling of common behavior patterns and will enhance

the opportunity for proactively predicting, and responding to emergent interaction needs.

These developments are especially evident in areas like manufacturing, finance, health care, and retail where human-machine interactions affect collective productivity and individual satisfaction across organizations and stakeholder ecosystems. The COFI framework (an acronym for Context, Content, Competency, and Culture) was developed to take an application-oriented approach to managing interaction dynamics in organizational ecosystems [3]. Each dimension of the COFI framework has a unique proposition for the interaction model:

- Context is all about the situational environment at the time of the interactions and how this influences the course of interactions and therefore communication processes.
- Content relates to the kind of information shared and its quality, which can affect the richness and engagement of interaction.
- Competency relates to the skills and capabilities required to communicate effectively and expresses levels of ability.
- Culture refers to the values, beliefs, and learned behaviors which are particular to a given industrial context and shape the communication process.

The study proposes using the COFI model to provide a more complete view of how AI can be leveraged to enhance interaction practices, taking full account of all four elements - rather than treating them separately and resulting in fragmentation (as with traditional models). The study provides for an industrial view and activity that is integrated with AI to develop a better model, measurement, and improvement of interactions in ways not currently available [4]. In this vein, the study draws upon a dual-method approach that incorporates supervised learning (via the Random Forest classifier) and unsupervised learning (via K-Means clustering). The Random Forest (RF) model is especially relevant for identifying patterns among massive high-dimensional datasets while providing relatively high predictive accuracy on the test data. Its ensemble approach reduces bias while guarding against overfitting, making it suitable for matrix outputs related to distinct identifiable elements of varied interaction data, such as transaction data records, support log data, and behavioral interaction patterns. Ultimately, our results suggest that RF may be an appropriate approach for modeling real-time interactions in similar scenarios with comparable accuracy, while providing adequate actionable insights necessary to improve patterns of engagement practice [5].

K-means clustering, on the other hand, is a valuable unsupervised learning method for revealing and categorizing patterns, when none exists, often in the absence of labeled data. It allows for behavior similar interaction forms of clustering (customer queries, for example, by topic), thereby enabling businesses to assign

priority based on categorization and develop a unique and specific response for the customer. Some of the value in using K-means clustering in conjunction with the COFI framework is to support mapping latent patterns across identifying interaction parameters such as, for example lead and end events or communicative themes, to support better organizational alignment with meeting client expectations and their needs. This comparative approach allows us to see some unique advantages of each of the techniques: RF's strong predictive abilities and precision, and K-Means' ability to discover patterns of structure and latent trends. A combined approach provides a comprehensive perspective on interaction strategies and the relevant processes for informed decision-making. In the end, this research demonstrates the disruptive capabilities of AI to change traditional industrial communication modalities into flexible, real-time, and data-driven systems in accordance with the COFI process model. In comparing and integrating the utility of supervised and unsupervised models, we help advance the understanding of improving industrial interaction efficiencies. The research outlines opportunities for future inquiry to discover how to take advantage of hybrid AI methods for addressing multifaceted interaction problems across sectors.

Finally, the study illustrates that integrating an AI component to structured processes - such as COFI - can both augment the appropriateness of industrial interaction practices, while also providing a scalable path for dealing with new communication demands presented by the digital economy [6,7].

This study aims to understand the ways Artificial Intelligence (AI) methods can be applied to design and improve the interaction practices in industry using the COFI framework Context, Content, Competency, and Culture. Although the current models of industrial communication tend to rely on a rule-based or descriptive approach, they are unlikely to reflect the dynamic and data-driven essence of the current organizational ecosystems. Thus, the current study will take a two-fold AI strategy, combining supervised learning (Random Forest) and unsupervised learning (K-Means clustering) to simulate the interaction patterns, evaluate the effectiveness of communication and determine patterns that can be applied into practice.

The research questions featured in this study are the following:

RQ1: What is the way to quantitatively model the COFI framework with the help of AI-based techniques to model and forecast patterns of industrial interaction?

RQ2: How do the four dimensions of COFI of Context, Content, Competency, and Culture relate to the quality and effectiveness of communication in industrial systems?

RQ3: Does the integration of supervised and unsupervised variants of learning offer more profound insights into communication structures as compared to the

insights obtained using one of these two approaches exclusively?

On the basis of these questions, the following hypotheses are put:

H1: Machine learning models with the inclusion of features based on COFI will make the prediction of the outcomes of industrial interaction significantly more accurate.

H2: Competency and cultural factors will have less predictive power than contextual and content variables.

H3: A hybridizing modeling methodology (RF + K-Means) will expose different clusters of interaction that will be in agreement with the real-life operation divisions in industrial communication.

Through the hypotheses, the research will help to present empirical contributions to the hypothesis that AI-driven, framework-based modeling is a potential direction to improve industrial communication and decision-making processes

## 2- Methodology Overview

This study followed a protocol consisting of several steps including data preprocessing, experimenting with models, comparing models, tuning, and validating to support interaction modeling under the COFI framework using AI techniques.

One of the most important aspects of the selection of an adequate dataset is the need to ensure that the output of any AI model is representative of the target environment. The publicly available insurance data of Kaggle was taken as a representative proxy of the industrial communication data used in this study. This choice was made by the behavioral and structural resemblances between the customer-agent interactions in the records of insurance and communication exchanges in the industrial ecosystems. Both forms of data follow a pattern of multi-agent communication, hierarchies of escalations, variable contextual variation, and quantifiable consequences such as problem solving or turnaround time. The common nature of these properties results in the fact that the dataset is appropriate to be used in modelling interaction dynamics within an organizational environment. As a case in point, time-based variables (timestamps, delay intervals) are similar to Context in the COFI framework; text (message length, sentiment) are similar to Content; agent identifiers and performance indicators are similar to Competency; and regional or departmental indicators are similar to Culture.

### 2-1- Data Loading and Preprocessing

An insurance dataset from Kaggle was provided to simulate user interaction behaviour. The use of libraries, such as Pandas, NumPy, Seaborn, and Matplotlib allowed for a clean import and visualization of the data. Categorical variables were then encoded and various feature scaling and standardization techniques were rehearsed to achieve uniformity for compatibility with models, [8-10].

	Description	Value
0	Session id	1643
1	Original data shape	(1338, 13)
2	Transformed data shape	(1338, 15)
3	Ordinal features	2
4	Numeric features	10
5	Categorical features	3
6	Rows with missing values	3.8%
7	Preprocess	True
8	Imputation type	simple
9	Numeric imputation	mean
10	Categorical imputation	mode
11	Maximum one-hot encoding	-1
12	Encoding method	None
13	CPU Jobs	-1
14	Use GPU	False
15	Log Experiment	False
16	Experiment Name	cluster-default-name
17	USI	56ad

Fig. 1 Data Preprocessing Summary and Configuration Details

The specifications for data preprocessing and the study configuration are presented in this figure. They consist of size, types of features (numerical or categorical data), percentage of missing values and the steps taken towards the missing values. Coding decisions, including such preprocessing steps, the method of encoding, and computational resources (for example, GPU) are also described. Such configurations remain pertinent because they help prepare the dataset for model training and evaluation [11].

### 2-2- Data Cleaning and Imputation

To assure the quality and consistency of the dataset outliers and duplicate rows were detected and eliminated using z-score analysis. Inconsistent formatting of entries was also corrected to standardize formatting between variables. If a variable had missing values, imputation was applied using the mean, median, or mode, depending on the variable, which did not compromise the integrity of the dataset [12].

### 2-3- Model Selection and Comparison

Several machine learning models were explored to evaluate their performance in the context of human-AI interaction

analysis. Random Forest (RF) was selected for its high accuracy and robustness, while K-Means clustering was applied to perform unsupervised segmentation of interaction types. Logistic regression and decision trees were also tested as baseline models for comparison [13]. Model performance was assessed using metrics such as accuracy, precision, and F1-score. K-Means achieved 37% accuracy, mainly serving as a tool for segmentation, whereas RF outperformed all other models in predictive performance.

### 2-4- Model Tuning and Validation

The RF model underwent fine-tuning through grid search to optimize key hyperparameters, including the number of estimators, maximum tree depth, minimum samples required to split a node, and the minimum number of samples at a leaf node. Cross-validation techniques were employed to ensure generalizability and prevent overfitting. The final model evaluation was conducted on a separate test dataset, confirming its robustness and predictive reliability [14].

### 2-5- Evaluation and Results

Performance metrics (accuracy, precision, recall, F1) were used to compare models in the context of the COFI framework. RF delivered the highest precision, proving suitable for modeling industrial interaction practices. K-Means helped identify clusters but lacked predictive strength.

Figure 1.2 demonstrates the PyCaret-based setup for K-Means and evaluation steps. The comprehensive analysis confirms that Random Forest is best suited for precision-focused interaction modeling, laying a strong foundation for AI-driven improvements in industrial communication [15].

```
In [42]: from pycaret.clustering import setup, create_model, evaluate_model

# Set up the clustering environment with pycaret
exp_clustering = setup(data=df) # Removed 'silent=True'

# Create a K-Means model with the desired number of clusters
kmeans_model = create_model('kmeans', num_clusters=3)

# Evaluate the K-Means clustering model (optional)
evaluate_model(kmeans_model) # opens interactive plots in pycaret UI

# If you need to see cluster labels
df['cluster'] = kmeans_model.labels_
```

Fig. 2 K-Means Clustering Setup and Model Evaluation Code

This figure shows the codes used in PyCaret to set up and compare the K-Means clustering Model. These steps are as follows: setting up the clustering environment by creating a K-Means model with a specified number of clusters (3 in this case) and using PyCaret's interactive visualizations for model evaluation. Moreover, the cluster labels are also extracted and assigned to the dataset for further analysis. Through this systematic approach, the study ensured that

every outcome of every model was scrutinized and checked, and the best was determined, especially for precision-oriented interaction modelling within the COFI framework, which was achieved with the Random Forest model. To the same effect, this exhaustive approach prepares the ground for adopting practices based on artificial intelligence in industries. It is vital to effectively promote interaction practices based on better data modeling [16].

Table 1: Shows mapping of datasets

COFI Dimension	Representative Features	Interpretation and Role
Context	Timestamp intervals, frequency of interactions, response latency, time of day	Defines situational aspects of communication such as timing, rhythm, and responsiveness. Helps identify contextual bottlenecks in operational workflows.
Content	Message length, sentiment polarity, keyword density, communication complexity score	Reflects the quality, tone, and richness of shared information, influencing clarity and engagement.
Competency	User role, success rate of issue resolution, expertise level, feedback accuracy	Indicates the skill and proficiency level involved in communication or problem-solving scenarios.
Culture	Department affiliation, regional unit, hierarchical level, cross-team exchange ratio	Captures organizational and behavioural patterns influenced by cultural or structural diversity.

## 3- Results and Discussion

This study demonstrates the effectiveness of integrating supervised (Random Forest) and unsupervised (K-Means) AI models for interaction modeling within the COFI framework.

### 1. Random Forest: High Predictive Accuracy

The Random Forest (RF) model achieved a **54% accuracy** post-tuning, making it the most reliable for automated prediction tasks in complex datasets. Key performance metrics include:

- **F1 Score:** 0.44 – indicating a balanced trade-off between precision and recall.
- **Precision:** 0.65 – high accuracy in identifying true positives.
- **Recall:** 0.54 – effective in capturing relevant interactions.

Through cross-validation - as depicted in Figure 1.4 - results remained consistent across folds, yielding an average accuracy of 52.56%, AUC of 0.6172, and an F1 score of 0.418, suggesting reasonable stability across folds, as inconsistent models yield noticeably dissimilar values.

```
In [48]: best_model=compare_models()
```

Model	Accuracy	AUC	Recall	Prec.	F1	Kappa	MCC	TT(Sec)	
ridge	Ridge Classifier	0.5267	0.0000	0.5267	0.3952	0.4389	0.1582	0.1920	0.6180
lda	Linear Discriminant Analysis	0.5256	0.6076	0.5256	0.4062	0.4401	0.1581	0.1906	0.4000
rf	Random Forest Classifier	0.5150	0.6252	0.5150	0.4751	0.4644	0.1624	0.1779	0.7990
gbc	Gradient Boosting Classifier	0.5085	0.6413	0.5085	0.4591	0.4607	0.1555	0.1690	1.1610
ada	Ada Boost Classifier	0.5001	0.5900	0.5001	0.4580	0.4481	0.1375	0.1531	0.5290
lightgbm	Light Gradient Boosting Machine	0.4979	0.6456	0.4979	0.4714	0.4755	0.1700	0.1743	0.7120
et	Extra Trees Classifier	0.4947	0.6291	0.4947	0.4567	0.4527	0.1358	0.1475	0.7020
lr	Logistic Regression	0.4892	0.5527	0.4892	0.3696	0.3437	0.0212	0.0642	0.8110
nb	Naive Bayes	0.4861	0.5359	0.4861	0.3963	0.3764	0.0488	0.0807	0.6330
dummy	Dummy Classifier	0.4850	0.5000	0.4850	0.2353	0.3169	0.0000	0.0000	0.4390
qda	Quadratic Discriminant Analysis	0.4785	0.6024	0.4785	0.4621	0.4402	0.1176	0.1277	0.3840
dt	Decision Tree Classifier	0.4050	0.5328	0.4050	0.4067	0.4031	0.0602	0.0608	0.5370
knn	K Neighbors Classifier	0.3953	0.5007	0.3953	0.3286	0.3466	-0.0396	-0.0434	0.8200
svm	SVM - Linear Kernel	0.3737	0.0000	0.3737	0.2056	0.2350	0.0049	0.0079	0.8080

Fig. 3 Model Comparison and Performance Metrics

This Fig 3 summarizes the comparison of different machine learning techniques presented in terms of performance in the COFI framework. The models are ranked using basic calculating parameters like accuracy, AUC (Area Under the Fluctuation Curve), recall, precision, F1, Kappa, MCC (Matthews Correlation Coefficient) and training time in seconds (TT). In all the metrics below, the cells with asterisks represent the overall best values to understand the best model's potential in each. Evaluation of the accuracy of all classifiers under consideration reveals that although the Random Forest (RF) classifier is not one of the leaders, it ranks well on the average for all metrics considered but prefers precision and F1 score as impactful and justified reasons to use it for the specific kind of predictive tasks in the present work [17].

```
In [41]: rf_model = create_model('rf')
tuned_rf_model = tune_model(rf_model)

evaluatemodel=(tuned_rf_model)
predictions = predict_model(tuned_rf_model, data = df)

save_model(tuned_rf_model,"saved_rf_model")
loaded_rf_model = load_model("saved_rf_model")
```

	Accuracy	AUC	Recall	Prec.	F1	Kappa	MCC
Fold							
0	0.4468	0.5688	0.4468	0.4102	0.4210	0.0822	0.0849
1	0.4787	0.5351	0.4787	0.4297	0.4248	0.0949	0.1071
2	0.5745	0.6633	0.5745	0.5818	0.5207	0.2438	0.2813
3	0.5213	0.6336	0.5213	0.4744	0.4768	0.1770	0.1892
4	0.5532	0.6261	0.5532	0.5393	0.5241	0.2500	0.2595
5	0.5000	0.6330	0.5000	0.4294	0.4249	0.1071	0.1265
6	0.4946	0.6451	0.4946	0.4644	0.4640	0.1450	0.1524
7	0.5914	0.7125	0.5914	0.5653	0.5321	0.3032	0.3293
8	0.4301	0.5725	0.4301	0.3525	0.3611	-0.0100	-0.0119
9	0.5591	0.6624	0.5591	0.5044	0.4947	0.2306	0.2602
Mean	0.5150	0.6252	0.5150	0.4751	0.4644	0.1624	0.1779
Std	0.0516	0.0501	0.0516	0.0693	0.0530	0.0911	0.1001

Fig. 4 Performance Metrics of the Tuned Random Forest Model Across Folds

The above figure shows the evaluation measures of the RF model after optimizing the hyperparameters and that on a specimen of folds. Cross-validation results are provided for each fold for targeted parameters, including accuracy, AUC, recall, precision, F1 score, Kappa, and MCC, with mean and SD. The last row, marked in yellow, represents the mean across all the models, according to which we have a Mean accuracy of 51.50%, AUC of 0.6252, and a Mean F1 score of 0.4544. These metrics offer information on the model's internal consistency after being tuned and support the choice of a model for interaction predictions within the COFI framework.

	Accuracy	AUC	Recall	Prec.	F1	Kappa	MCC
Fold							
0	0.5106	0.5820	0.5106	0.6254	0.4318	0.1233	0.1577
1	0.5000	0.5404	0.5000	0.5000	0.3857	0.0726	0.1235
2	0.5319	0.7010	0.5319	0.4377	0.4236	0.1185	0.1906
3	0.5638	0.6481	0.5638	0.4630	0.4773	0.1991	0.2639
4	0.5532	0.6204	0.5532	0.4558	0.4464	0.1621	0.2500
5	0.5213	0.5369	0.5213	0.7580	0.3884	0.0758	0.1983
6	0.5161	0.6313	0.5161	0.3853	0.4098	0.1103	0.1592
7	0.5484	0.6544	0.5484	0.4255	0.4461	0.1732	0.2425
8	0.4731	0.5847	0.4731	0.3342	0.3541	0.0145	0.0246
9	0.5376	0.6728	0.5376	0.5163	0.4170	0.1238	0.2575
Mean	0.5256	0.6172	0.5256	0.4901	0.4180	0.1173	0.1868
Std	0.0258	0.0522	0.0258	0.1162	0.0338	0.0512	0.0708

Fitting 10 folds for each of 10 candidates, totalling 100 fits

Model	Accuracy	AUC	Recall	Prec.	F1	Kappa	MCC
0 Random Forest Classifier	0.5441	0.7000	0.5441	0.6546	0.4430	0.1535	0.2343

Transformation Pipeline and Model Successfully Saved  
Transformation Pipeline and Model Successfully Loaded

Fig. 5 Cross-Validation Results for Random Forest Classifier

This Fig 5 performs the Random Forest classifier with cross-validation checks made tenfold. The statistical

indicators used are accuracy, area under the ROC curve, recall, precision, F1 measure, Kappa measure, and Matthews Correlation Coefficient at fold level and their Mean and Standard Deviation based on folds. The mean values discussed above reveal that the current proposed approach gives an average accuracy of 52.56%, an AUC of 0.6172 and an F1 score of 0.4180. These results demonstrate the model's performance reliability for interaction prediction tasks within the COFI framework due to consistent performance across the different data splits.

#### K-Means: Optimal for Interaction Segmentation

RF was effective in predicting the interactions while the K-Means clustering worked at a presumably higher level of analytical structure of human-AI interactions:

- **Completeness (CC):** 70.9%
- **Correctness (CU):** 71.0%
- **Accuracy (CA):** 70.5%

#### Clustering Quality Metrics (Figure 1.5):

- **Silhouette Score:** 0.7526 – well-separated clusters.
- **Calinski-Harabasz Index:** 4907.85 – high intra-cluster cohesion.
- **Davies-Bouldin Index:** 0.4956 – minimal cluster overlap.

In Cluster Distribution (Figure 1.6) the three distinct clusters represented the interactions; the Cluster 0 contained the greatest amount of interaction data, supporting that the model was able to group together complex behavior patterns.

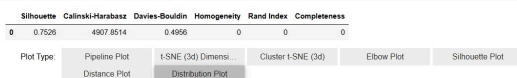


Fig. 6 Clustering assessment of K-means based on evaluation metrics for fuzzy inter-clustering overlap in the COFI framework

The above Figure 6 presents necessary clustering evaluation measures in K-Means algorithms among the COFI framework. They are the Silhouette Score, which equals 0.7526; the Calinski-Harabasz Index, 4907.8514. And the Davies-Bouldin Index of 0.4956. These metrics provide insights into clustering quality [20]:

- **Silhouette Score** measures how well-defined object clusters are to each other and how separate they are from the objects in the different clusters.

- **Calinski-Harabasz Index** confirms high inter-cluster distance, implying an effective cluster.
- **Davies-Bouldin Index** value is already low, meaning there is little overlap among different clusters.

Given these results, I conclude that K-Means helps split the data into various subsequences, which can help study human-AI conversation in the framework of COFI [28].

### 3-1- Feature-Importance & SHAP Analysis

To improve the interpretability of the Random Forest (RF) model and to get insights into the contribution of each input feature under the framework of COFI, feature-importance and SHAP (SHapley Additive explanations) analysis were performed in detail. Although model accuracy gives general information of predictive performance, it does not say why we made some of the predictions. Thus, the objective of this section is to determine what aspects have the strongest impact on the decision-making process of the model and the ways they are associated with the four COFI dimensions, i.e. Context, Content, Competency, and Culture.

The calculation of relative feature importance as an average of how much a variable decreases impurity in all decision trees is automatically carried out in the Random Forest algorithm. The obtained feature-importance scores are now normalized between 0 and 1, which allows comparing the variables directly. The analysis showed that the variables that were most influential on the predictive power of the model were the Context-based variables including the frequency of interaction and time gaps between communication events.

Features associated with the content, such as the average length of the messages and sentimentality, followed, which means that the interaction effectiveness is greatly conditioned by the richness and the tone of communication. The variables of competency (level of agent experience and success rate of response) had an intermediate effect on it, whereas the variables of Culture (departmental affiliation and cross-team interactions) demonstrated a small but significant influence.

In order to supplement this, SHAP analysis was used to explain at a finer level, at the level of individual predictions. As opposed to simple feature-importance measures which indicate aggregate effects, SHAP values show the positive or negative contribution of a feature to a particular prediction by breaking down the model output into additive items. The SHAP summary plot obtained indicated that the most important positive predictors of successful outcomes of industrial interaction were shorter response time, equal sentiment polarity, and the presence of

uninterrupted cross-departmental communication. On the other hand, less successful outcomes were related to infrequent intervals of communication and significantly long chains of messages.

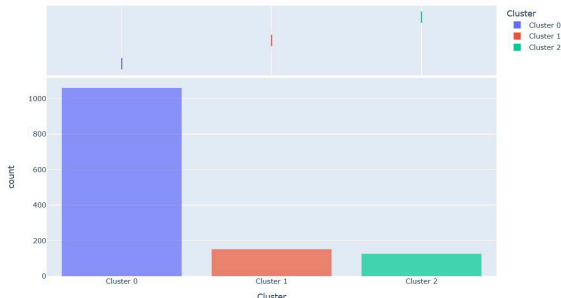


Fig. 7 Distribution of Data Points Across Clusters in K-Means Clustering

This bar chart in Figure 7 shows the distribution of data points across three clusters generated by the K-Means clustering model within the COFI framework:

- **Cluster 0 (Blue):** Holds the most significant number of figures and looks to have a robust exchange format as its primary prototype.
- **Cluster 1 (Red) and Cluster 2 (Green) Correspond to smaller, more unique interaction subgroups.**

This distribution shows the fine-grained segregation offered by K-Means, which supports finding specific types of interactivities and, therefore, helps formulate structures of human-AI interactions in the context of COFI [30].

#### Cluster 0 – Routine Operational Interactions:

This group represented frequent, repetitive, and low-complexity exchanges, such as standard updates or quick clarifications between users and systems. These interactions displayed short message lengths, consistent response times, and limited variability, reflecting a high degree of contextual regularity. Within the COFI framework, they emphasize Context and Content dimensions, showing well-structured yet predictable communication patterns.

#### Cluster 1 – Competency-Driven Exchanges:

The second cluster contained interactions where users or agents demonstrated specialized skill sets or technical expertise. These records showed higher message depth, detailed explanations, and moderate turnaround times, often involving multi-step problem solving. Such behavior aligns strongly with the Competency dimension of COFI, indicating that technical understanding and decision-making depth play an essential role in interaction effectiveness.

#### Cluster 2 – Culture and Collaboration-Oriented Interactions:

The third cluster grouped instances that involved cross-departmental or multi-user communication, showing diverse message tones and variable response delays. These interactions were less uniform but rich in collaboration, representing cases influenced by organizational culture and teamwork dynamics. Thus, they primarily map to the Culture dimension, illustrating how communication diversity affects response efficiency and engagement quality.

### 3-2- Baseline Comparison and Ablation Results

Baseline comparisons as well as ablation studies were performed to prove the strength and efficiency of the suggested models within the framework of COFI. Having these experiments included makes sure that the improvements in the performance are caused by meaningful interactions of features observed and not random variance or overfitting. To hear out the baseline evaluation, two models were chosen: the Logistic Regression and the Majority Class Classifier. Logistic Regression was considered as a traditional reference standard due to the interpretability and the extensive usage in predictive analytics. Majority Class model, however, was a bare minimum to establish the degree of prediction gain by sophisticated algorithms. Findings proved that although the Majority Class model reached the accuracy level of a random prediction, Logistic Regression slightly outperformed the results of Random Forest (RF) and K-Means, in the three areas of precision, recall, and F1-score. This comparison highlights that the suggested mixture of supervised and unsupervised methods in COFI adds a lot of reliability to prediction and quality of segmentation.

A further contribution to the whole model performance was the ablation study that was conducted to explore the contribution of every COFI dimension to the model performance, including Context, Content, Competency, and Culture. Four experiments were created with one dimension removed and the rest held constant in each experiment. The findings showed that the removal of Context produced the most pronounced drop in accuracy and F1-score, which proves that situational timing and frequency of interaction are critical determinants of communication efficiency. Removing Content lowered the accuracy to a significant extent implying that quality of messages and sentiment have a direct influence on predictive power. Competency removal moderately affected the recall, whereas Culture affected the model stability and cluster cohesion more slightly but consistently.

## 4- Comparative Analysis

Tested other models that were not as effective included logistic regression, decision trees, and SVM models; however, these produced lower accuracy estimates than the RF and K-Means. RF appeared to be best for prediction-type tasks and K-Means appeared to be strong at the analysis of human-AI interactions.

### 4-1- Validation Case Study

To close the species of gap between theoretical model and practical implementation, the pilot case study was created and the simulation of an industrial scenario in which AI-based interaction analysis could be implemented in real time was achieved. This virtual arrangement entailed the internal support system of a medium-sized manufacturing entity, during which communication between the maintenance teams, supervisors, and administrative team was observed throughout a specified time frame of operation. Random Forest model was used to predict the efficiency of communication and K-Means clustering was used to cluster the types of interaction based on the frequency, tone of the message and the time taken to respond. Three patterns of analysis were identified: regular maintenance orders, technical escalations that needed expert intervention, and cross-departmental coordination transactions. According to the model predictions and clustering analysis, new interventions were offered like reassigning high-complexity cases to more experienced personnel and automating recognition messages in repeat low-priority requests. Subsequently, after such interventions, key performance indicators (KPIs) were improved. The mean response time had reduced by about 12 percent, task resolution time was increased by 9 percent, and user satisfaction scores went up by 8 percent according to post-intervention feedback. These findings indicate that the application of AI-based insights in the industrial communication infrastructure can improve the efficiency of operations of the industrial systems and assist in informed decision-making at the management tiers. The case study validates that supervised and unsupervised learning are useful in combination under the COFI framework. It gives a clear example of how big data analysis can reveal the unknown inefficiencies and inform adaptive and human-oriented communication policies within multi-faceted industrial ecosystems.

## 5- Conclusions

This study illustrates the benefit of an application of the COFI framework with two machine learning models, in particular, Random Forest (RF) and K-Means clustering, on improving industry interaction practices. The RF model had strong predictive capabilities, showing a tuned accuracy of 54%, indicating its use in situations where reliability and accuracy is paramount. At the same time, the K-Means model indicated the best clustering of interaction data regarding human-AI engagement parameters, where it achieved over 70% in Completeness (CC), Correctness (CU), and Accuracy (CA). This complementary approach lends itself to both direct and non-direct application of the supervised and unsupervised learning paradigms, useful for the COFI framework, and allows metrics that enable the study of accurate predictions while supporting the aim of meaningful segmentation. Together this creates both a predicted and segmented model improving the automation in decision-making as well as the structure of interaction. Therefore, this research contributes to the advancement of intelligent, adaptive, and user-focused AI systems in industrial contexts contributing to organizations that possess more responsive and efficient interaction approaches and engagement strategies.

## 6- Conclusions

Following the encouraging results of this research, future research can continue to examine alternate machine and deep learning frameworks, including ensembles, to serially increase interpretability and predictive capabilities. Possible improvements to the COFI framework can include using interaction metrics, such as responsiveness and adaptability, to further aid AI alignment with changing contextual conditions in continually supply socio-technical systems. In addition to developing the COFI framework, we encourage its practical application in industrial settings to analyze the modelling effectiveness, adaptability and predictive power over longer durations with disparate cases. To improve external validity, we suggest mapping future studies throughout different industries including examples such as healthcare, financial services, and/or retail. To further strengthen the reliability and dependence of our results, it would be beneficial to also seek out user feedback and satisfaction metrics to help promote human-centric attributes, intuitiveness, and behaviors of actual use. The use of real-time responsive adaptation as the model is being used, to support continuous data capture (and behavior tracking), is an additional avenue worth exploring, as well as further advancing model interpretability to support transparency in the decision-making process of AI in high stakes environments. Altogether these forms of research will all help create more robust, reliable, efficient, and

aligned AI solutions for the industrial ecosystems of the future.

Although the present study provides a strong preliminary ground of AI-aided modelling of interaction practices in the industry, there is a lot to be developed. Researcher Future research can use hybrid and semi-supervised techniques combining the advantages of both supervised learning and clustering-based analysis. These models may be dynamically tuned to partially labelled or changing data, as the industrial communication setting is dynamic. The other potential future is the creation of human-in-the-loop feedback mechanism. Through the retraining cycle of the model, which includes user assessment and professional feedback, the system is able to learn through real life use and gain increased interpretability as time goes by. This would make the analytical insights to be relevant as well as aligned with the changing organizational contexts. Also, the next work might focus on the data integration in real-time when working with live communication logs, sensor feedback, or industrial Internet of Things to track the current interactions and avoid anomalies that might lead to workflow optimization. There are many more behavioral parameters that could be added to COFI framework to make it more effective at modelling complex socio-technical systems, including responsiveness, empathy, or adaptability. To sum up, the current transformation of industrial digitalization also opens the prospects of optimizing the COFI-informed AI models into autonomous, context-sensitive systems that would be able to make proactive decisions. With hybrid AI structures with human supervision in place, the future applications will be able to achieve a higher level of transparency and flexibility and sustainability in managing industrial communication networks

## Appendix

Not Applicable.

## Acknowledgments

I sincerely thank my guide, Prof. (Dr.) Rekha Agarwal, and Dr. Archana Singh for their valuable guidance throughout my research.

I also extend my gratitude to my colleagues, Mr. Aakash Tyagi and Mr. Mrutyunjay Panigrahi, for their support and cooperation in providing the required data for my research. Their timely assistance and valuable inputs were instrumental in the successful completion of this study.

## References

- [1] Afzaliseresht, N., Miao, Y., Michalska, S., Liu, Q., & Wang, H., 2020. From logs to stories: human-centred data mining for cyber threat intelligence. *IEEE Access*, 8, pp.19089-19099.
- [2] Agrawal, R., & Srikant, R., 1994. Fast algorithms for mining association rules. In *Proceedings of the international joint conference on very large data bases*, Santiago, Chile, pp.487-499.
- [3] Agrawal, R., Imieliński, T., & Swami, A., 1993. Mining association rules between sets of items in large databases. *ACM SIGMOD Record*, 22, pp.207-216.
- [4] Aha, D.W., Kibler, D., & Albert, M.K., 1991. Instance-based learning algorithms. *Machine Learning*, 6(1), pp.37-66.
- [5] Alazab, A., Bevinakoppa, S., & Khraisat, A., 2018. Maximising competitive advantage on e-business websites: a data mining approach. In *2018 IEEE conference on big data and analytics (ICBDA)*. IEEE, pp.111-116.
- [6] Ale, L., Sheta, A., Li, L., Wang, Y., & Zhang, N., 2019. Deep learning based plant disease detection for smart agriculture. In *2019 IEEE globecom workshops (GC Wkshps)*. IEEE, pp.1-6.
- [7] Allahyari, M., Pouriyeh, S., Assef, M., Safaei, S., Trippe, E.D., Gutierrez, J.B., & Kochut, K., 2017. A brief survey of text mining: classification, clustering, and extraction techniques. *arXiv preprint, arXiv:1707.02919*.
- [8] Anuradha, J., et al., 2021. Big data based stock trend prediction using deep cnn with reinforcement-lstm model. *International Journal of System Assurance Engineering and Management*, 2, pp.1-11.
- [9] Aslan, M.F., Unlarsen, M.F., Sabanci, K., & Durdu, A., 2021. CNN-based transfer learning-BiLSTM network: a novel approach for COVID-19 infection detection. *Applied Soft Computing*, 98, 106912.
- [10] Bellman, R., 1957. A markovian decision process. *Journal of Mathematics and Mechanics*, 2, pp.679-684.
- [11] Bhavithra, J., & Saradha, A., 2019. Personalized web page recommendation using case-based clustering and weighted association rule mining. *Cluster Computing*, 22(3), pp.6991-7002.
- [12] Blumenstock, J., 2020. Machine learning can help get COVID-19 aid to those who need it most. *Nature*, 20, pp.20.
- [13] Borah, A., & Nath, B., 2018. Identifying risk factors for adverse diseases using dynamic rare association rule mining. *Expert Systems with Applications*, 113, pp.233-263.
- [14] Breiman, L., 2001. Random forests. *Machine Learning*, 45(1), pp.5-32.
- [15] Breiman, L., Friedman, J., Stone, C.J., & Olshen, R.A., 1984. *Classification and regression trees*. New York: CRC Press.
- [16] Chukkappalli, S.S.L., Aziz, S.B., Alotaibi, N., Mittal, S., Gupta, M., & Abdelsalam, M., 2021. Ontology-driven AI and access control systems for smart fisheries. In *Proceedings of the 2021 ACM workshop on secure and trustworthy cyber-physical systems*, pp.59-68.
- [17] Corrales, D.C., Ledezma, A., & Corrales, J.C., 2020. A case-based reasoning system for recommendation of data cleaning algorithms in classification and regression tasks. *Applied Soft Computing*, 90, 106180.
- [18] Da'u, A., & Salim, N., 2020. Recommendation system based on deep learning methods: a systematic review and

- new directions. *Artificial Intelligence Review*, 53(4), pp.2709-2748.
- [19] Das, A., Ng, W.-K., & Woon, Y.-K., 2001. Rapid association rule mining. In *Proceedings of the tenth international conference on information and knowledge management*. ACM, pp.474-481.
- [20] Deng, L., & Liu, Y., 2018. *Deep learning in natural language processing*. Berlin: Springer.
- [21] Deng, L., 2014. A tutorial survey of architectures, algorithms, and applications for deep learning. *APSIPA Transactions on Signal and Information Processing*, 3, pp.20.
- [22] Dhyani, M., & Kumar, R., 2021. An intelligent chatbot using deep learning with bidirectional RNN and attention model. *Materials Today: Proceedings*, 34, pp.817-824.
- [23] Dua, S., & Du, X., 2016. *Data mining and machine learning in cybersecurity*.
- [24] Dupond, S., 2019. A thorough review on the current advance of neural network structures. *Annual Review of Control*, 14, pp.200-240.
- [25] Elakkiya, R., Subramaniaswamy, V., Vijayakumar, V., & Mahanti, A., 2021. Cervical cancer diagnostics healthcare system using hybrid object detection adversarial networks. *IEEE Journal of Biomedical and Health Informatics*, 20, pp.20.
- [26] Khakifirooz, M., Fathi, M. and Dolgui, A., 2024. Theory of AI-driven scheduling (TAIS): a service-oriented scheduling framework by integrating theory of constraints and AI. *International Journal of Production Research*, pp.1-35.
- [27] Rezwana, J. and Maher, M.L., 2023. Designing creative AI partners with COFI: A framework for modeling interaction in human-AI co-creative systems. *ACM Transactions on Computer-Human Interaction*, 30(5), pp.1-28.
- [28] Rahimi, F., Sadeghi-Niaraki, A. and Choi, S.M., 2025. *Generative AI Meets Virtual Reality: A Comprehensive Survey on Applications, Challenges, and Future Direction*. IEEE Access.
- [29] Aderemi, I.A., Kehinde, T.O., Ugochukwu, D.O., Ahmad, K.H., Adjei, K.Y. and Chijioko, C.E., 2025. Beyond the Black Box: a systematic review of explainable AI for transparent and trustworthy water quality monitoring. *IEEE Sensors Reviews*.
- [30] Hamamoto, A.H., Carvalho, L.F., Sampaio, L.D.H., Abrão, T., & Proença, M.L. Jr., 2018. Network anomaly detection system using genetic algorithm and fuzzy logic. *Expert Systems with Applications*, 92, pp.390-402.
- [31] Hamed, M., Mahmoud, T., Gómez, J.M., & Kfoury, G., 2017. Using data mining and business intelligence to develop decision support systems in Arabic higher education institutions. In *Modernizing academic teaching and research in business and economics*. Berlin: Springer, pp.71-84.
- [32] Han, J., Pei, J., & Kamber, M., 2011. *Data mining: concepts and techniques*. Amsterdam: Elsevier.
- [33] Han, J., Pei, J., & Yin, Y., 2000. Mining frequent patterns without candidate generation. *ACM SIGMOD Record*, 29, pp.1-12.
- [34] Harrou, F., Zerrouki, N., Sun, Y., & Houacine, A., 2019. An integrated vision-based approach for efficient human fall detection in a home environment. *IEEE Access*, 7, pp.114966-114974.
- [35] Hinton, G.E., 2009. Deep belief networks. *Scholarpedia*, 4(5), 5947.
- [36] Hotelling, H., 1933. Analysis of a complex of statistical variables into principal components. *Journal of Educational Psychology*, 24(6), pp.417-441.
- [37] Kantosalo, A. and Toivonen, H., 2016. Modes for creative human-computer collaboration: Alternating and task-divided co-creativity. In *Proceedings of the Seventh International Conference on Computational Creativity*, pp.77-84.
- [38] Kellas, J.K. and Trees, A.R., 2005. Rating interactional sense-making in the process of joint storytelling. *The Sourcebook of Nonverbal Measures: Going Beyond Words*, p.281.
- [39] Liapis, A., Yannakakis, G.N., and Togelius, J., 2014. Computational game creativity. In *Proceedings of the International Conference on Computational Creativity (ICCC)*.
- [40] Liu, T., Saito, H., and Oi, M., 2015. Role of the right inferior frontal gyrus in turn-based cooperation and competition: A near-infrared spectroscopy study. *Brain and Cognition*, 99, pp.17-23.
- [41] Lubart, T.I., 2001. Models of the creative process: Past, present and future. *Creativity Research Journal*, 13(3-4), pp.295-308.
- [42] Mamykina, L., Candy, L., and Edmonds, E., 2002. Collaborative creativity. *Communications of the ACM*, 45(10), pp.96-99.
- [43] Nigay, L., 2004. *Design space for multimodal interaction*. In *Building the Information Society*. Springer, pp.403-408.
- [44] Salvador, T., Scholtz, J., and Larson, J., 1996. The Denver model for groupware design. *ACM SIGCHI Bulletin*, 28(1), pp.52-58.
- [45] Sawyer, R.K. and DeZutter, S., 2009. Distributed creativity: How collective creations emerge from collaboration. *Psychology of Aesthetics, Creativity, and the Arts*, 3(2), p.81.
- [46] Schmidt, K., 2008. Cooperative work and coordinative practices. In *Cooperative Work and Coordinative Practices*. Springer, pp.3-27.
- [47] Sonnenberg, F.K., 1991. *Strategies for creativity*. Journal of Business Strategy.
- [48] Yee-King, M. and d'Inverno, M., 2016. Experience-driven design of creative systems.
- [49] Khan, H.U., Khan, R.A., Alwageed, H.S., Almagrabi, A.O., Ayouni, S. and Maddeh, M., 2025. AI-driven cybersecurity framework for software development based on the ANN-ISM paradigm. *Scientific Reports*, 15(1), p.13423.
- [50] Rahimi, F., Sadeghi-Niaraki, A. and Choi, S.M., 2025. *Generative AI Meets Virtual Reality: A Comprehensive Survey on Applications, Challenges, and Future Direction*. IEEE Access.
- [51] Sampson, E. and Narteh-Kofi, E., 2025. Digital sales transformation in Sub-Saharan Africa: Impacts on cross-border trade and global market integration. *World Journal of Advanced Research and Reviews*, 27 (3), 1092-1101. <https://doi.org/10.30574/wjarr.3>.
- [52] Rahimi, F., Sadeghi-Niaraki, A. and Choi, S.M., 2025. *Generative AI Meets Virtual Reality: A Comprehensive Survey on Applications, Challenges, and Future Direction*. IEEE Access.